

## CHAPTER 3

# CALIBRATION OF LOAD FACTORS FOR COMBINATIONS OF EXTREME EVENTS

This chapter describes the procedure followed during the reliability analysis of bridges subjected to extreme events and combinations of events. The calibration of appropriate load factors is also described. Following the research approach described in Chapter 1, the first step of the process requires the calculation of the reliability index,  $\beta$ , for a set of typical bridge configurations designed to satisfy current AASHTO LRFD specifications. Because the AASHTO LRFD specifications are primarily concerned with medium- to short-span bridge spans, the basic configuration used in this chapter consists of a three-span bridge with span lengths of 18 m/30 m/18 m (60 ft/100 ft/60 ft). The bridge is assumed to be supported by either single-column bents in which each bent's column is 1.8 m (6 ft) in diameter or two-column bents in which each bent consists of two 1.1-m (3.5-ft) diameter columns at 8 m (26 ft) center to center. The bridge geometry and structural properties for these cases are further described in Section 3.1. The reliability analysis of these two basic bridge configurations is first performed for each of the pertinent extreme hazards individually. The results of these calculations are provided in Section 3.2. Section 3.3 gives the results of the reliability calculations for the combination of events and also describes the load factor calibration process. Section 3.4 gives a summary of the load combination factors. These are also presented in an AASHTO specifications format in Appendix A. Additional details of the calculations described in this chapter are provided in Appendixes C and D. Some of the models and assumptions made during the calculations are based on the analyses and models presented in Appendixes B, E, F, H, and I.

### 3.1 DESCRIPTION OF BASIC BRIDGE CONFIGURATIONS AND STRUCTURAL PROPERTIES

The basic bridge configuration used in this study consists of a three-span 66-m (220-ft) bridge having the profile shown in Figure 3.1. The bridge is also assumed to span over a small river that may produce local scour around the bridge columns. The geometric properties of the columns for each of the bents considered are shown in Figure 3.2.

#### 3.1.1 One-Column Bent

The first option for substructure configuration consists of a bridge with two bents, each formed by a single 1.8-m (6-ft) diameter concrete column with concrete strength,  $f'_c$ , of 28 MPa (4,000 psi). The cap beam is 1.5 to 2.1 m (5 ft to 7 ft) deep carrying 6 Type-6 AASHTO girders and a 0.25-m (10-in.) deck slab plus wearing surface. The deck is 12-m (40-ft) wide with a 0.9-m (3-ft) curb on each side. The required column capacity is calculated to satisfy each of the pertinent loads using the current AASHTO LRFD specifications. Specifically, the required moment capacity is calculated for the one-column bent when subjected to the effects of gravity loads, wind loads, earthquakes, and vessel collision forces. The required foundation depth is determined to satisfy the requirements for each load type and also for scour. In addition, the column axial capacity and foundation bearing capacity are estimated to satisfy the requirements for applied gravity loads. The applied loads and load factors used in the calculations performed in this section to estimate the structural properties of the basic configuration are those specified by the AASHTO LRFD. A short description of the procedure is provided below for each load and limit state analyzed. More details are provided in Appendixes C and D.

#### *Gravity Loads*

The weight applied on each bent is calculated as follows:

- Superstructure weight per span length = 156 kN/m (10.7 kip/ft);
- Weight of cap beam = 690 kN (154 kips); and
- Weight of wearing surface and utilities = 36 kN/m (2.5 kip/ft).

The weight of the column above the soil level is 390 kN (88 kips). The analysis of the distributed weights will produce a dead weight reaction at the top of the column equal to 5.4 MN (1,209 kips) from the superstructure plus 690 kN (154 kips) from the cap and 390 kN (88 kips) from the column, producing a total weight equal to 6.5 MN (1,450 kips).

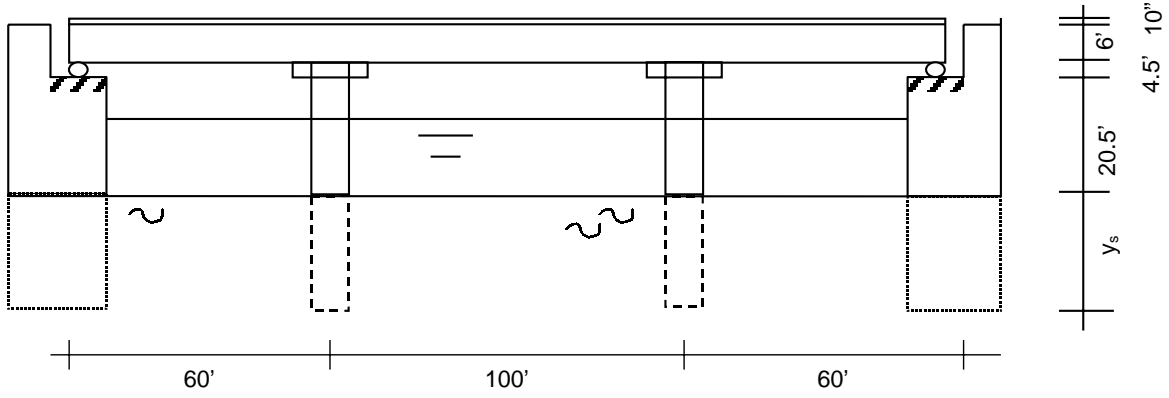


Figure 3.1. Profile of example bridge.

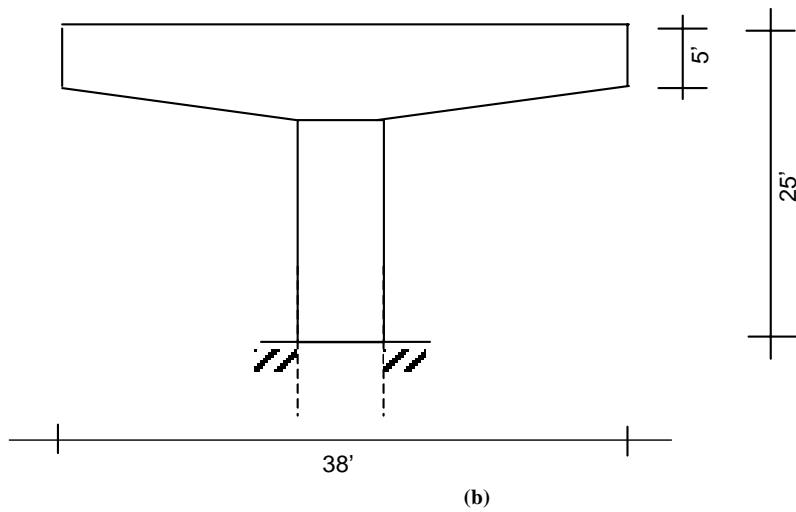
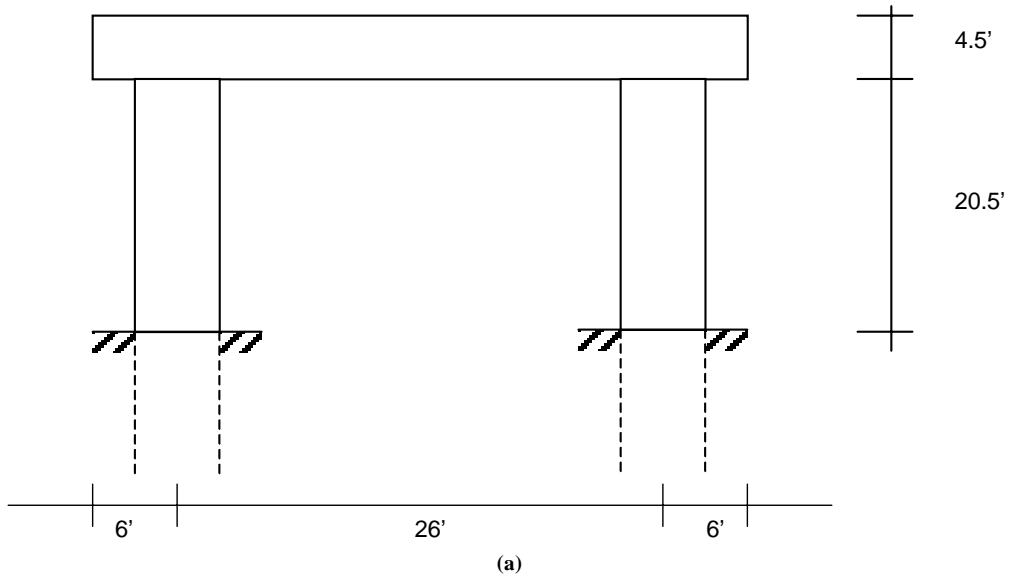


Figure 3.2. Configurations of (a) two-column and (b) one-column bents.

If designed to carry gravity loads alone (live and dead loads), the column and foundations of the one-column bent should be designed to support either two lanes of HL-93 live load that produce an unfactored live load on top of the column equal to 1.9 MN (423 kips) at an eccentricity of 2 m (7 ft), or one lane of loading that is 1.1 MN (254 kips) (including a multiple presence correction factor of 1.20) at an eccentricity of 3.7 m (12 ft) from the center of the column. The free body diagram for the one-column bent subjected to gravity loads is shown in Figure 3.3 in which  $F_{LL}$  is the force caused by live load and  $F_{DC}$  is the force from the dead weight.

The design equation used for axial and bearing capacity is as follows:

$$\phi R = 1.25 DC + 1.75 LL \tag{3.1}$$

where

$DC = 6.5 \text{ MN (1,450 kips)}$  = the permanent weight of components;

$LL$  = the live load = 1.9 MN (423 kips); and

$\phi$  = the resistance factor, which for column strength is equal to 0.75 and for foundation bearing capacity is taken as 0.50; and

$R$  = the nominal axial capacity in kips.

The required nominal resistance capacity is obtained from Equation 3.1 for each case as listed in Table 3.1.

For bending moment capacity of the column, the following equation used is:

$$\phi R = 1.75 LL \tag{3.2}$$

where  $LL$  is the live load moment = 4.1 kN-m (3,048 kip-ft = 254 kip × 12 ft) and  $\phi$  is the resistance factor which for bending is equal to 0.90. In this case,  $R$  is the nominal moment capacity in kN-m.

In the case of foundation overtipping, the permanent weight of the bridge would help resist overtipping, hence the design equation used is

$$\phi R = 0.90 DC + 1.75 LL \tag{3.3}$$

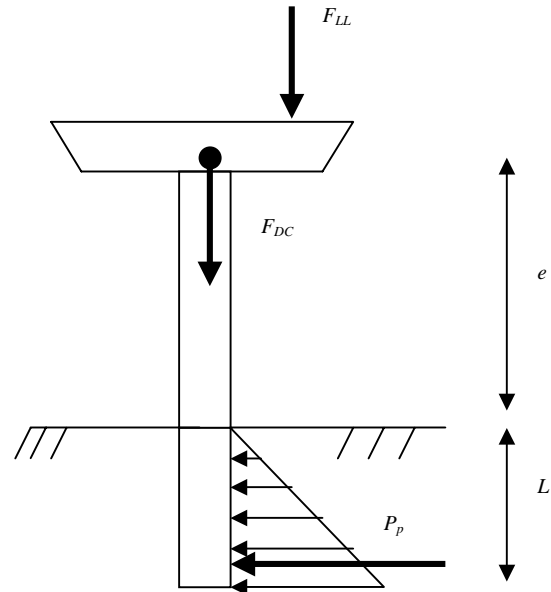


Figure 3.3. Free body diagram of one-column bent under gravity loads.

where

$DC = 5.9 \text{ kN-m (4,350 kip-ft = 1,450 kip} \times 3 \text{ ft)}$  is the moment caused by the permanent weight of components about the edge of the column shaft;

$LL = 3.1 \text{ kN-m (2,286 kip-ft = 254 kip} \times 9 \text{ ft)}$ ; and

$\phi$  = the resistance factor, which for foundation lateral resistance is taken as 0.50.

The 2.7-m (9-ft) moment arm is used as the distance between the live load and the edge of the column rather than the center, which is used when calculating the column bending moment. In this case, also  $R$  is a moment capacity in kN-m. The required foundation depth (embedded length),  $L$ , is obtained from the  $R$  value calculated from Equation 3.3, assuming a triangular distribution of soil pressure using the free body diagram shown in Figure 3.3. If  $P_p$  is calculated from Equations 2.15 and 2.16 of Chapter 2 using a soil unit weight,  $\gamma = 960 \text{ kg/m}^3 \text{ (60 lb/ft}^3\text{)}$ ; an angle of friction for sand,

TABLE 3.1 Required design capacities of one-column bent under gravity load

Hazard	Member	Limit State	Current Design Load Factors	Resistance Factor $\phi$	Required Nominal Capacity
Gravity load	Column	Axial capacity	$1.25 DC + 1.75 LL$	0.75	3,404 kips
		Moment capacity	$1.25 DC + 1.75 LL$	0.90	5,908 kip-ft
	Foundation	Vertical bearing capacity	$1.25 DC + 1.75 LL$	0.50	5,106 kips
		Foundation depth to prevent overtipping	$0.90 DC + 1.75 LL$	0.50	6 ft

$\phi_s = 35^\circ$ ; and a column diameter,  $D = 1.8 \text{ m}$  (6 ft); then  $L$  is found by setting  $R = P_p L/3$ . Knowing  $R$  from Equation 3.3, the foundation depth,  $L$ , required to resist overturning can be calculated as  $L = 1.8 \text{ m}$  (6 ft).

Table 3.1 summarizes the results of the nominal design capacities for the column axial force, column bending moment, foundation bearing resistance, and foundation depth for the one-column bent.

*Wind Loads*

The design of the single-column bridge bent for wind load in interior regions of the United States uses a design wind speed of 145 km/h (90 mph) as stipulated in the AASHTO LRFD wind maps. The AASHTO LRFD design equation for the moment capacity of the column when the system is subjected to wind is given as follows:

$$\phi R = 1.40 WS \tag{3.4}$$

where  $R$  is the required moment capacity of the column and  $WS$  is the applied moment. For overturning about the base of the foundation system, the equation used is of the form

$$\phi R = 0.90 DC + 1.40 WS. \tag{3.5}$$

In Equation 3.5,  $DC$  is the moment produced by the permanent weight about the bottom edge of the column, and  $WS$  is the moment about the base of the column produced by the wind load on the structure.

In Equation 3.4, the maximum bending moment in the column occurs at a point located at a distance  $f$  below the soil surface.  $f$  corresponds to the point in which the lateral force  $P_p$  in the soil is equal to the applied lateral force from the wind. The free body diagram for column bending is illustrated in Figure 3.4(b). For Equation 3.5, which checks the safety of the system against overturning about the base, the free body diagram is illustrated in Figure 3.4(a).

The forces  $F_1$  applied on the superstructure and  $F_2$  applied on the column because of the wind are calculated from the AASHTO LRFD wind pressure equation, which is given as follows:

$$P_D = P_B \frac{V_{DZ}^2}{25,600} \tag{3.6}$$

where  $P_B$  is base wind pressure = 0.0024 MPa for beams and  $V_{DZ}$  is the design wind velocity at design elevation  $Z$ , which is calculated from

$$V_{DZ} = 2.5V_0 \left( \frac{V_{10}}{V_B} \right) \ln \left( \frac{Z}{Z_0} \right) \tag{3.7}$$

where

- $V_{10}$  = wind velocity above ground level = 145 km/h (90 mph) in the case studied herein;
- $V_0$  = friction velocity = 13.2 km/h (8 mph) for open country;
- $V_B$  = base wind velocity = 160 km/h (100 mph); and
- $Z_0$  = friction length = 70 mm for open country.

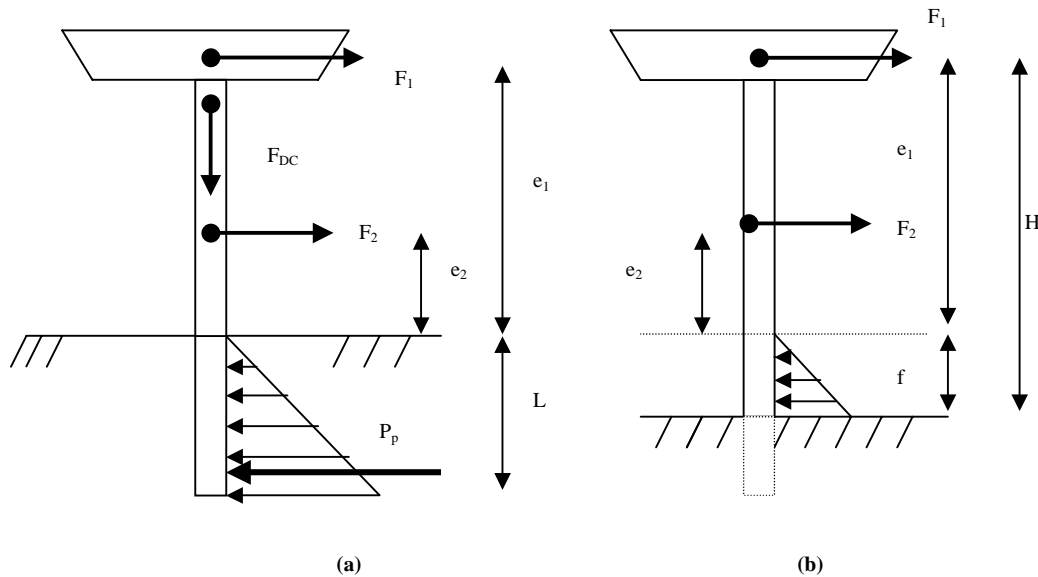


Figure 3.4. Free body diagram of bridge foundation system: (a) free body diagram for a short pile, dominant failure mode is tipping at base; (b) diagram for a long pile, dominant failure mode is column bending at distance  $f$  below soil level.

Using a superstructure depth of 2.4 m (8 ft), the wind force transmitted from the superstructure to the column is calculated to be  $F_1 = 140$  kN (31.6 kips) applied at a height  $e_1 = 8.8$  m (29 ft) from the soil surface. The force applied on the substructure is  $F_2 = 27$  kN (6 kips) at a height  $e_2 = 3.6$  m (11.8 ft). For long columns, the point of maximum moment is at  $f = 1.6$  m (5.14 ft) below the soil surface. Thus, the moment from the wind on the structure  $WS = 1600$  kN (1,180 kip-ft). The corresponding nominal design bending moment of 2500 kN-m (1,835 kip-ft) is obtained from Equation 3.4 using a resistance factor  $\phi = 0.90$ .

The results of Equation 3.5 show that the column is able to resist overturning simply because of the counteracting effects of the permanent weight. Thus, the foundation depth is controlled by effects other than the wind load (e.g., the effect of live load as shown in the previous section). Table 3.2 summarizes the wind load design requirements.

### Earthquakes

When performing a dynamic analysis in the transverse direction and assuming that the point of fixity for lateral deformation is 5.5 m (18 ft) below soil level, the effective weight of the column above the point of fixity is equal to 747 kN (168 kips). In this latter case, the center of mass is 8 m (27 ft) above soil level (= 45 ft from the point of fixity). Following common practice in earthquake engineering and assuming a tributary length of 28 m (91.75 ft = 50% of the distance to other bent and 70% of distance to abutment), the total weight from the superstructure and wearing surface applied on one bent adds up to 5360 kN (1,205 kips). Thus, the total weight on one bent is equal to 6800 kN (1,527 kips). This assumes that the lateral connection of the superstructure to the abutments will not break because of the earthquake-induced lateral motions. Notice that the total weight is slightly higher than for the gravity load because of the inclusion of the weight of the pile up to the point of fixity. The center of mass is calculated to be at 8.2 m (27 ft) above the soil surface.

The inertial forces applied on the bent because of the earthquake accelerations may be represented as shown in Figure 3.5. The point of fixity at a distance  $L_e$  below the soil surface can be calculated as a function of the soil elastic modulus,  $E_s$ , the foundation depth,  $L$ , and the stiffness of the column represented by  $E_p I_p$  where  $E_p$  is the modulus of the concrete pile and  $I_p$  is the moment of inertia of the concrete pile. The foundation is assumed to consist of a drilled pile shaft (pile extension) that

extends 15 m (50 ft) into the soil. The soil is assumed to have an elastic modulus  $E_s = 69$  MPa (10,000 psi) corresponding to moderately stiff sand. The point of fixity of the floating foundation can be calculated using the relationship provided by Poulos and Davis (1980) given as follows:

$$\left(\frac{L_e}{L}\right)^3 + 1.5 \frac{e}{L} \left(\frac{L_e}{L}\right)^2 = 3K_R \left(I_{\rho H} + \frac{e}{L} I_{\rho M}\right) \quad (3.8)$$

where

$L_e$  = the effective depth of the foundation (distance from ground level to point of fixity);

$L$  = the actual depth;

$e$  = the clear distance of the column above ground level;

$K_R$  = the pile flexibility factor, which gives the relative stiffness of the pile and soil;

$I_{\rho H}$  = the influence coefficient for lateral force; and

$I_{\rho M}$  = the influence coefficient for moment.

The pile flexibility factor is given as follows:

$$K_R = \frac{E_p I_p}{E_s L^4} \quad (3.9)$$

If the pile is made of 28 MPa (4,000 psi) concrete, then  $E_p = 25$  GPa (3,600 ksi =  $57\sqrt{4,000}$ ) and the diameter of the column being  $D = 1.8$  m (6 ft) result in a moment of inertia  $I_p = 0.55$  m<sup>4</sup> (63.62 ft<sup>4</sup> =  $\pi r^4/4$ ). Thus, for a pile length of 15 m (50 ft), the pile flexibility becomes  $K_R = 0.0037$ . The charts provided by Poulos and Davis (1980) show that for  $K_R = 0.0037$  the influence coefficients  $I_{\rho H}$  and  $I_{\rho M}$  are respectively on the order of 5 and 15. The root of Equation 3.8 produces a ratio  $L_e/L = 0.35$ , resulting in an effective depth,  $L_e$ , of 18 ft below ground surface. Thus, the effective total column height until the point of fixity becomes  $H = 13.7$  m (45 ft = 27 ft + 18 ft).

The natural period of the column bent can be calculated from

$$T = 2\pi \sqrt{\frac{M}{K}} \quad (3.10)$$

where the column stiffness is given as  $K = 3E_p I_p / H^3$  and the mass  $M$  is the equal to weight 6.8 MN (1,527 kips) divided by  $g$ , the acceleration due to gravity. Given the material and geometric properties, the natural period of the column is found to be  $T = 1.31$  sec.

**TABLE 3.2 Required design capacities of one-column bent under wind load**

Hazard	Member	Limit State	Current Design Load Factors	Resistance Factor $\phi$	Required Nominal Capacity
Wind load	Column	Moment capacity	1.40 WS	0.90	1,835 kip-ft
	Foundation	Overturning	0.90 DC + 1.40 WS	0.50	0 ft

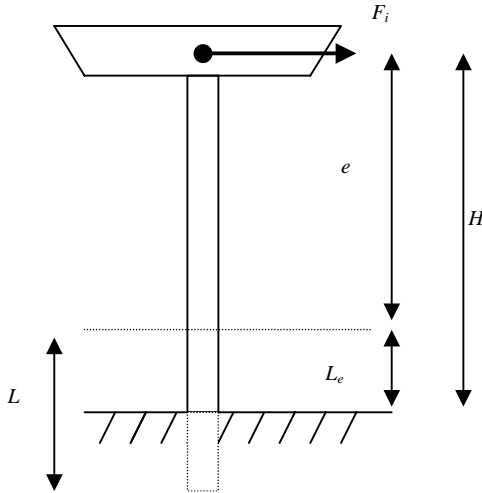


Figure 3.5. Dynamic analysis model.

The natural period of the system is used along with Equations 2.17 through 2.19 and Table 2.4 of Chapter 2 to find the spectral accelerations,  $S_a$ , for different bridge site locations. The soil is assumed to be of type *D*. The spectral accelerations calculated for the 2,500-year return period (2% probability of exceedance in 50 years) are shown in Table 3.3. The equivalent inertial forces,  $F_i$ , for nonlinear columns are obtained using Equation 3.11:

$$F_i = \frac{S_a W}{R_m} \tag{3.11}$$

where

- $S_a$  = the spectral acceleration as a function of the acceleration due to gravity,  $g$ ;
- $W$  = the weight of the structure; and
- $R_m$  = the response modification factor.

Assuming a response modification factor  $R_m = 1.50$  as specified in the proposed AASHTO LRFD earthquake design specifications in *NCHRP Report 472* (ATC and MCEER, 2002), the equivalent inertial forces accounting for column nonlinearity are calculated as shown in Table 3.3. Using the free body diagrams of Figure 3.4(b) with  $F_1 = F_i$  and  $F_2 = 0$ , the required moment capacities for the bridge column for different earthquake sites are given as shown in Table 3.3.

Table 3.3 also shows the required foundation depth,  $L$ , calculated using the free body diagram of Figure 3.4(a). In this case, the  $R_m$  value used is  $R_m = 1.0$  because rigid body overturning is assumed to occur in short columns where the maximum moment capacity has not been reached yet (i.e., when the column’s bending moment is still in the linear elastic range). For these cases, the required foundation depth,  $L$ , is given in the last column of Table 3.3.

Note that following common practice, the stiffness and the natural period of the system are calculated using Equations 3.8 and 3.9, which are based on the elastic behavior of the system. The design uses Equation 3.11 and the free body diagram of Figure 3.4, which are based on ultimate capacity.

### Scour

It is herein assumed that the bridge is constructed over a 67-m (220-ft) wide rectangular river channel as shown in Figure 3.1. To obtain realistic results for the effect of scour, different possible discharge rate data from different small rivers are used, and design scour depths are calculated for each of these river discharge rates. The rivers chosen for this analysis consist of the following: (1) Schohaire Creek in upstate New York, (2) Mohawk River in upstate New York, (3) Cuyahoga River in northern Ohio, (4) Rocky River in Ohio, and (5) Sandusky River in Ohio. Data on the peak annual discharge rates for each of the five rivers were obtained from the USGS website. Lognormal probability plots and Kolmogorov–Smirnov (K-S) goodness-of-fit tests showed that the peak annual discharge rate,  $Q$ , for all five rivers can be reasonably well modeled by lognormal probability distributions. The mean of the log  $Q$  and its standard deviation were calculated using a maximum likelihood estimator. These data are provided in Table 2.8 of Chapter 2. Assuming a slope of  $S_0 = 0.2\%$  and a Manning roughness coefficient of  $n = 0.025$ , the flow depth for the 100-year flood,  $y_{max}$ , can be calculated along with the corresponding flow velocity,  $V$ , for each of the five rivers, using Equations 2.22 through 2.28. Assuming a 67-m (220-ft) wide rectangular channel and a pier diameter of  $D = 1.8$  m (6 ft), the maximum design scour depth for the one-column bent bridge for each river data is obtained as shown in Table 3.4.

To avoid failure caused by scour, the foundation depth should be designed for a length,  $L$ , greater than or equal to the design scour depth,  $Y_{max}$ , which is given in Table 3.4.

TABLE 3.3 Earthquake design requirements for five sites

Site	Spectral Acceleration, $S_a$	Equivalent Inertial Force, $F_i$	Required Moment Capacity, $M_{cap}$	Required Foundation Depth, $L$
San Francisco	1.15 g	1,171 kips	55,950 kip-ft	86 ft
Seattle	0.64 g	652 kips	28,320 kip-ft	66 ft
Memphis	0.50 g	510 kips	21,050 kip-ft	59 ft
New York	0.17 g	173 kips	6,500 kip-ft	37 ft
St. Paul	0.05 g	51 kips	1,670 kip-ft	20 ft

**TABLE 3.4 Design scour depth for five rivers**

River	$Q$ 100-year (ft <sup>3</sup> /sec)	$V$ (ft/sec)	$Y_0$ - flood depth (ft)	$Y_{max}$ - design scour depth (ft), one-column bent
Schohaire	78,146	17.81	20.56	17.34
Mohawk	32,747	12.87	11.78	13.99
Sandusky	36,103	13.35	12.52	14.33
Cuyahoga	19,299	10.50	8.45	12.26
Rocky	19,693	10.58	8.56	12.32

*Vessel Collision*

The basic bridge configuration shown in Figure 3.1 does not allow for the passage of vessels under the bridge span. Hence, a different bridge configuration is assumed to study the vessel collision problem. For the purposes of this study, the bridge configuration selected is similar to that of the Interstate 40 (I-40) bridge over the Mississippi River in Memphis, which is fully described in Appendix D. The bridge pier and water channel configurations are represented as shown in Figure 3.6. USACE provided data on the types of barges that travel the Mississippi River near Memphis along with their weights. The data are used along with the model of the AASHTO guide specifications (1991) following the recommendations proposed by Whitney et al. (1996) to find the required design vessel impact force that would produce a nominal annual failure rate of  $AF = 0.001$ .

The calculations use Equation 2.32 through 2.38, which are given in Chapter 2. According to the analysis summarized in Table 3.5 the design impact force should be  $H_{CV} = 35$

MN (7,900 kips). This design impact force is assumed to be applied at 4.9 m (16 ft) above soil level on a column that has a diameter  $D = 6.1$  m (20 ft). The free body diagram for designing the column and foundation capacities is similar to that depicted in Figure 3.4, with  $F_1 = 0.0$ ,  $F_2 = H_{CV}$ , and  $e_2 = 4.9$  m (16 ft). Given the very large permanent weight that is applied on the bent from the large superstructure needed to span the river channel, the possibility of overturning because of vessel collision is negligibly small. Hence, only two limit states are investigated for this case: (1) failure of the column in shear, and (2) failure of the column in bending moment.

The design for shear is checked using an equation of the form

$$\phi R = 1.00 CV \tag{3.12}$$

where  $CV$  is the vessel collision force  $CV = H_{CV} = 35$  MN (7,900 kips) and is the resistance factor for shear, which according to the AASHTO LRFD should be equal to 0.90 for normal density concrete. This would result in a required shear

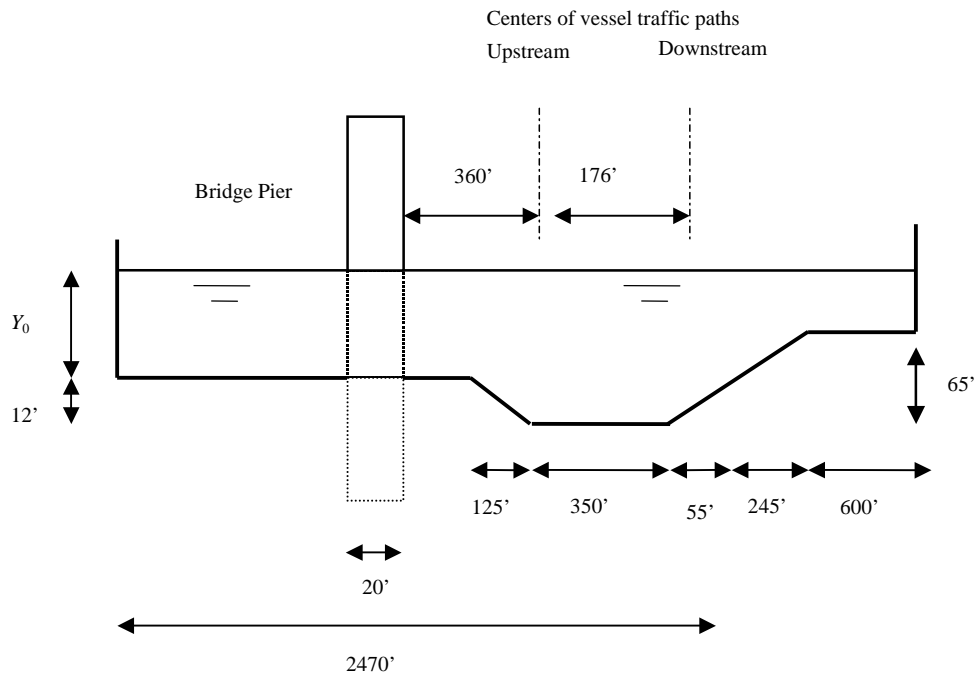


Figure 3.6. Profile of river channel for vessel collisions.

**TABLE 3.5 Details of calculations of annual failure rates for vessel collisions by flotilla type**

Type <sup>a</sup>	Frequency	Number of		Mean			Distances (m)		Normalized		PG <sup>d</sup>	PA <sup>d</sup>	PC <sup>d</sup>	N*PA*PG*PC
		columns	rows	weight(MN)	LOA(m) <sup>b</sup>	Bm <sup>c</sup>	d1 <sup>c</sup>	d2 <sup>c</sup>	d1	d2				
AB	91	4	1.9	22.92	18.74	9.45	152.56	176.62	2.04	2.36	0.01	1.77E-04	0.00	0.00
BC	126	5.93	2.05	138.44	44.52	16.11	145.03	184.15	0.55	0.70	0.05	1.77E-04	0.00	0.00
BD	1	5.11	2.93	128.28	45.35	16.49	137.39	191.80	0.59	0.83	0.07	1.77E-04	0.00	0.00
CC	79	5.11	2.93	92.63	54.70	12.24	143.62	185.57	0.51	0.66	0.05	1.77E-04	0.00	0.00
DC	35610	5.38	3.21	116.19	59.44	10.67	144.41	184.77	0.45	0.58	0.04	1.77E-04	0.00	0.00
EA	6	5	1	119.22	60.96	7.62	157.73	171.45	0.52	0.56	0.02	1.77E-04	0.00	0.00
EB	6	5	1	124.82	60.96	9.30	156.90	172.29	0.51	0.57	0.02	1.77E-04	0.00	0.00
EC	33026	5.38	3.3	129.44	61.53	10.81	143.71	185.47	0.43	0.56	0.04	1.77E-04	0.00	0.00
FC	1043	4.5	3	209.20	79.81	15.96	137.60	191.58	0.38	0.53	0.05	1.77E-04	0.00	0.00
GC	648	4	2.8	195.75	90.01	16.17	138.91	190.27	0.39	0.53	0.05	1.77E-04	0.00	0.00
GD	19	3.23	2.3	173.97	90.71	16.49	142.58	186.60	0.49	0.64	0.05	1.77E-04	0.00	0.00
HC	17	3.23	2.3	166.98	96.53	16.17	142.95	186.24	0.46	0.60	0.05	1.77E-04	0.00	0.00
Up-bound														
AB	219	4	1.9	22.60	18.73	9.42	97.73	121.73	1.30	1.63	0.04	1.77E-04		
AC	78	4	1.9	72.28	30.30	16.46	91.04	128.41	0.75	1.06	0.08	1.77E-04		
BB	4	4	1.9	9.97	35.05	8.84	98.28	121.17	0.70	0.86	0.05	1.77E-04		
BC	760	5.93	2.05	147.40	44.40	15.99	90.29	129.16	0.34	0.49	0.05	1.77E-04	1.97E-02	1.43E-04
BD	151	5.11	2.93	138.53	45.35	16.49	82.52	136.93	0.36	0.59	0.08	1.77E-04	1.15E-02	2.57E-05
CC	396	5.11	2.93	159.39	53.79	16.07	83.14	136.32	0.30	0.50	0.07	1.77E-04	1.69E-02	8.45E-05
DC	14698	5.38	3.21	119.36	59.44	10.74	89.43	130.02	0.28	0.41	0.05	1.77E-04		
EB	1	5	1	116.89	60.96	9.30	102.03	117.42	0.33	0.39	0.02	1.77E-04		
EC	12097	5.38	3.3	131.09	61.62	11.05	88.45	131.01	0.27	0.40	0.05	1.77E-04	2.90E-03	3.01E-04
ED	1	4.5	3	68.03	73.46	17.68	80.16	139.29	0.24	0.42	0.07	1.77E-04		
FC	697	4.5	3	193.33	81.43	16.02	82.66	136.80	0.23	0.37	0.06	1.77E-04	1.96E-02	1.36E-04
FD	2	4.5	3	125.15	81.38	17.68	80.16	139.29	0.22	0.38	0.06	1.77E-04	3.20E-03	6.97E-08
GC	2028	4	2.8	197.23	90.03	16.25	83.93	135.52	0.23	0.38	0.05	1.77E-04	1.58E-02	3.10E-04
GD	158	3.23	2.3	145.12	90.71	16.49	87.72	131.74	0.30	0.45	0.06	1.77E-04		
HC	73	3.23	2.3	145.11	96.55	15.67	88.66	130.79	0.28	0.42	0.05	1.77E-04		
HD	17	2	1	103.57	117.98	21.76	95.80	123.65	0.41	0.52	0.04	1.77E-04		

NOTES:

(a) The definitions of barge flotilla types are provided in Appendix E (on CRP-CD-30).

(b) LOA = length overall of flotilla.

(c) These terms are defined in Figure 2.12, shown as  $x_1$  and  $x_2$ .

(d) See Section 2.4.5 for definitions of the probabilities PA, PG, and PC.

column capacity equal to  $V_{cap} = 39$  MN (8,780 kips). The point of fixity is found to be at  $f = 10.5$  m (34.5 ft) below the soil level. Using the free body diagram of Figure 3.4(b) and a moment resistance factor,  $\phi$ , also equal to 0.90, the required column moment capacity is found to be equal to  $M_{cap} = 464$  MN-m (342,333 kip-ft). The design requirements for the column subjected to vessel collision are summarized in Table 3.6.

### 3.1.2 Two-Column Bents

The second design option is for the same bridge superstructure described in Figure 3.1, but where the substructure

consists of two bents, each formed by two 1.1-m (3.5-ft) diameter columns spaced at 7.9 m (26 ft) center to center as described in Figure 3.2(a). The clear column height is 6.3 m (20.5 ft) connected by a 1.4-m (4.5-ft) cap carrying six Type-6 AASHTO girders and a 10-in. deck slab plus wearing surface. The bent carries the same 12.2-m (40-ft) wide deck with a 0.91-m (3-ft) curb on each side as that of the one-column bent. The required column capacities are calculated to satisfy each of the pertinent loads using the current AASHTO LRFD specifications. Specifically, the required moment capacity is calculated for the two-column bent when subjected to the effects of wind loads, earthquakes, and vessel collision forces. The analysis assumes that the bent cap is very stiff compared

**TABLE 3.6 Required design capacities of one-column bent under vessel collision forces**

Hazard	Member	Limit State	Current Design Load Factors	Resistance Factor $\phi$	Required Nominal Capacity
Vessel Collision	Column	Moment capacity	1.00 VC	0.90	342,333 kip-ft
	Column	Shearing capacity	1.00 VC	0.90	8,780 kips

with the columns. Thus, vertical loads will produce negligible moments in the columns, and only the lateral loads will produce moments. Because of the presence of the two columns, no overturning is possible, although foundation depth is controlled by the scour requirements. In addition, the column axial capacity and foundation bearing capacity are determined to satisfy the requirements for applied gravity loads. The applied loads and load factors used in the calculations performed in this section are those specified by the AASHTO LRFD. A short description of the procedure is provided below for each load and limit state analyzed. More details are provided in Appendix C.

*Gravity Loads*

The weight applied on each bent is calculated as follows:

- Superstructure weight = 156 kN/m (10.67 kip/ft),
- Weight of cap beam = 480 kN (109 kips), and
- Weight of wearing surface = 35.9 kN/m (2.46 kip/ft).

The weight of the each column above the soil level is 138 kN (31 kips). The analysis of the distributed weights will produce a dead weight reaction at the top of the bent equal to

5400 kN (1,209 kips) from the superstructure plus 480 kN (109 kips) from the cap. These will result in 2900 N (659 kips) for each column for a total of 3000 kN (690 kips) per column.

If designed to carry vertical loads alone, each column of the two-column bent should be designed to support two lanes of HL-93 live load that produce an unfactored live load on top of the column equal to 188 kN (423 kips) at an eccentricity of 1.8 m (6 ft). For one lane of traffic, the live load is 1100 kN (254 kips) at an eccentricity of 0.3 m (1 ft). The free body diagram is shown in Figure 3.7 with the lateral forces  $F_1 = F_2 = 0$ . In Figure 3.7,  $e_3$  denotes the eccentricity of the applied live load,  $F_{LL}$ , relative to the center of a column. Assuming a rigid cap beam compared with the column stiffness, the applied moment on the columns caused by vertical loads is small, and the columns need to resist mostly vertical loads. Using design Equation 3.1 results in a required nominal column axial capacity and a nominal foundation bearing capacity, as are shown in Table 3.7.

*Wind Loads*

The design of the two-column bridge bent for wind load in interior regions of the United States uses a design wind speed

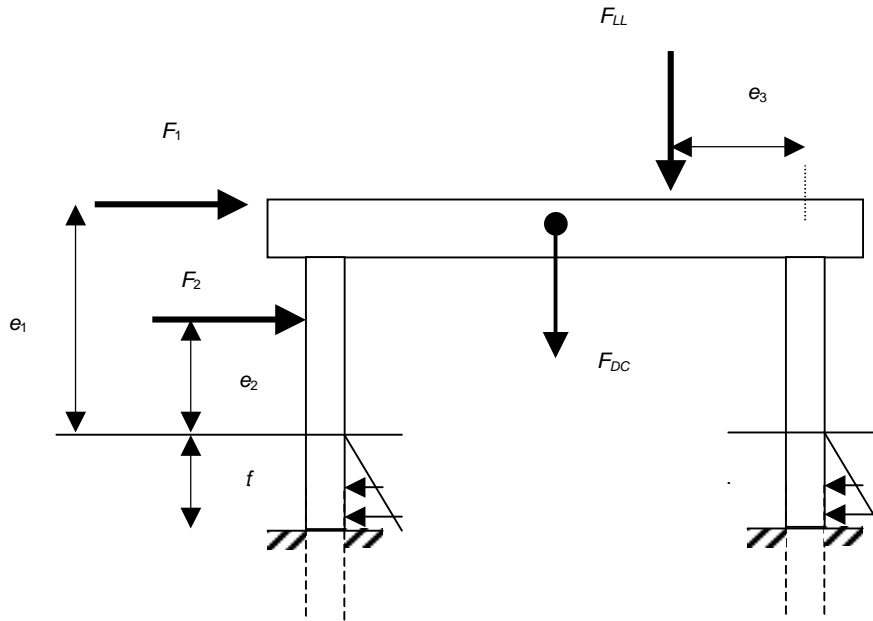


Figure 3.7. Basic free body diagram of two-column bent.

TABLE 3.7 Required design capacities of two-column bent under gravity load

Hazard	Member	Design Parameter	Current Design Load Factors	Resistance Factor $\phi$	Required Nominal Capacity
Gravity load	Column	Axial capacity	$1.25 DC + 1.75 LL$	0.75	1,909 kips
	Foundation	Vertical bearing capacity	$1.25 DC + 1.75 LL$	0.50	2,864 kips

of 145 km/h (90 mph) as stipulated in the AASHTO LRFD wind maps. The free body diagram for the wind analysis problem is as shown in Figure 3.7 with  $F_{LL} = 0$ ,  $F_1 = 140$  kN (31.6 kips) at  $e_1 = 8.8$  m (29 ft), and  $F_2 = 18$  kN (3.95 kips) at  $e_2 = 4$  m (13 ft). The design column bending moment capacity to resist the applied lateral caused by wind and allowing for a resistance factor of 0.90 and a wind load factor of 1.40 is equal to 600 kN-m (440 kip-ft) for each column as shown in Table 3.8. The simplified analysis model assumes fixity at the top because of the presence of a stiff column cap and at the base at a distance  $f = 1.4$  m (4.6 ft) below the soil level.

*Earthquakes*

When performing a dynamic analysis in the transverse direction and assuming that the point of fixity for lateral deformation is 3 m (10 ft) below soil level, the effective weight of the column above the point of fixity is equal to 200 kN (45 kips). In this case, the center of mass is 8 m (27 ft) above soil level (= 11.3 m or 37 ft from the point of fixity). Following common practice in earthquake engineering and assuming a tributary length of 28 m (91.75 ft = 50% of the distance to other bent and 70% of distance to abutment), the total weight of superstructure and wearing surface add up to 5360 kN (1,205 kips) for one bent. This will result in a total weight on one column equal to 2.9 MN (650 kips).

As a first step it is assumed that the foundation consists of a drilled pile shaft (pile extension) that extends 15 m (50 ft) into the soil. A sensitivity analysis is performed at a later stage to check other foundation depths. The soil is assumed to have an elastic modulus  $E_s = 10,000$  psi corresponding to moderately stiff sand. As explained in Appendix C, the point of fixity of the floating foundation can be calculated using the relationship provided by Poulos and Davis (1980) to produce a point of fixity  $L_e = 3$  m (10 ft) below soil level. Given a clear height of the column  $e = 6.2$  m (20.5 ft), the effective total column height until the point of fixity becomes 9.3 m (30.5 ft = 20.5 ft + 10 ft). For transverse seismic motion, the bent is

taken as fixed at the base of the effective pile depth and also fixed on the top of the column because of the presence of the stiff column cap. Thus, the natural period of the bent system,  $T$ , is 0.72 sec. The natural period is used to find the inertial forces and the required moment capacities for different earthquake sites using the same method described in Section 3.1.1 for bridges with one-column bent as provided in Equation 3.10, but with  $K = 12E_p I_p / L^3$ . Given the natural period,  $T$ , the spectral accelerations are calculated from Equation 2.17 through 2.19 of Chapter 2. The inertial forces are calculated using Equation 3.11 with a response modification factor  $R_m = 1.5$ . The spectral accelerations along with the inertial forces are listed in Table 3.9 for earthquake data from five different sites. The free body diagram described in Figure 3.7 is used with  $F_1$  equal to the inertial force while all other forces are set equal to zero. The required column moment capacities are calculated as shown in Table 3.9 using a resistance factor,  $\phi = 0.90$ .

*Scour*

The analysis of the two-column bent for scour follows the same exact method used for the one-column bent. The only difference is the diameter of the column where  $D = 1.1$  m (3.5 ft) is used for the two-column bent rather than the value  $D = 1.8$  m (6 ft), which is used for the one-column bent. The required foundation depths for different river flood data are shown in Table 3.10. The required foundation depth,  $L$ , for each river should then be equal to or greater than the values of  $y_{max}$  given in Table 3.10.

*Vessel Collision*

The vessel collision design force of  $H_{cv} = 35$  MN (7,900 kips) for the two-column bent is calculated following the same exact procedure described above for the single-column bent. The free body diagram for determining the maximum moment in the column is as shown in Figure 3.7, with  $F_2 = H_{CV}$  at  $e_2 = 4.9$  m (16 ft) and  $F_1 = F_{LL} = 0$ . In the case of the

**TABLE 3.8 Required design capacities of two-column bent for wind load**

Hazard	Member	Design Parameter	Current Design Load Factors	Resistance Factor $\phi$	Required Nominal Capacity
Wind load	Column	Moment capacity	1.40 WS	0.90	440 kip-ft

**TABLE 3.9 Earthquake design requirements for two-column bent using earthquake data from five sites**

Site	$S_a$ Spectral Acceleration	$F_i$ Equivalent Inertial Force	$M_{cap}$ , Required Moment Capacity
San Francisco	1.81 g	784 kips	13,500 kip-ft
Seattle	1.19 g	516 kips	8,370 kip-ft
Memphis	0.92 g	399 kips	6,260 kip-ft
New York	0.32 g	139 kips	1,970 kip-ft
St. Paul	0.09 g	39 kips	514 kip-ft

**TABLE 3.10 Design scour depth for five rivers**

River	$Q$ 100-year (ft <sup>3</sup> /sec)	$V$ (ft/sec)	$Y_0$ flood depth (ft)	$Y_{max}$ – design scour depth (ft), two- column bent
Schohaire	78146	17.81	20.56	12.31
Mohawk	32747	12.87	11.78	9.93
Sandusky	36103	13.35	12.52	10.17
Cuyahoga	19299	10.50	8.45	8.70
Rocky	19693	10.58	8.56	8.75

vessel collision analysis, the column width is taken as 6.1 m (20 ft) and the clear height of the bent is 46 m (150 ft), which is the same height as the I-40 bridge over the Mississippi River described in Appendix D. Because the clear column height of 46 m (150 ft) is so much higher than the point of application of the force, which is at 4.9 m (16 ft) above the soil level, most of the applied load remains in the lower portion of the impacted column. The maximum shearing force in the lower part of the column is calculated to be 0.95 times the applied force. Hence, the design shearing capacity should be 37 MN (8,340 kips) using a resistance factor  $\phi = 0.90$ . The point of maximum moment is approximated to be at 10 m (33 ft) below the soil surface. Hence, using a resistance factor  $\phi = 0.90$ , the required moment capacity at the base will be 430 MN-m (317,000 kip-ft). The required moment and shear capacities are listed in Table 3.11

### 3.2 RELIABILITY ANALYSIS FOR EXTREME EVENTS

The reliability index,  $\beta$ , is calculated in this section for bridges designed to satisfy the current AASHTO LRFD criteria for the various extreme load events of interest to this project. The purpose is to study the level of bridge structural safety provided by the current AASHTO LRFD for each of the extreme events. Also, the reliability analysis shows how changes in the design criteria would affect the safety of bridge systems. This information will also be used to choose the target reliability indexes that will form the basis for calibrating the load factors for load combinations. The reliability analysis uses the methodology and the statistical models described in Chapter 2. In this section, the reliability analysis is performed for gravity loads consisting of live load and dead loads, for wind loads in combination with the permanent loads when applicable, for earthquakes alone, for scour, and for vessel collisions. The bridges analyzed have the basic geometries described in Figures 3.1 and 3.2. Modifications on the basic

bridge geometry are assumed in order to allow for barge traffic under the bridge and, thus, also to study the reliability under vessel collision.

The reliability calculations are performed using a Monte Carlo simulation. The random numbers were generated using the method described by Deng and Lin (2000). This method has proven to be more stable and capable of generating large numbers of independent random variables than are similar routines provided in commercially available mathematical packages. An excessively large number of independent random variables are needed in this study in which Monte Carlo simulations have to be performed for a relatively large number of random variables and to study probabilities of failure on the order of  $10^{-5}$  to  $10^{-6}$  (reliability index,  $\beta$ , up to the range of 4.0). Monte Carlo simulations are used rather than a FORM algorithm because some of the cumulative distributions identified in Chapter 2 (e.g., for earthquake intensities and vessel collision forces described in Figures 2.4 and 2.13) are given in discrete forms that render them difficult to implement in a FORM algorithm because of the discontinuities of their slopes.

#### 3.2.1 Reliability Analysis for Gravity Loads

In this section, the reliability index implicit in the AASHTO LRFD design criteria is calculated for bridge columns subjected to the effect of live loads in combination with dead loads. Four different limit states are studied:

1. Failure of the column under axial load,
2. Failure of the foundation caused by exceedance of bearing capacity,
3. Overtipping of a column with a short pile shaft, and
4. Failure of a long pile shaft in bending.

For the analysis of the column for overtipping, the soil's contributions in resisting bending are included using the free body diagram in Figure 3.3. The failure functions for each of

**TABLE 3.11 Required design capacities of two-column bent under vessel collision forces**

Hazard	Member	Limit State	Current Design Load Factors	Resistance Factor $\phi$	Required Nominal Capacity
Vessel Collision	Column	Moment capacity	1.00 VC	0.90	317,000 kip-ft
	Column	Shearing capacity	1.00 VC	0.90	8,340 kips

the four limit states considered for one-column bents are given as follows:

$$Z_1 = P_{\text{col}} - F_{DC} - F_{LL}, \quad (3.13)$$

$$Z_2 = P_{\text{soil}} - F_{DC} - F_{LL}, \quad (3.14)$$

$$Z_3 = \frac{3\gamma DK_p L^2}{2} \frac{L}{3} + F_{DC} \frac{D}{2} - F_{LL} \left( e_3 - \frac{D}{2} \right), \quad \text{and} \quad (3.15)$$

$$Z_4 = M_{\text{col}} - F_{LL} e_3. \quad (3.16)$$

For each limit state,  $i$ , failure occurs when  $Z_i$  is less than or equal to zero.  $P_{\text{col}}$  is the column's axial capacity,  $F_{DC}$  is the dead weight applied on the column,  $F_{LL}$  is the live load,  $P_{\text{soil}}$  is the soil's bearing capacity at the column's tip,  $\gamma$  is the specific weight of the soil,  $D$  is the column diameter,  $K_p$  gives the Rankine coefficient,  $L$  is the foundation depth,  $e_3$  is the eccentricity of the live load relative to the center of the column, and  $M_{\text{col}}$  is the column's bending moment capacity. All the variables used in Equations 3.13 through 3.16 are considered random except for the column diameter,  $D$ , the eccentricity,  $e_3$ , and the foundation depth,  $L$ . Adjustments to Equations 3.13 and 3.14 are made when analyzing the two-column bents to find the portion of  $F_{LL}$  and  $F_{DC}$  applied on each column. The statistical models used to describe the random variables are provided in Tables 2.1, 2.2 and 2.3. Specifically, the live load  $F_{LL}$  is composed of time-dependent and time-independent random variables and can be represented as follows:

$$F_{LL} = \lambda_{LL} I_{LL} HL_{93} I_{IM} \quad (3.17)$$

where

$\lambda_{LL}$  = the live load modeling factor,

$I_{LL}$  = the live load intensity coefficient,

$HL_{93}$  = the AASHTO LRFD live load model, and

$I_{IM}$  = the dynamic amplification factor.

All the terms in Equation 3.17 except for  $HL_{93}$  are random with statistical properties provided in Table 2.3 of Chapter 2.  $I_{LL}$  is a time-dependent random variable that varies as a function of the return period as described in Equations 2.11 and 2.14.

It is noted that the columns are subjected simultaneously to axial compression and bending moment. Thus, the column's load-carrying capacity is governed by a  $P$ - $M$  (axial load versus moment) interaction curve as shown in Figure 2.2. However, for the sake of simplicity and because reliability models for the combined behavior of bridge columns are not readily available, Equations 3.13 through 3.16 treat each effect separately.

For the one-column bent, the column is first assumed to have the nominal capacities provided in Table 3.1. The columns of the two-column bent are first assumed to have the nominal capacities listed in Table 3.7. In addition, a sensitivity analysis is performed to study how the reliability index

for each limit state changes as the nominal capacities are varied from the required AASHTO LRFD values of Tables 3.1 and 3.7. During the reliability calculations, the resistance biases, COVs, and probability distribution types listed in Tables 2.1 and 2.2 of Chapter 2 are used to model the variables that contribute to resisting the failure in each limit state.

Statistical data for modeling the dead and live loads' effects are described in Section 2.4.1 of Chapter 2. The biases, COVs, and probability distributions of all the random variables that describe the effects of gravity loads are provided in Table 2.3. These values are used as input during the reliability calculations. Following the model used by Nowak (1999), the bridge is assumed to carry 1,000 individual heavy truck load events or 67 occurrences of heavy side-by-side truck events each day. This would result in  $27.4 \times 10^6$  single truck events or  $1.825 \times 10^6$  side-by-side events in a 75-year design period. The 75-year design period is used in this report to remain compatible with the AASHTO LRFD specifications. Equation 2.14 with  $m = 27.4 \times 10^6$  or  $1.825 \times 10^6$  is used to obtain the probability distribution of the maximum live load intensity in 75 years given the probability distribution for one event as listed in Table 2.3. The reliability calculations also account for the modeling factor and the dynamic amplification factors. Only the live load intensity is considered to be time-dependent. All the other variables are time-independent in the sense that they are not affected by the 75-year design period. During each cycle of the Monte Carlo simulation, the worst of the one-lane loading or the two-lane loading is used as the final load applied on the bridge structure.

The results of the reliability analysis for the four limit states considered are presented in Figures 3.8 through 3.11 for the two- and one-column bents. The figures give the reliability index,  $\beta$ , for each limit state as a function of the nominal capacity of the column. The abscissas are normalized such that a value of 1.0 indicates that the column is designed to exactly satisfy the requirements of the AASHTO LRFD specifications for the limit state under consideration. The required nominal design capacities for the columns under the effect of gravity loads are listed in Tables 3.1 and 3.7 for the one- and two-column bents. Thus, a value of 1.0 for the failure of the column under axial load (i.e., the first limit state) means that the column analyzed has a nominal capacity  $P_{\text{cap}}$  equal to the AASHTO LRFD required design capacity or  $P_{\text{cap}} = P_{\text{design}} = 15 \text{ MN}$  (3,404 kips). A value of 1.1 indicates that the capacity is 10% higher than the required design capacity such that  $P_{\text{cap}} = 16.6 \text{ MN}$  (3,744 kips).

The steepness of the slope of each curve gives an assessment of the cost implied when an increase in the reliability index is desired. For example, a steep positive slope would indicate that large increases in the reliability index could be achieved as a result of small increases in the member capacities while a shallow positive curve would indicate that large increases in the member capacities would be required to achieve small increases in the reliability index.

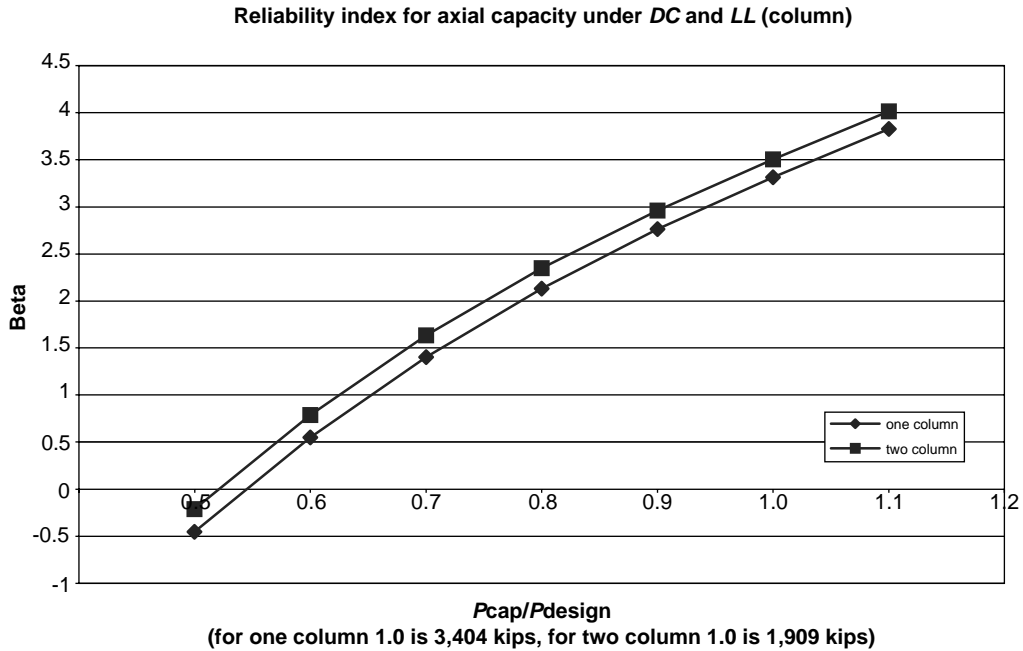


Figure 3.8. Reliability of concrete columns under axial load due to gravity.

The results in Figure 3.8 for the columns under axial load show that the current AASHTO LRFD produces reliability indexes of 3.50 for the two-column bent and 3.32 for the one-column bent. This indicates that the AASHTO LRFD code produces reliability index levels close to the 3.5 target beta set by the AASHTO LRFD code writers for columns under axial compression even though this particular limit state was not specifically considered during the calibration of the AASHTO LRFD specifications (Nowak, 1999). The figure also shows

that an increase in column capacity of 10% ( $P_{cap}/P_{design} = 1.1$ ) would result in an average reliability index on the order of 3.90. This indicates that improvement in the reliability index can be achieved with relatively small increases in column axial capacities.

The results for the failure of the soil bearing capacity are illustrated in Figure 3.9. These results show that the current AASHTO LRFD produces reliability indexes of 2.53 for the two-column bent and 2.47 for the one-column bent, which

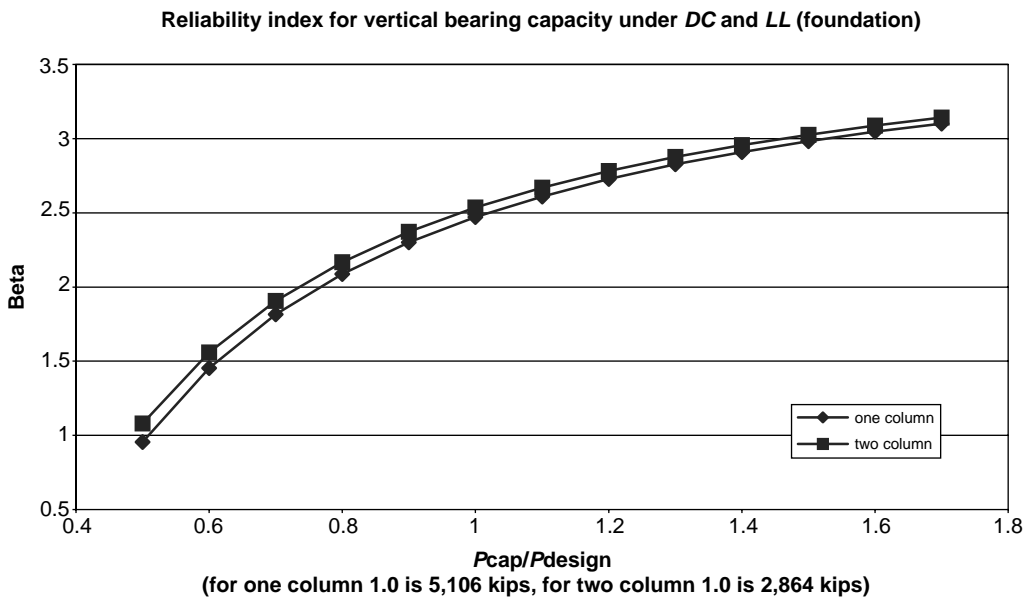


Figure 3.9. Reliability of foundation bearing capacity under axial load due to gravity.

indicates that the current code produces lower reliability levels for foundation design than for the design of structural elements despite the higher resistance factor of 0.50 used for the design of foundations. This is due to the high level of uncertainty associated with current methods for designing foundations and in estimating soil properties. The data are applicable to the models described by Poulos and Davis (1980). It should be noted that there are several different methods used in current practice for the design of foundations. These will produce different reliability indexes depending on the biases and implicit safety factors included when the methods are developed. NCHRP Project 12-55, entitled “Load and Resistance Factors for Earth Pressures on Bridge Substructures and Retaining Walls,” is addressing some of these issues. Figure 3.9 shows that an increase in foundation bearing capacity of 50% ( $P_{cap}/P_{design} = 1.5$ ) would result in an average reliability index on the order of 3.0 when  $P_{design}$  is calculated based on the Poulos and Davis method (1980). A much higher increase would be required to achieve a reliability index of 3.50. Hence, increases in the reliability indexes for bridge foundations would require large increases in the foundation depths and sizes because of the relative shallowness of the reliability index curve.

Figures 3.8 and 3.9 also show that the reliability indexes for the two- and one-column bents are reasonably similar despite the differences in bent configurations and column sizes.

Figure 3.10 illustrates how the reliability index against foundation overturning for one-column bents varies with foundation depth. The figure shows that if the foundation is built to a depth of  $L = 1.8$  m (6 ft) as required using current AASHTO LRFD design standards along with the Broms method for foundation analysis as described in Poulos and Davis (1980), the reliability index against overturning is then equal to 3.58.

The reliability analysis is based on the free body diagram of Figure 3.3 and the random variables associated with soil resistance listed in Table 2.2.

It is noticed that doubling of the foundation depth from 1.8 m to 3.7 m (6 ft to 12 ft) would result in increasing the reliability index to 4.73. The higher reliability index for foundation overturning compared with that for foundation bearing capacity is due to the fact that the Broms method has an implicit bias of about 1.50, as reported by Poulos and Davis (1980). On the other hand, the model proposed by Poulos and Davis (1980) for calculating the ultimate pile shaft bearing capacity for vertical load is not associated with any bias. The differences emphasize the need to develop more consistent reliability-based models for bridge foundation design. As mentioned earlier, NCHRP Project 12-55 is addressing some of these issues. The last failure mode considered for gravity loads only is the failure of the one-column bent because of bending. Although the live load eccentricity of the one-column bent is relatively small and the column will mostly behave as a member under axial loading, the possibility of bending failures is considered in this section producing the results presented in Figure 3.11. These results will be used in subsequent sections when studying the combination of live loads and other lateral loads that will produce high bending moments. If the column is designed to resist the applied moment produced because of the eccentricity of the live load, then the AASHTO LRFD specifications require a nominal moment capacity  $M_{cap} = 8$  MN-m (5,908 kip-ft), as shown in Table 3.1. According to Figure 3.11, such a moment capacity would produce a reliability index of  $\beta = 3.71$ . This value is higher than the  $\beta_{target} = 3.5$  used to calibrate the AASHTO LRFD and is also higher than the value observed in Figure 3.8 for column axial capacity. The difference is partially due to the fact that the dead load does not

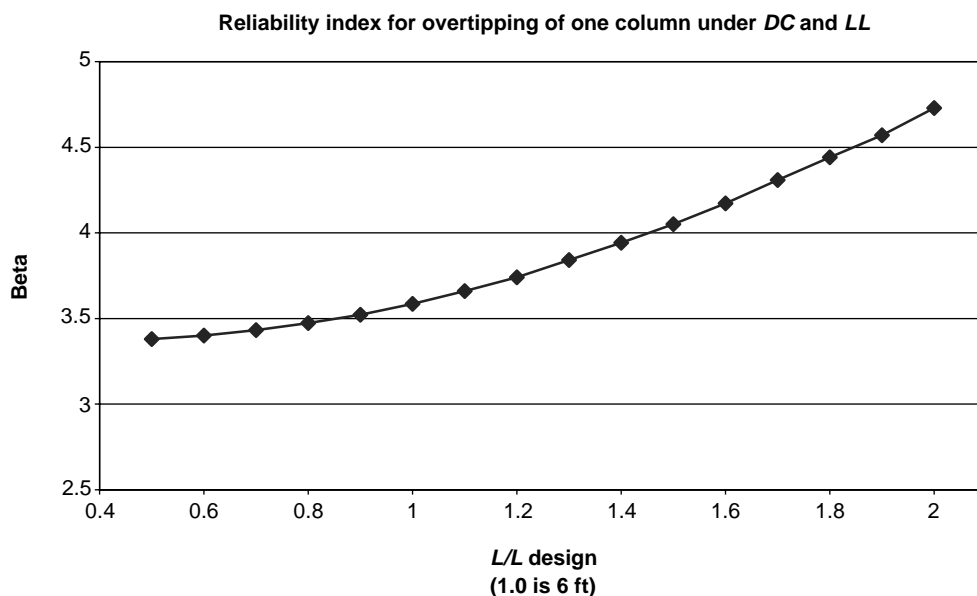


Figure 3.10. Reliability for foundation overturning caused by live and dead loads.

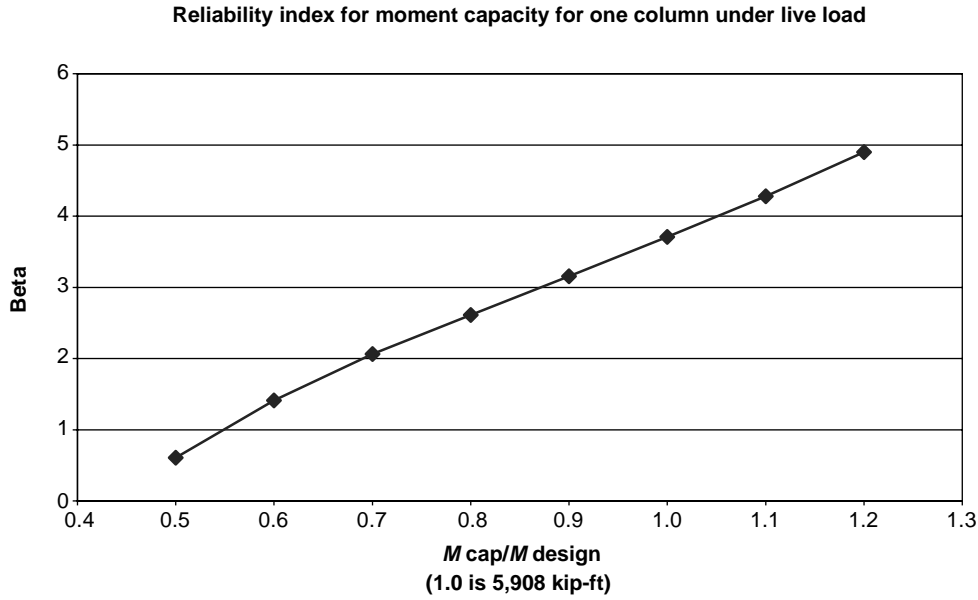


Figure 3.11. Reliability index for bending moment of one-column bent.

contribute in either resisting or increasing the bending moment in one-column bents. The slope of the reliability index curve shows that an increase in moment capacity by 10% would produce a reliability index equal to 4.28 (i.e., an increase in beta of more than 0.57).

The results presented in Figures 3.8 through 3.11 further illustrate that, based on the data assembled in Chapter 2, the AASHTO LRFD specifications have achieved a reasonably uniform reliability index close to the target value of 3.5 for structural members subjected to gravity loads. The reliability indexes for foundation design, however, greatly depend on the design methodology followed. Several different foundation design methodologies are used in practice that would require different safety factors to achieve a uniform reliability level. NCHRP Project 12-55 is currently addressing the issue of the foundation safety and the calibration of resistance factors for bridge foundation design. The slopes of the reliability index curves demonstrate that by increasing the structural properties of the bridge columns by 10%, a relatively large increase in the reliability index on the order of 0.40 to 0.60 is achieved. On the other hand, very large increases in the foundation capacities are required to effect small increases in the reliability index values associated with column overturning or foundation bearing failures.

The results shown in Figures 3.8 through 3.11 show the reliability index values calculated for member failure. When the column in a single-column bent fails, it leads to the failure of the whole system. On the other hand, when one member of a multicolumn bent system fails in bending, the presence of ductility and redundancy will help the system redistribute the load to provide additional reserve strength. In this case, system failure will occur at a higher load. Failures in shear or com-

pression do not provide much ductility. Because under gravity load the failure of multicolumn bents is primarily due to axial compression and soil-bearing capacity rather than due to bending, all types of bents subjected to gravity loads will have no redundancy.

### 3.2.2 Reliability Analysis for Wind

The reliability analysis of the one-column and two-column bents under wind loads is also executed using the model described in Chapter 2 and using the free body diagrams of Figures 3.4 and 3.7 with the live load  $F_{LL} = 0$ . Referring to Figure 3.4(b), the failure function for column bending in the one-column bent can be represented by an equation of the following form:

$$Z_5 = M_{col} + \frac{3\gamma DK_p f^2}{2} \frac{f}{3} \lambda_{cyc} - [F_{WL1}(e_1 + f) + F_{WL2}(e_2 + f)] \quad (3.18)$$

where

- $M_{col}$  = the column bending moment capacity,
- $F_{WL1}$  = the wind load on the superstructure,
- $F_{WL2}$  = the wind load on the column,
- $\gamma$  = the specific weight of the soil,
- $D$  = the column diameter,
- $K_p$  = the Rankine coefficient,
- $e_1$  and  $e_2$  = the distance of  $F_{WL1}$  and  $F_{WL2}$  from the soil level,
- $f$  = the distance from the soil level to the point of maximum moment, and

$\lambda_{cyc}$  = the model of the effect of applying cyclic loads on the foundation.

The distance,  $f$ , is calculated by setting the sum of  $F_{WL1} + F_{WL2}$  = to the lateral load pressure, or

$$\frac{3\gamma DK_p f^2}{2} = F_{WL1} + F_{WL2} \tag{3.19}$$

Referring to Equation 3.18, failure occurs when  $Z_5$  is less than or equal to zero. All the variables used in Equations 3.18 and 3.19 are considered random except for the column diameter,  $D$ , and the eccentricities,  $e_1$  and  $e_2$ . Adjustments to Equations 3.18 and 3.19 are made when analyzing the two-column bents to find the portion of  $F_{WL1}$  and  $F_{WL2}$  applied on each column. The statistical models used to describe the random variables are provided in Tables 2.1, 2.2, and 2.7. Specifically, the wind load  $F_{LW}$ , for either wind on the structure or on the column, is composed of time-dependent and time-independent random variables and can be represented as

$$F_{WL} = cC_p E_z G(\lambda_v V)^2 \tag{3.20}$$

where

- $c$  = an analysis constant,
- $C_p$  = the pressure coefficient,
- $E_z$  = the exposure coefficient,
- $G$  = the gust factor,
- $\lambda_v$  = the statistical modeling factor for wind speeds, and
- $V$  = the wind speed.

All the terms in Equation 3.20 are random with statistical properties provided in Table 2.6 of Chapter 2. The wind speed,  $V$ , is a time-dependent random variable that varies as a function of the return period as described in Equations 2.11 and 2.14. Mean and COV values of wind speed at different interior sites throughout the United States are provided in Table 2.7 for the annual maximum winds and the 50-year maximum wind.

The reliability analysis is performed in this section to study the safety of bridge columns in bending caused by the effect of wind alone. The return period used is 75 years in order to remain compatible with the AASHTO LRFD criteria. Notice that Equation 3.18 does not include the effect of dead loads. Only the bending in the column failure mode is considered because preliminary calculations performed in this study have indicated that the safety of the one-column bent against overturning is very high and thus overturning of one-column bents because of wind loads is not considered in this report.

The results of the reliability index calculations for the failure of one column in bending are illustrated in Figure 3.12 for the one-column bent and Figure 3.13 for the two-column bents. The calculations are effected for different wind data collected by Simiu, Changery, and Filliben (1979) and summarized by Ellingwood et al. (1980) at seven sites within the interior of the United States. The results show that bridge structures designed to satisfy the current AASHTO LRFD specifications for wind loads (i.e., for  $M_{cap}/M_{design} = 1.0$ ) produce an average reliability index value from all the sites analyzed equal to 3.07 for the one-column bent and 3.17 for the two-column bent. However, the variability of the results for

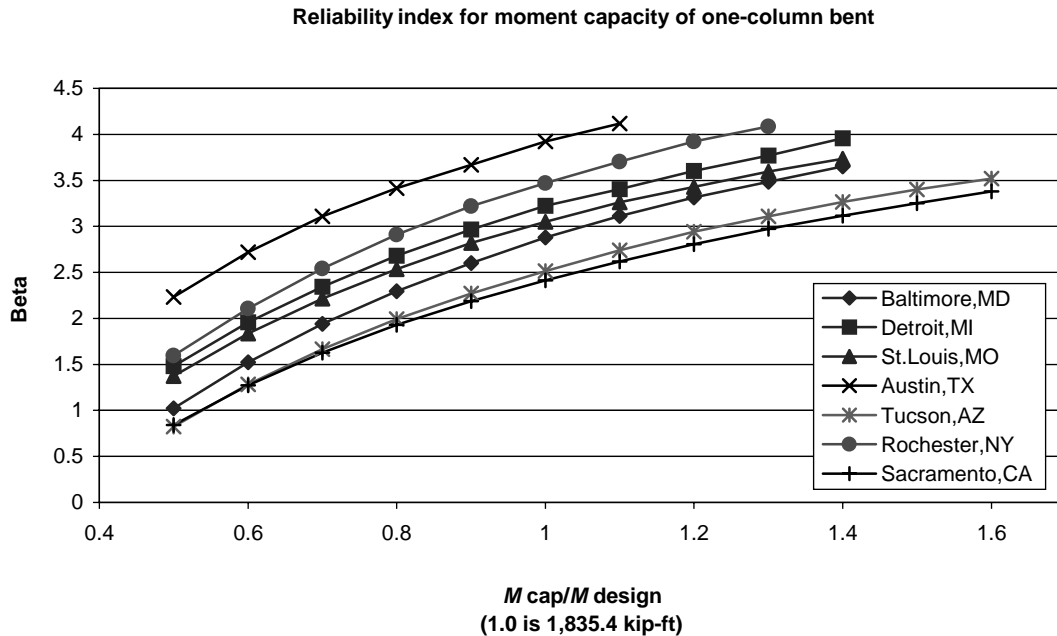


Figure 3.12. Reliability index for bending moment of one-column bent under wind loads.

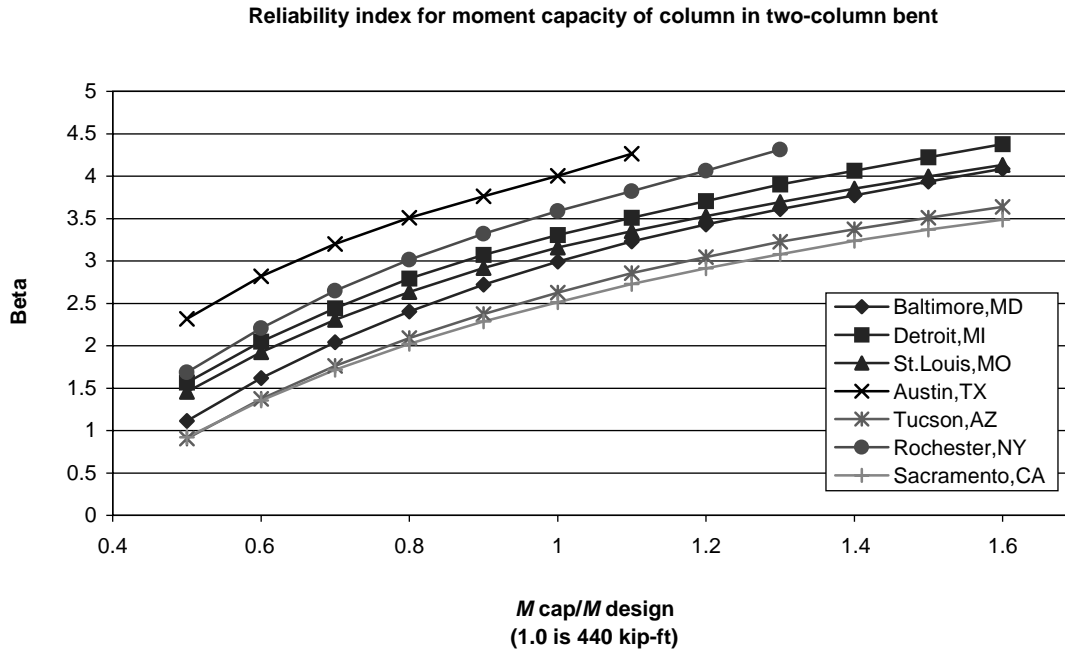


Figure 3.13. Reliability index for bending moment in two-column bent under wind loads.

different sites is large: the range of the reliability index is from 2.41 to 3.92 for one-column bents and from 2.51 to 4.00 for two-column bents. This large spread in  $\beta$  is due to the fact that the ASCE-7 design wind speed maps that are adopted by AASHTO use a common design wind of  $V = 145$  km/h (90 mph) for all interior regions; the actual data collected (see Table 2.7) show a large range of values for the mean maximum winds and their COVs. It is herein recommended that future wind maps account for the different wind speeds observed in different regions.

The results shown for the 7.6-m (25-ft) high bridge produce low applied moments from the wind load as compared with the moments caused by the effect of live load. Thus, a sensitivity analysis is performed to study the effect of changing the bridge height on the reliability of the bridge column. The results for failure of the one-column bent in bending are shown in Figure 3.14 for different column bents with heights varying between 7.6 m and 23 m (25 ft and 75 ft). The results illustrate that column height does not significantly affect the reliability index of bridges for the failure mode in bending although a small drop in the reliability index is observed as the column height increases. The drop in  $\beta$  between the heights of 7.6 m and 23 m (25 ft and 75 ft) is generally less than 0.30 such that the average reliability index from the three sites studied—namely St. Louis, Sacramento, and Austin—reduces from a value of 3.13 to an average value of 2.87. The  $M_{\text{design}}$  values used to normalize the abscissa of the curve shown in Figure 3.14 are the nominal bending moment capacities required for exactly satisfying the current AASHTO LRFD criteria. The drop in  $\beta$  is primarily due to the uncertainty in identifying the location of the point of maximum

moment,  $f$ , calculated from Equation 3.19. The value of  $f$  is highly uncertain because of the uncertainty in the soil properties and the modeling of the soil capacity to resist lateral forces. The drop in the reliability index caused by increases in column height is clearly less significant than the difference observed in the effects of site variations in wind speeds on the reliability index.

The results illustrated in Figures 3.12 through 3.14 show the reliability index values calculated for member failure. When the column in a single-column bent fails, it leads to the failure of the whole system. On the other hand, when one member of a multicolumn bent system fails in bending, the presence of ductility and redundancy will help the system redistribute the load to provide additional reserve strength. In this case, system failure would occur at a higher load. Liu et al. (2001) have shown that typical two-column bent systems formed by pile extensions subjected to lateral loads provide an additional reserve strength equal to 15% higher than the strength of one column. Using a system capacity ratio of 1.15 with a COV of 8% (as described in Table 2.1 for unconfined columns) would lead to higher system reliability index values as compared with those of one column. Figure 3.15 illustrates the difference between the reliability indexes for one column versus for the two-column bent system. The wind data used as the basis of the calculations are from the St. Louis site. The results show an increase from the 3.16 reliability index for one column to a value of 3.40 for the two-column system, or an increase of about 0.24. Higher increases in the reliability index would be expected if the concrete columns are highly confined because of the effect of the higher ductility levels associated with confined columns.

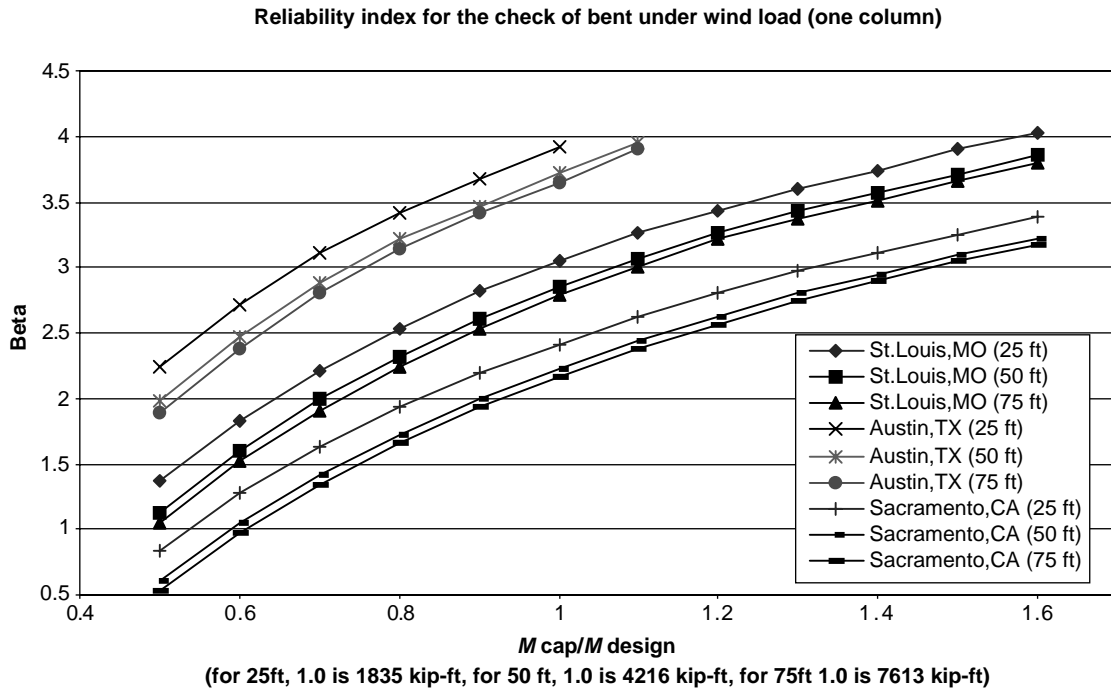


Figure 3.14. Reliability index for bending moment in one-column bent of different height under wind loads.

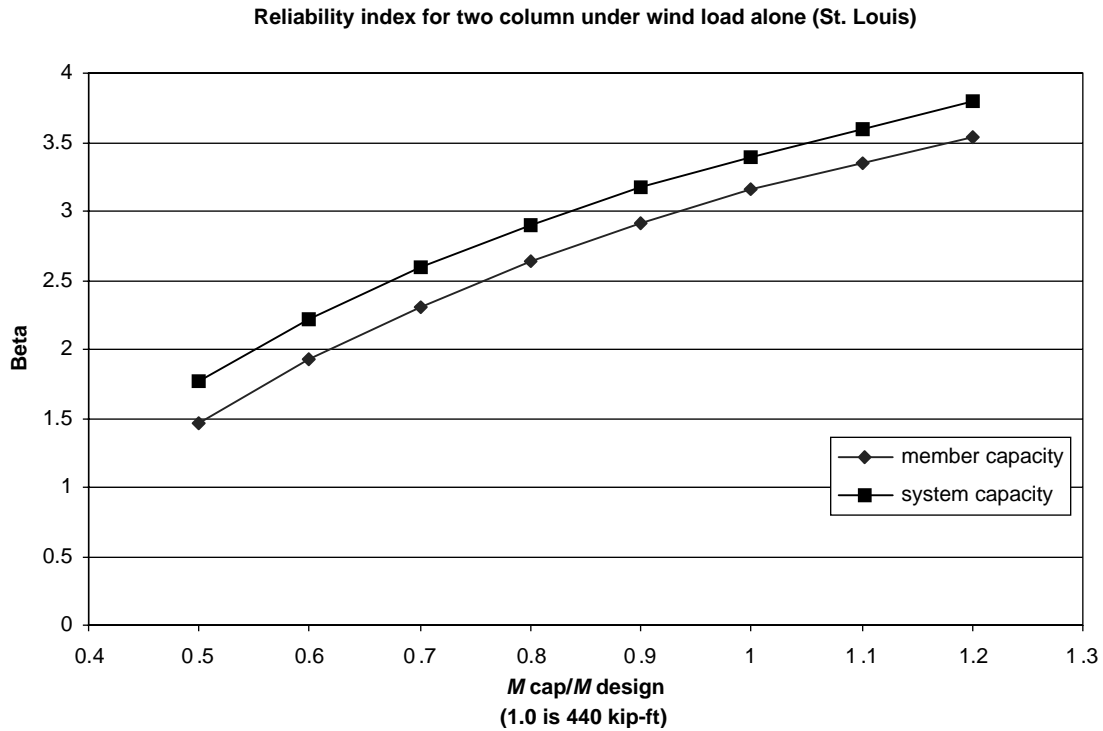


Figure 3.15. Comparison of system reliability to member reliability for two-column bent under wind load.

### 3.2.3 Reliability Analysis for Earthquake Alone

The reliability analysis of the one-column and two-column bents under earthquakes is also executed using the model described in Chapter 2 and using the free body diagrams of Figures 3.4 and 3.7 with the live load of  $F_{LL} = 0$ . For the case of earthquakes, two limit states are considered: (1) the bending of the columns of one- and two-column bents because of lateral inertial forces and (2) the overturning of the one-column bent. Referring to Figure 3.4(a) and (b), the failure functions for column bending in the one-column bent can be represented by an equation of the following form:

$$Z_6 = M_{\text{col}} + \frac{3\gamma DK_p f^2}{2} \frac{f}{3} \lambda_{\text{cyc}} - F_{EQ}(e_1 + f) \quad (3.21)$$

where

- $M_{\text{col}}$  = the column bending moment capacity,
- $F_{EQ}$  = the equivalent earthquake lateral load on the column,
- $\gamma$  = the specific weight of the soil,
- $D$  = the column diameter,
- $K_p$  = the Rankine coefficient,
- $e_1$  = the distance of  $F_{EQ}$  from the soil level,
- $f$  = the distance from the soil level to the point of maximum moment, and
- $\lambda_{\text{cyc}}$  = the model of the effect of cyclic loading on the foundation.

The distance  $f$  is calculated by setting the equivalent lateral earthquake load,  $F_{EQ}$ , equal to force,  $P_p$ , of Figure 3.4 produced from the earth pressure.

Based on Figure 3.4(a), the failure equation for overturning can be represented as follows:

$$Z_7 = \frac{3\gamma DK_p L^2}{2} \frac{L}{3} \lambda_{\text{cyc}} - F_{EQ}(e_1 + L) \quad (3.22)$$

where  $L$  is the depth of the foundation. Notice that Equation 3.22 does not consider the counter effects of the dead weights. This is because it is herein assumed that vertical accelerations caused by the earthquake may significantly reduce the contributions of the dead weight in resisting the risk for overturning.

Referring to Equations 3.21 and 3.22, failure occurs when either  $Z_6$  or  $Z_7$  are less than or equal to zero. All the variables used in Equations 3.21 and 3.22 are considered random except for the column diameter,  $D$ ; the eccentricity,  $e_1$ ; and foundation depth,  $L$ . The statistical models used to describe the random variables are provided in Tables 2.1, 2.2, and 2.6. Specifically, the equivalent lateral earthquake load,  $F_{EQ}$ , is composed of time-dependent and time-independent random variables and can be represented as follows:

$$F_{EQ} = \lambda_{EQ} C' S_a(t' T) \frac{AW}{R_m} \quad (3.23)$$

where

- $\lambda_{EQ}$  = an analysis modeling factor;
- $C'$  = the spectrum's modeling factor;
- $S_a(\cdot)$  = the spectral acceleration calculated as a function of the calculated nominal period,  $T$ ;
- $t'$  = the period's modeling factor;
- $A$  = the earthquake intensity in terms of the ground acceleration,  $g$ ;
- $W$  = the weight of the structure; and
- $R_m$  = the response modification factor.

When studying overturning, the response modification factor is  $R_m = 1.0$ , and it is deterministic. For column bending,  $R_m$  is random. The variables  $\lambda_{EQ}$ ,  $C'$ , and  $t'$  are also random.  $W$  is assumed to be deterministic although the uncertainties in estimating  $W$  are considered in  $\lambda_{EQ}$  as well as in  $t'$ . The earthquake intensity,  $A$ , is the only time-dependent random variable that varies as a function of the return period, as is described in Equations 2.11 and 2.14. The probability distribution of  $A$  is described in Figure 2.4 for five different sites. The probability of exceedance curves of Figure 2.4 are for the annual maximum earthquake intensity. The calculations performed in this report are executed for a 75-year design period in order to remain consistent with the AASHTO LRFD specifications.

The reliability analysis of one-column bent and two-column bent bridges has been performed using data from the five different sites listed in Table 2.4 and Figure 2.4. Figures 3.16 and 3.17 show the reliability index for the bending failure limit state for each of the five sites as a function of the column moment capacity for the one-column bent and the two-column bent, respectively. The abscissa of the plot is normalized such that a ratio of 1.0 indicates that the bridge is designed to exactly satisfy the proposed NCHRP Project 12-49 requirements [ATC and MCEER, 2002] with a nominal response modification factor  $R_m = 1.5$ . The design column moment capacities and foundation depths required to resist overturning are provided in Tables 3.3 and 3.9 for five different site conditions. For the purposes of this study, the bridges are subjected to earthquake input motions similar to those expected in San Francisco, Seattle, St. Paul, New York, or Memphis. The reliability analysis is then performed for each bridge configuration and for each of the five site data assuming a 75-year design life. The object is to verify whether the proposed NCHRP Project 12-49 specifications would provide reasonably uniform reliability levels for any site within the United States.

Figure 3.16 shows that the proposed NCHRP Project 12-49 specifications using a nominal response modification factor of  $R_m = 1.5$  will produce a reliability index,  $\beta$ , that varies between 2.56 and 2.88. The average from the five sites is equal to 2.78. If a response modification factor of  $R_m = 1.0$  is used (such as proposed for columns with hinges that cannot be inspected), then the reliability indexes will have an average value of 3.00 with a range of 2.80 to 3.16. These values can be observed in Figure 3.16 for an  $M_{\text{cap}}/M_{\text{design}}$  ratio of 1.50

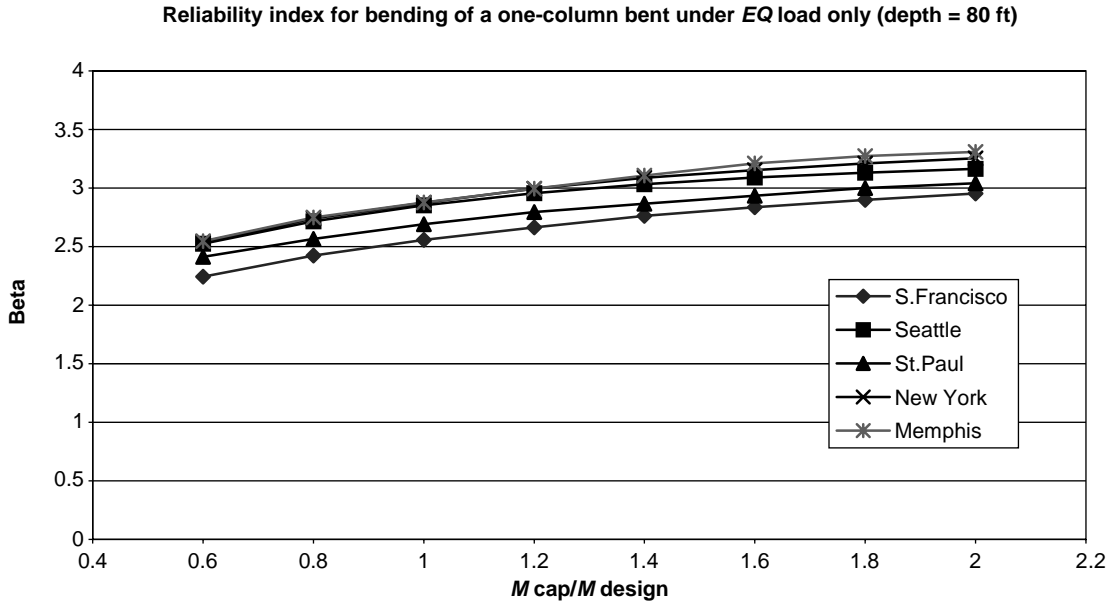


Figure 3.16. Reliability index for one-column bent under earthquakes.

because changing the nominal response modification factor will result in increasing the moment capacity by the same ratio. The small increase in the reliability index caused by the 50% change in  $M_{cap}$  reflects the high costs that would be required to produce only an incremental change in the reliability of bridges subjected to earthquakes. This is due to the fact that the uncertainties in estimating the earthquake intensities are very high.

Figure 3.17 shows that the range of the reliability indexes for the two-column bent is slightly higher than that of the one-column bent. The average reliability index for the five earthquake data is 2.82 with a minimum  $\beta$  equal to 2.70 and a maximum value equal to 2.91. Since member ductility is already taken into consideration by using the response modification factor, the reliability indexes shown in Figures 3.16 and 3.17 are for the complete system.

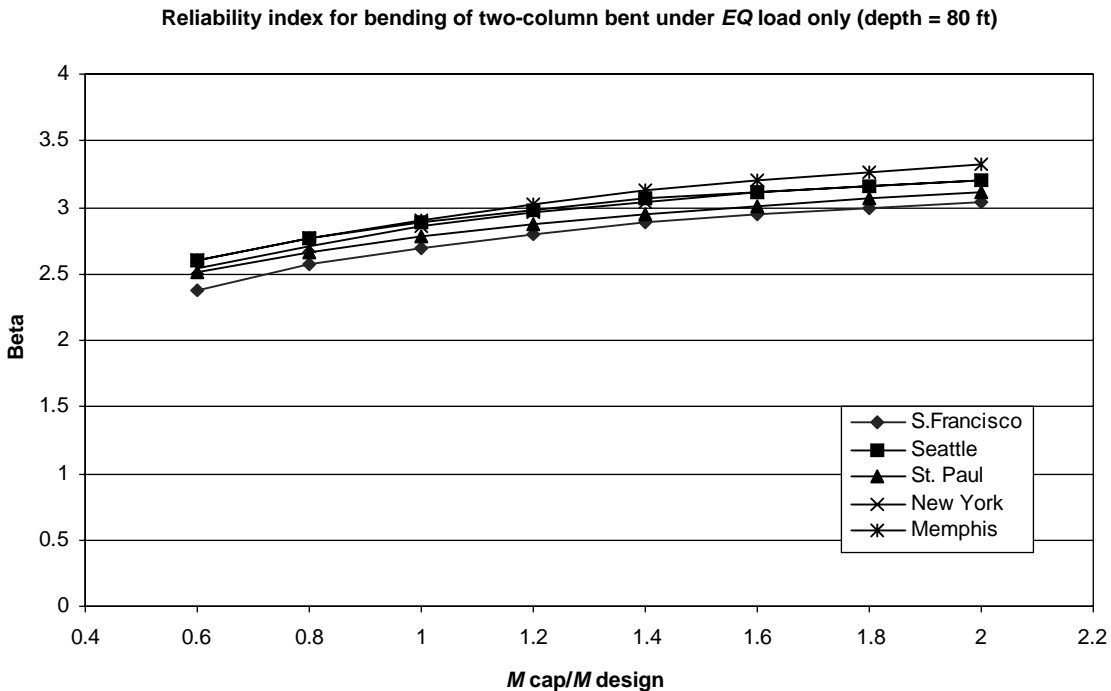


Figure 3.17. Reliability index for two-column bent under earthquakes.

The results shown in Figures 3.16 and 3.17 are for a foundation depth  $L = 24$  m (80 ft). The effect of the foundation depth on the bridge safety is illustrated in Figures 3.18 and 3.19. Figure 3.18 shows how the reliability index for the bending limit state for the one-column bent varies with foundation depth. It is noticed that the effect is negligibly small. This is due to the fact that a shallow foundation would reduce the stiffness of the system, thus increasing its natural period, which in turn leads to lower spectral accelerations and lower moments in the column. The maximum difference between

the reliability indexes for each site is less than 0.03. Similarly, it is observed that the depth of the foundation does not significantly affect the reliability index for the bending limit state of the two-column bent. The reliability indexes shown in Figure 3.19 range from a low value of 2.69 to a high of 2.95 for all foundation depths and site data.

Unlike what was observed for column bending, the depth of the foundation affects the safety of the column against overturning, as is illustrated in Figure 3.20. In Figure 3.20, the reliability index is calculated using the failure function of

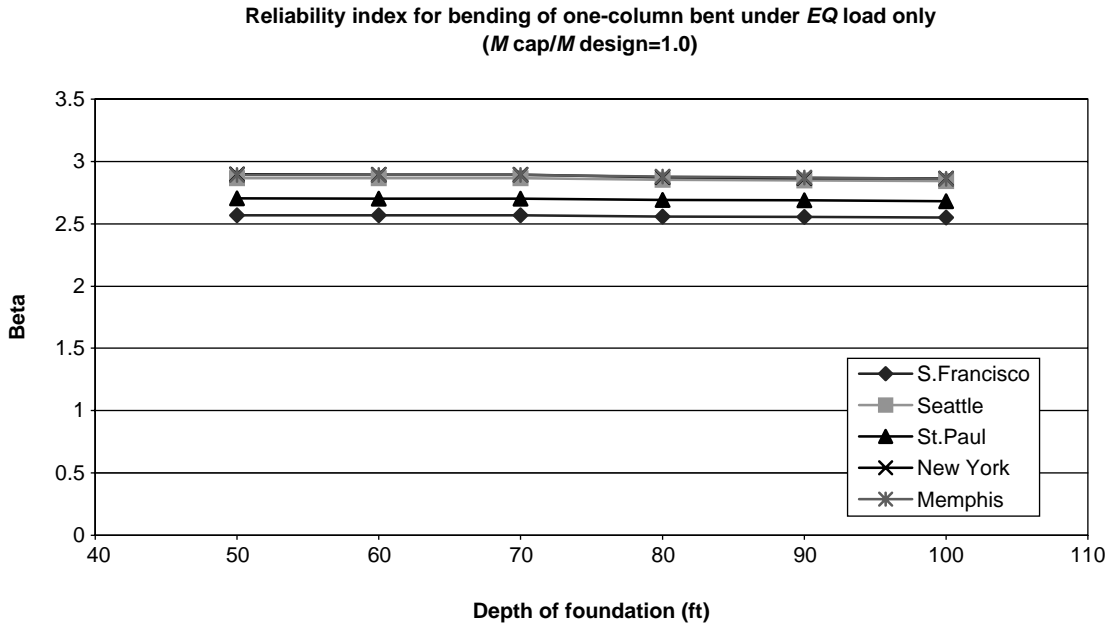


Figure 3.18. Reliability index for one-column bent under earthquakes for different foundation depths.

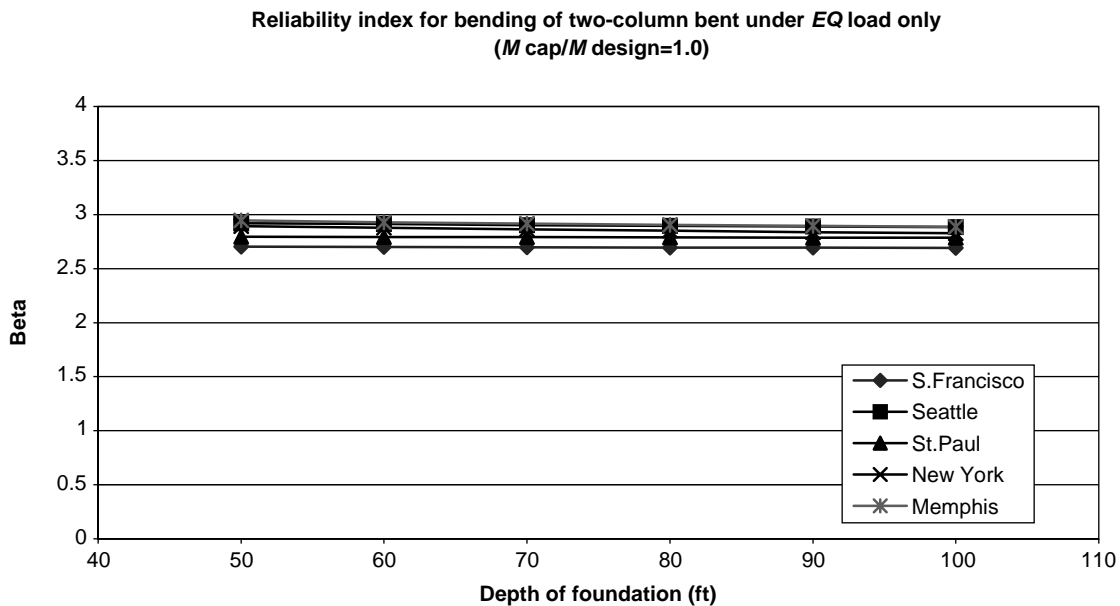


Figure 3.19. Reliability index for two-column bent under earthquakes for different foundation depths.

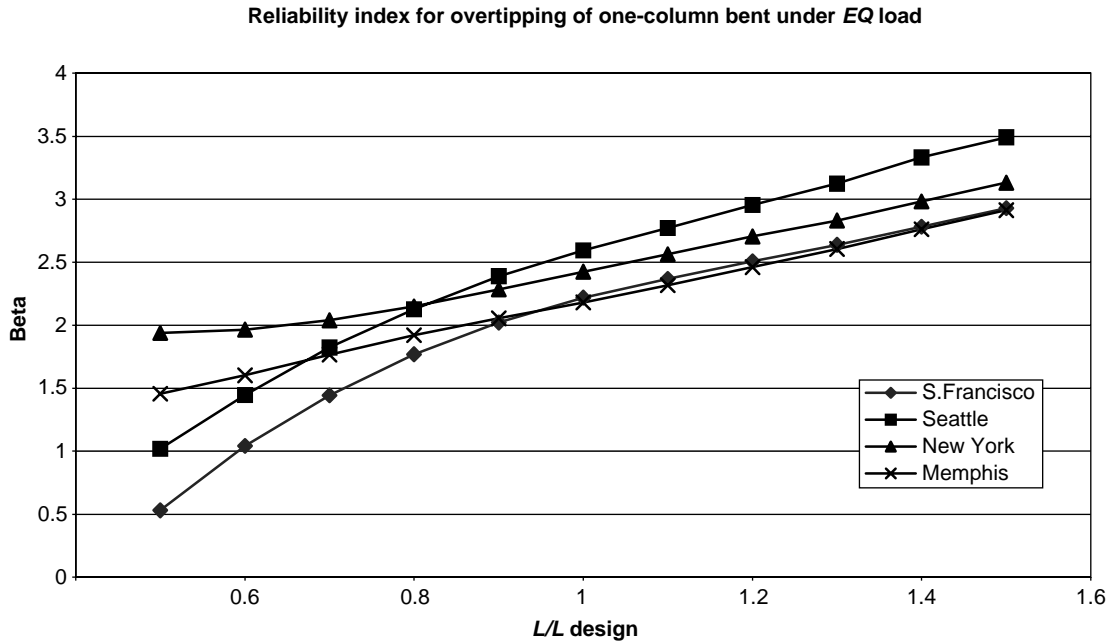


Figure 3.20. Reliability index for one-column bent for overturning caused by earthquakes.

Equation 3.22 for different values of foundation depth,  $L$ . The required design foundation depth  $L_{\text{design}}$  is given in Table 3.3 for the different site data. The results show that the effect of the foundation depth becomes significant because the shallower foundations will not be able to resist the tendency of columns to overturn under the effect of the inertial forces at the top of the column. If the column depth is designed to satisfy the requirements of the proposed specifications of NCHRP Project 12-49 (ATC and MCEER, 2002), then the reliability index will vary between 2.22 and 2.59 for the sites analyzed in this report. It is noticed that the trends of the curves for the New York and Memphis data differ from those of San Francisco and Seattle because of the shallowness of the foundations that are required in the first two cases compared with the second set. The inertial forces observed for St. Paul are so small that the probability of overturning is negligibly small. It is also noted that the results shown in Figures 3.16 through 3.19 ignore the possibility of vertical accelerations. These, according to the NCHRP Project 12-49, can be ignored except for near-field motions in which the vertical accelerations may be significant. The reliability calculations for overturning did not include the vertical earthquake accelerations, nor did they account for the counter effect of the dead weight.

The analyses performed above are based on isolating a single bent from the bridge system that is founded on an extension pile and on modeling it as an SDOF system after determining its point of fixity. The reliability analysis is performed based on a design that uses a response modification of  $R_m = 1.5$ . Appendix H performs a reliability analysis of the columns of a bridge founded on a multiple-pile foundation system when the bridge is modeled as a multidegree-of-freedom (MDOF)

system. In this case, the bridge columns were designed using a design response modification factor  $R_m = 6.0$  as recommended by NCHRP Project 12-49. The results of the analysis described in Appendix H demonstrate the following points:

1. The simplified analysis using an SDOF system as performed in this section yields values for the reliability index,  $\beta$ , that are consistent with those obtained from the more advanced multimodal structural analysis.
2. The use of a response modification factor  $R_m = 6.0$  for bridge columns associated with the 2,500-year NEHRP spectrum produces system reliability index values on the order of 1.75, which is considerably lower than the 2.82 average value observed for multicolumn systems with members designed using  $R_m = 1.5$ . The 1.75 value that is for system safety is much lower than the member reliability equal to 3.5 that is used as the basis for calibrating the LRFD code for members under gravity loads.

In summary, large differences in the reliability indexes are observed for the different components of bridge subsystems subjected to seismic events. For example, the foundation systems produce much higher reliability index values than the bridge columns do. This difference has been intentionally built into the bridge seismic design process by seismic design code writers in order to account for the consequences of the failure of different members. However, the difference is rather large, producing a reliability index close to  $\beta = 3.0$  when a response modification factor equal to  $R_m = 1.0$  is used to about  $\beta = 1.75$  when a response modification factor  $R_m = 6.0$  is used during the design process. It is noted that the use

of a response modification  $R_m = 1.0$  implies a design based on the elastic behavior of members while a value of  $R_m = 6.0$  accounts for the plastic behavior of bridge columns. These differences, however, will not affect the results of the calibration of load factors for combinations of extreme events that include earthquakes as long as the target reliability level used during the calibration is based on the reliability index obtained when earthquakes alone are applied on the bridge. This point will be further elaborated upon in Section 3.3.1.

### 3.2.4 Reliability Analysis for Scour Alone

The scour model described in Chapter 2 can be used in a Monte Carlo simulation program to find the probability that the scour depth in a 75-year period will exceed a given value  $y_{CR}$ . In this case, the failure function is given as follows:

$$Z_8 = y_{CR} - y_{SC} \tag{3.24}$$

The scour depth,  $y_{SC}$ , for rounded piers set in non-cohesive soils is calculated from

$$\ln y_{\max} = -2.0757 + 0.6285 \ln D + 0.4822 \ln y_0 + 0.6055 \ln V + \varepsilon \tag{3.25}$$

where

- $D$  = the pier diameter,
- $y_0$  = the flow depth,
- $V$  = the flow velocity, and
- $\varepsilon$  = the residual error.

As explained in Chapter 2,  $D$  is a deterministic variable because the pier diameter can be accurately known even before the actual construction of the bridge;  $y_0$  and  $V$  are random variables that depend on Manning’s roughness coefficient,  $n$ , and the 75-year maximum discharge rate, which are random variables having the properties listed in Table 2.9. Based on the analysis of the residuals affected in Appendix I,  $\varepsilon$  may be considered to follow a normal distribution with mean equal to zero and a standard deviation equal to 0.406. The flow depth,  $y_0$ , and velocity,  $V$ , are calculated from the geometry of the channel (which is assumed to be deterministic), from the Manning roughness coefficient ( $n$ ), and from the hydraulic discharge rate ( $Q$ ) using the relationships provided in Section 2.4.4 of Chapter 2. In addition, the estimation of the discharge rate will be associated with statistical uncertainties represented by a statistical modeling random variable,  $\lambda_Q$ . The pertinent random variables and their properties are listed in Table 2.9 of Chapter 2. Only the discharge rate,  $Q$ , is a time-dependent random variable as it increases with longer return periods. Given the cumulative distribution for the maximum 1-year discharge rate,  $Q$ , the probability distribution can be calculated for different return periods using Equation 2.14. In the calculations performed in this report, a 75-year return period is used in order to remain compatible with the AASHTO LRFD. The calculations are executed for the discharge data from the five sites listed in Table 2.8.

The probability that  $y_{SC}$  will exceed a critical scour depth,  $y_{CR}$ , is calculated for different values of  $y_{CR}$  as shown in Figure 3.21 for the one-column pier for hydraulic discharge data collected from five different rivers. Figure 3.22 gives the same results for the two-column pier. The differences between

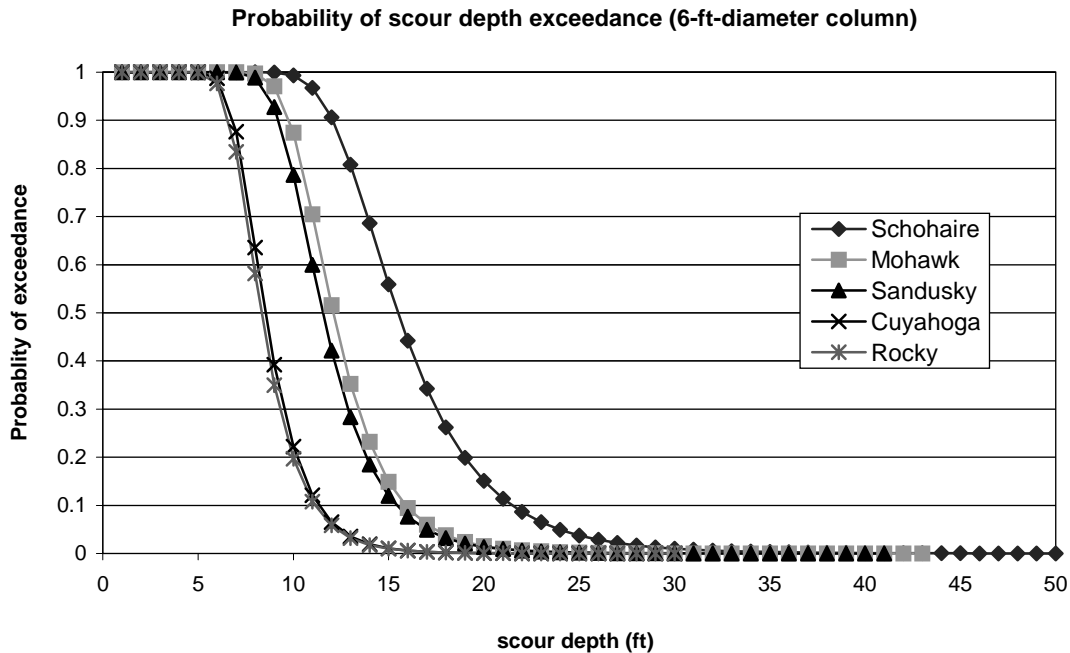


Figure 3.21. Probability that actual scour will exceed critical depths for 6-ft-diameter column.

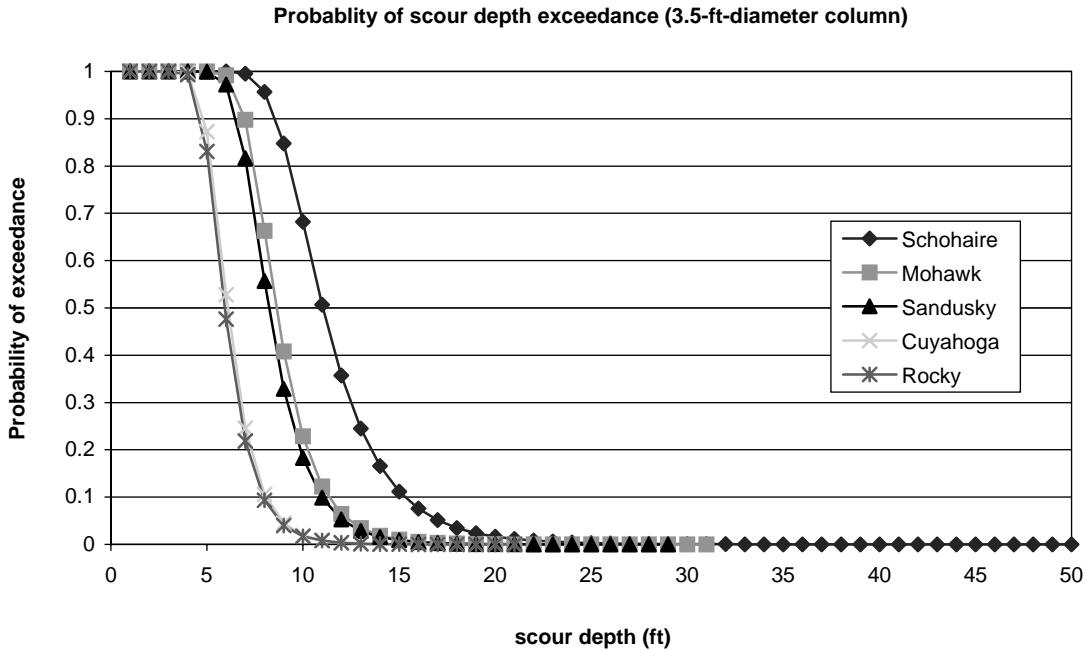


Figure 3.22. Probability that actual scour will exceed critical depths for 3.5-ft-diameter column.

the results of the two figures are due to the influence of the column diameter,  $D$ , in Equation 3.25.

Figures 3.23 and 3.24 show the reliability index,  $\beta$ , versus the normalized critical foundation depth such that a factor of 1.0 indicates that the foundation is designed to exactly satisfy the foundation depth requirement of HEC-18 for each of the river data considered. The safety of bridges against

scour is expressed in terms of the reliability index,  $\beta$ , that is obtained from

$$P_f = \Phi(-\beta) \tag{3.26}$$

where, in this case, the probability of failure  $P_f$  is the probability that the scour depth,  $y_{sc}$ , will exceed the design scour

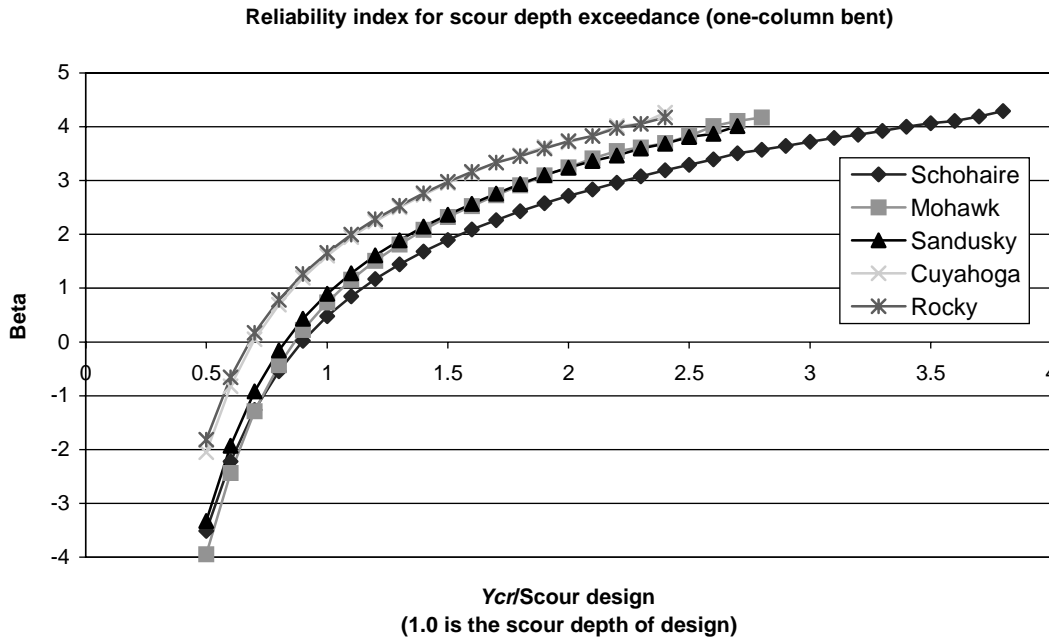


Figure 3.23. Reliability index for scour at different critical depths for  $D = 6$  ft.

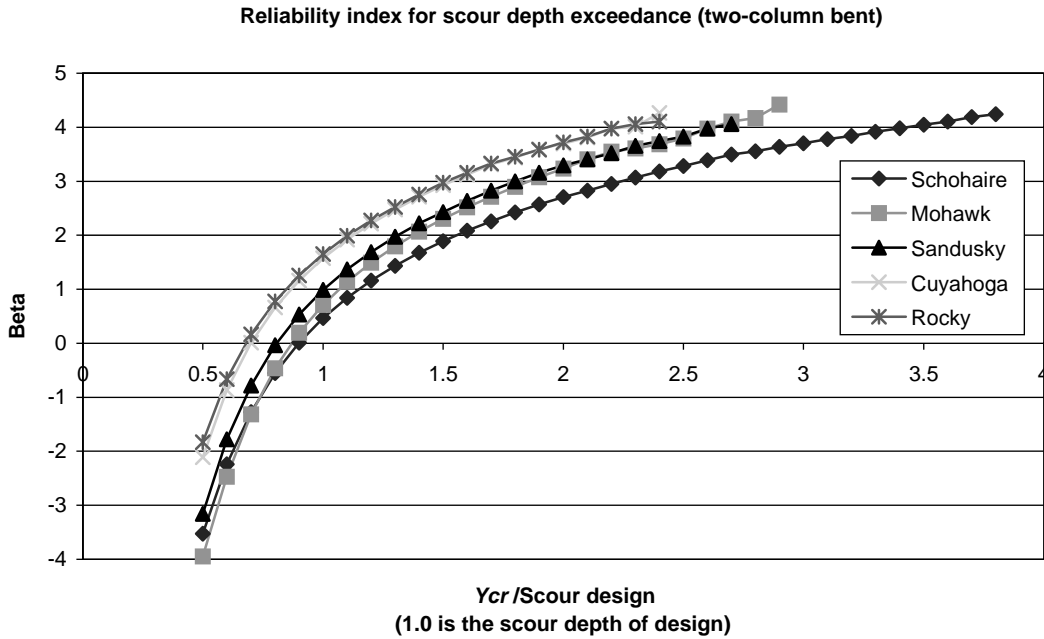


Figure 3.24. Reliability index for scour at different critical depths for  $D = 3.5$  ft.

depth.  $\Phi$  is the standard Gaussian cumulative distribution function.

The results shown in Figures 3.23 and 3.24 demonstrate that the HEC-18 method provides varying degrees of reliability for the different river data analyzed. The results of the simulation are also summarized as shown in Tables 3.12 and 3.13 for the five rivers. The two tables show the average 75-year discharge rate and the COV for the 75-year discharge rate for the one- and two-column bents. They also show the 75-year maximum scour depth along with its COV. These are com-

pared with the design scour depths as calculated from Equation 2.22 and listed in Tables 3.4 and 3.10.

The results in Tables 3.12 and 3.13 show that the reliability index,  $\beta$ , implied in current scour design procedures varies from about 0.47 to 1.66 with an average value of 1.08. These values are much lower than  $\beta = 3.5$ , which is the reliability index used as the basis for the calibration of the load factors for the combination of live and dead loads in the AASHTO LRFD specifications. Also, the target  $\beta = 3.5$  is for member reliability while a foundation failure caused by scour will generally lead to the collapse of the complete system. The

TABLE 3.12 Summary of simulation results for one-column pier

River	Average $Q_{75yr}$ ( $Q$ for 75 years) (ft <sup>3</sup> /sec)	COV of $Q_{75yr}$	Average $y_{s75}$ (max. scour depth in 75 yrs)	COV of $y_{s75}$	Design depth (ft)	Reliability index, $\beta$
Schohaire	85,000	29%	16.3	25%	17.3	0.48
Mohawk	34,000	12%	12.6	21%	14.0	0.73
Sandusky	38,000	18%	12.0	22%	14.3	0.90
Cuyahoga	20,000	16%	8.88	21%	12.3	1.60
Rocky	21,000	19%	8.68	22%	12.3	1.66

TABLE 3.13 Summary of simulation results for two-column pier

River	Average $Q_{75yr}$ ( $Q$ for 75 years) (ft <sup>3</sup> /sec)	COV of $Q_{75yr}$	Average $y_{s75}$ (max. scour depth in 75 yrs)	COV of $y_{s75}$	Design depth (ft)	Reliability index, $\beta$
Schohaire	85,000	29%	11.6	25%	12.3	0.47
Mohawk	34,000	12%	8.95	21%	9.93	0.71
Sandusky	38,000	18%	8.57	22%	10.2	0.99
Cuyahoga	20,000	16%	6.33	21%	8.70	1.57
Rocky	21,000	19%	6.18	22%	8.75	1.65

results show that the rivers with lower discharge rates have higher reliability levels than do those with the higher discharge rates. This confirms the observation made in Appendix I that the “design” scour depths as calculated from the HEC-18 equations give different levels of safety (or bias) when compared with observed scour depths with the safety level decreasing as the observed scour depth increases. In addition, the low overall reliability level observed for foundations designed to exactly satisfy the HEC-18 equations imply that although the scour design equation involves a safety factor equal to 2.0 (the first term in Equation 2.30), the large differences between the observed scour depths and those predicted (see Figure 2.10) lead to an overall low reliability index for scour as compared with the reliability index for bridge structural members. Based on this observation, it is recommended that a revision of current scour design procedures be initiated in order to improve our ability to predict the depth of scour and to increase the safety levels of bridges that may be subject to foundation erosion caused by scour. An increase in the safety levels for scour design is also justified based on the observation by Shirole and Holt (1991), who have reported that a majority of the bridges that have failed in the United States and elsewhere have failed because of scour. In fact, Shirole and Holt state that over a 30 year-period, more than 1,000 of the 600,000 U.S. bridges have failed and that 60% of these failures are due to scour. This would constitute a failure rate of 0.001 in 30 years, or 0.0025 failures in 75 years. However, since many of the U.S. bridges are not founded in water channels, the data reported by Shirole and Holt indicate a very high probability of failure for bridges founded in water channels. If one guesses that 12,500 bridges are exposed to scour, then the rate of failure would be about 12%. A reliability index of about 1.10 would mean a probability of failure of roughly 13.6% in 75 years.

Tables 3.14 and 3.15 give the additional load factor that should be applied on the scour design equation in order to produce different values of the reliability index when Equation 2.22 is used to determine the design scour depth. According to this approach, the results for  $y_{\max}$  obtained from Equation 2.22 should be further multiplied by an additional load factor to produce reliability index values compatible with those observed with the other extreme events studied in this

**TABLE 3.14 Design scour depths required for satisfying different target reliability levels for one-column pier**

Target index	$\beta = 3.5$		$\beta = 3.0$		$\beta = 2.5$	
	Depth	Load factor	Depth	Load factor	Depth	Load factor
River						
Schohaire	46.5	2.69	38.6	2.23	32.0	1.85
Mohawk	30.2	2.16	25.9	1.85	22.3	1.59
Sandusky	31.9	2.23	26.3	1.84	22.5	1.57
Cuyahoga	22.4	1.82	18.8	1.53	16.0	1.30
Rocky	22.5	1.83	18.6	1.51	15.9	1.29
<i>Average</i>		<i>2.15</i>		<i>1.79</i>		<i>1.52</i>

**TABLE 3.15 Design scour depths required for satisfying different target reliability levels for two-column pier**

Target index	$\beta = 3.5$		$\beta = 3.0$		$\beta = 2.5$	
	Depth	Load factor	Depth	Load factor	Depth	Load factor
River						
Schohaire	33.5	2.72	27.6	2.24	22.8	1.85
Mohawk	21.4	2.16	18.5	1.86	15.9	1.60
Sandusky	22.2	2.18	18.4	1.80	15.6	1.53
Cuyahoga	16.0	1.84	13.4	1.54	11.4	1.31
Rocky	16.0	1.83	13.2	1.51	11.3	1.29
<i>Average</i>		<i>2.15</i>		<i>1.79</i>		<i>1.52</i>

report. For example, if a target reliability index of  $\beta_{\text{target}} = 3.50$  is desired, then the design scour depth that should be used when designing bridge foundations for scour should be equal to 2.15 times the value calculated from Equation 2.22. It is noted that two of the rivers selected have relatively low discharge volumes, two rivers have average discharge volumes and only one river has a relatively high discharge volume. If a weighted average is used, then a factor of 2.24 should be used rather than the 2.15 calculated above.

On the other hand, if a reliability index of  $\beta_{\text{target}} = 2.50$  is to be used as the target index for the design of bridge foundations for scour, then the average load factor should be equal to 1.52 while the weighted average would be 1.57. For a target of  $\beta_{\text{target}} = 3.00$ , the average load factor is 1.79 while the weighted average would be 1.87. It is important to note that significant differences are observed in the load factors calculated from different sites. On the other hand, no difference is observed for different column diameters. Sensitivity analyses performed in Appendixes C and D have also shown that variations in the shape and geometry of the water channel do not seem to influence the reliability index value significantly. Some of the other extreme events have shown lower average reliability indexes than 3.5. For example, wind loads have an average reliability index value on the order of 3.12 for the 25-ft-high columns, and the reliability index for the failure of columns in bending to ship collisions is found to be on the order of 2.78. Hence, for the sake of keeping the safety levels relatively uniform for the different extreme events considered, it would be justified to use a target reliability index of 3.0 for scour. It is noted that the reliability calculations for seismic events produced a reliability index even lower than those of the other events. However, as mentioned earlier, the costs associated with increasing the safety level for earthquake effects have prevented the use of the higher safety levels for earthquakes. Because the AASHTO LRFD specifications are primarily directed toward short- to medium-span bridges, which are normally set over small rivers with relatively low discharge rates, it is herein concluded that the use of a scour factor on the order of  $\gamma_{sc} = 2.00$  would provide reliability levels slightly higher than the 3.0 target that is similar to the average reliability index observed for the other extreme events. The 2.00 value proposed herein is a rounded up value to the 1.87 value calculated above.

**3.2.5 Reliability Analysis For Vessel Collision Forces**

The reliability analysis of the one-column and two-column bents is also executed for vessel collision forces following the model described in Section 2.4.5 of Chapter 2. Using the free body diagram of Figure 3.4(b) and a force of  $F_2 = F_{CV}$  where  $F_{CV}$  is the vessel collision force, two limit states are considered: (1) the bending of the columns of one- and two-column bents because of lateral collision force and (2) the shear failure of the impacted column. Referring to Figure 3.4(b), the failure function for column bending in the one-column bent can be represented by an equation of the form

$$Z_9 = M_{col} + \frac{3\gamma DK_p f^2}{2} \frac{f}{3} \lambda_{cyc} - F_{CV}(e_2 + f) \quad (3.27)$$

where

- $M_{col}$  = the column bending moment capacity,
- $F_{CV}$  = the vessel collision force on the column,
- $\gamma$  = the specific weight of the soil,
- $D$  = the column diameter,
- $K_p$  = the Rankine coefficient,
- $e_2$  = the distance of  $F_{CV}$  from the soil level,
- $f$  = the distance from the soil level to the point of maximum moment, and
- $\lambda_{cyc}$  = the model of the effect of cyclic loading on the foundation.

The distance  $f$  is calculated by setting the equivalent vessel collision force,  $F_{CV}$ , equal to the force from the soil pressure

on the foundation,  $P_p$ , of Figure 3.4 produced from the earth pressure. For shearing failure of the column, the failure function is as follows:

$$Z_{10} = V_{col} - F_{CV} \quad (3.28)$$

where  $V_{col}$  is the shearing capacity. The vessel collision force is calculated from

$$F_{CV} = x w P_B \quad (3.29)$$

where  $x$  is the vessel collision modeling factor, and  $w$  is a factor that accounts for the statistical modeling of the calculated impact force,  $P_B$ . All the variables listed in Equations 3.27 through 3.29 are random except for the column diameter,  $D$ , and the distance,  $e_2$ . The statistical properties for all the random variables are listed in Tables 2.1, 2.2, and 2.12.  $P_B$  is the only time-dependent variable. The cumulative probability distribution of the maximum value of  $P_B$  in 1 year is provided in Figure 2.13 of Chapter 2. The calculations executed in this report are for a 75-year return period. The probability distribution for a 75-year return period for  $P_B$  is found by using Equation 2.14.

The results of the reliability calculations are shown in Figures 3.25 and 3.26. As shown in Figure 3.25, the reliability index for shearing failure of the column is calculated to be 3.15 when the column is designed to exactly meet the requirement of the AASHTO LRFD specifications for vessel collisions. A 10% increase in the column shearing capacity will increase the reliability index by 0.35, leading to a reliability index of 3.5. This demonstrates that it would not be very

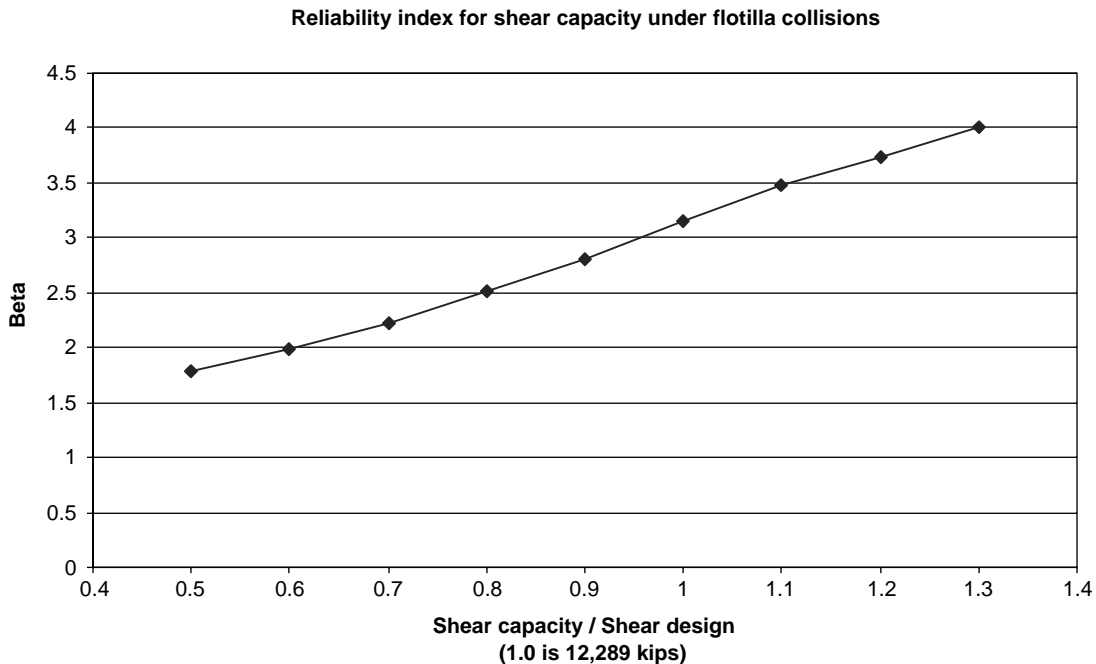


Figure 3.25. Reliability index for shearing failure caused by vessel collisions.

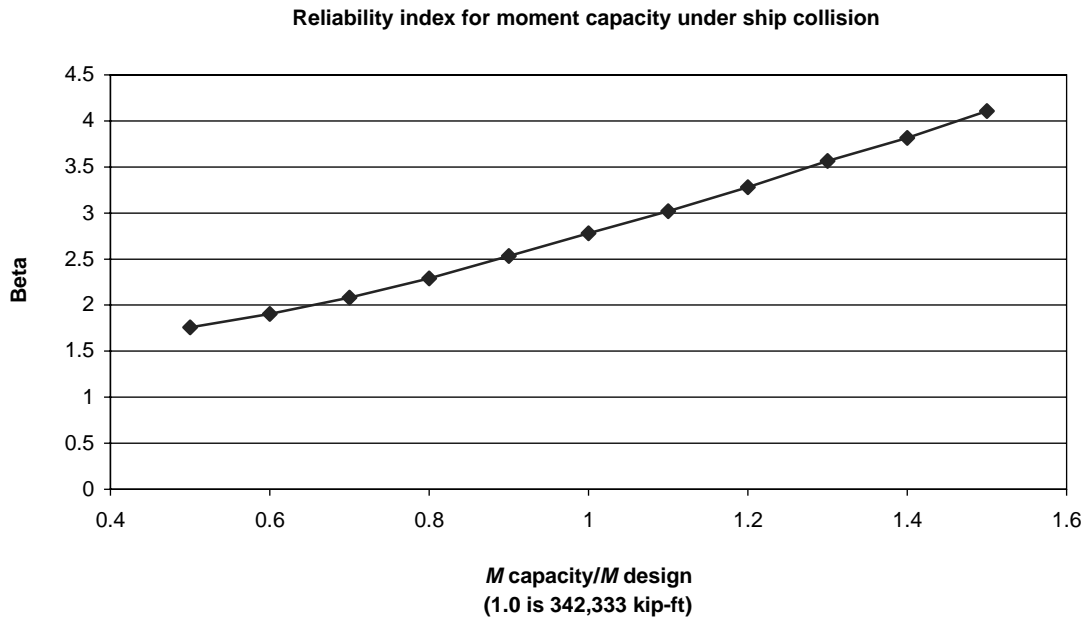


Figure 3.26. Reliability index for bending failure caused by vessel collisions.

costly to increase the target reliability level for shearing failures caused by vessel collisions. For column bending (see Figure 3.26), the reliability index is found to be equal to 2.78 if the column is exactly designed to satisfy the AASHTO LRFD specifications. A 10% increase in the column moment capacity will lead to a 0.24 improvement in  $\beta$ . The lower reliability index for moment failures is due to the inherent biases and conservatism implied in the shear design equations.

The reliability calculations executed in this section for each of the extreme events will be used in Section 3.3 to determine the target reliability levels and, subsequently, the load factors for the combination of extreme events.

### 3.3 RELIABILITY ANALYSIS FOR COMBINATIONS OF EXTREME EVENTS AND CALIBRATION OF LOAD FACTORS

This section presents the results of the reliability analysis executed for combinations of extreme events. The results are also used to perform the calibration of the load factors for combinations of events. Specifically, the section studies the following combinations:

1. Combinations involving live loads:
  - Earthquakes, *EQ*, and live loads, *LL*;
  - Wind loads, *WS*, plus live loads, *LL*;
  - Scour, *SC*, and live loads, *LL*.
2. Combinations involving scour:
  - Earthquakes, *EQ*, and scour, *SC*;
  - Wind loads, *WS*, plus scour, *SC*;

- Collision of vessels and scour, *SC*, in addition to the case of live load plus scour addressed earlier.
- 3. Combinations involving vessel collision forces:
  - Wind loads, *WS*, plus vessel collision forces, *CV*;
  - Wind loads, *WS*, plus collision of vessels, *CV*, and scour, *SC*.

Because the results obtained in Section 3.2 have shown very little difference between the reliability indexes of two-column bents and one-column bents when these columns are designed to satisfy the same AASHTO LRFD specifications, this section will concentrate on studying the reliability of one-column bents.

#### 3.3.1 Combination of Earthquakes and Live Loads (*EQ + LL*)

The single-column bent described in Figure 3.1 is analyzed to illustrate how the combined effects of earthquake and live loads will affect the bent's reliability. The data from the five earthquake sites with probability distribution curves described in Figure 2.4 are used. The live load data are obtained from the models developed by Nowak (1999) under NCHRP Project 12-33 as described in Section 2.4.1 (Table 2.3). The reliability calculations follow the Ferry-Borges model described in Section 2.5. The following conservative assumptions are made:

- All earthquakes last 30 sec ( $\frac{1}{2}$  min), during which time the moment at the base of the column remains at its highest value. The intensity of the earthquake response is constant as shown in Figure 2.15 for the  $\frac{1}{2}$ -min duration of the earthquake.

- The number of earthquakes expected in 1 year are 8 for the San Francisco site data, 2 for Seattle, 0.50 for Memphis, 0.40 for New York, and 0.01 for St. Paul. This means that the expected number of earthquakes in a 75-year return period in San Francisco will be 600, 150 earthquakes for Seattle, 38 in Memphis, 30 in New York, and 1 in St. Paul.
- The probability distribution of the maximum yearly earthquake may be used to find the probability distribution for a single event using Equation 2.14.
- The live load model for the applied vertical load has the same biases as those provided in Table B-16 of Nowak's report (1999) for the mean maximum negative moments of two equal continuous spans. Particularly, the results provided by Nowak for the 80-ft spans are used as the basis for the calculations. These results show that for each one-lane loading event, the load effect is on the average 0.79 times the load effect obtained from the HL-93 loading configuration of the AASHTO LRFD specifications for one lane of traffic with a COV of 10%. For two lanes, the average load effect is 1.58 times the effect of one lane of HL-93 with a COV of 7%. These results assume 1,000 single-lane heavy truck events in 1 day and 67 two-lane truck events in 1 day based on the assumptions of Nowak (1999) and Moses (2001).
- Equation 2.11 is used to find the probability distribution of the live load for different return periods. In particular, the live load for a  $t = 1/2$  min period is calculated for combination with the earthquake load effects when an earthquake is on.
- The effects of each earthquake are combined with the effects of the  $1/2$  min live load magnitude and projected to provide the maximum expected combined load in the 75-year bridge design life period using the Ferry-Borges model described in Section 2.5. The calculations account for the cases in which the earthquake occurs with the  $1/2$  min live load and the cases in which the live load arrives when no earthquake is on (which constitute most of the time).
- The reliability calculations are executed for a column bending failure limit state.
- The reliability calculations account for the uncertainties associated with predicting the  $EQ$  intensity, estimating the bridge response given an  $EQ$  intensity, the uncertainty in projecting the live load magnitude, and the uncertainty in estimating the column capacities.
- The failure equation for bending of the column under the combined effect may be represented as follows:

$$Z = M_{col} + \frac{3\gamma DK_p f^3}{6} - M_{EQ+LL,75} \quad (3.30)$$

where

$M_{col}$  = the column's moment capacity;  
 $\gamma$  = the specific weight of the soil;

$D$  = the column diameter;

$K_p$  = the Rankine coefficient;

$f$  = the distance below the soil level at which point the maximum bending moment occurs; and

$M_{EQ+LL,75}$  = the applied moment caused by the combined effects of the live load,  $LL$ , and the earthquake load,  $EQ$ , in a return period of  $T = 75$  years.

The maximum effect of the combined load can be represented as follows:

$$M_{EQ+LL,75} = \max \left\{ \begin{array}{l} \max_{n_1} [c_{EQ}A + \max_{n_2} [c_{LL}I_{LL}]] \\ \max_{n_3} [c_{LL}I_{LL}] \end{array} \right\} \quad (3.31)$$

where

$n_1$  = the number of earthquakes expected in a 75-year period;

$n_2$  = the number of live loads expected in a  $1/2$  min period;

$n_3$  = the number of live load events expected in a period equal to 75 years minus the times when an earthquake is on (i.e.,  $n_3$  = number of live load events in 75 years  $- n_1 \times 1/2$  min, which is almost equal to the number of truck events in 75 years);

$A$  = the earthquake intensity for one event;

$I_{LL}$  = the intensity of the live load for one event; and

$c_{EQ}$  and  $c_{LL}$  = the analysis coefficients that convert the earthquake intensity and the live load intensity to moment effects (e.g., Equations 3.16 and 3.17 show how to convert the intensity of the live load into a moment effect, and Equations 3.22 and 3.23 show how to convert the intensity of the earthquake acceleration into a moment effect).

The results of the reliability analysis are provided in Figure 3.27 for the San Francisco earthquake data for different values of the column capacity to resist applied bending moment. The results obtained by considering the reliability of the bridge structure when only earthquakes are considered—that is, by totally ignoring the effects of live loads—are also illustrated in Figure 3.27. The plot illustrates how, for this site, the effects of earthquakes dominate the reliability of the bridge when subjected to the combined effects of live loads and earthquakes. The results for the San Francisco site, as well as results for the other sites, are summarized in Table 3.16. As an example, if the bridge column is designed to satisfy the proposed revised AASHTO LRFD specifications (the seismic provisions)

Reliability index for one column under EQ and live load (San Francisco)

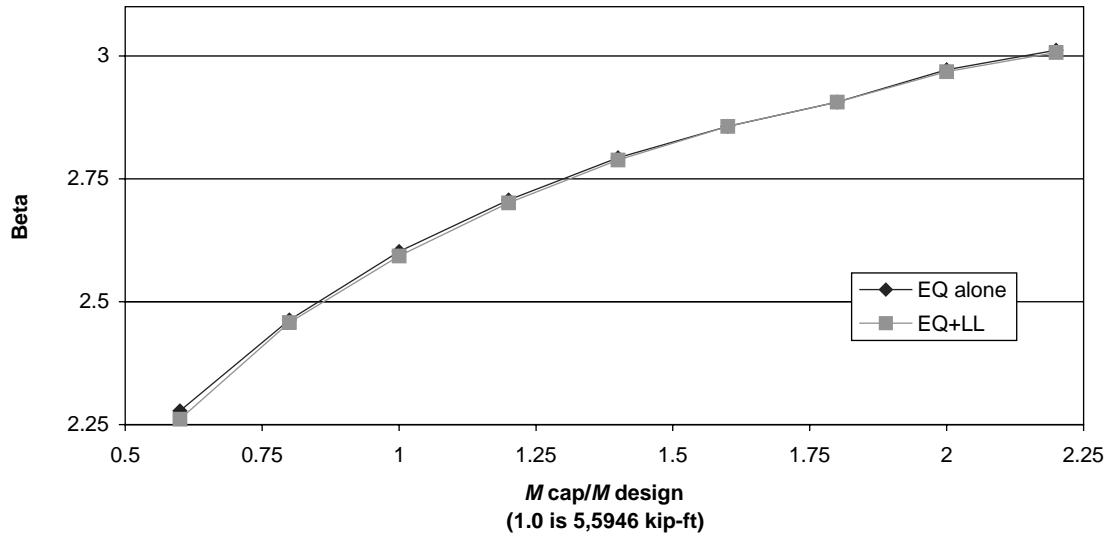


Figure 3.27. Reliability index for moment capacity under earthquakes plus live loads (San Francisco).

developed under NCHRP Project 12-49 (ATC and MCEER, 2002), then the required moment capacity for the drilled column shaft using a 2,500-year earthquake return period and a response modification factor equal to  $R_m = 1.5$  will be  $M_{cap} = M_{design} = 76$  MN-m (55,950 kip-ft). This will produce a reliability index (for a 75-year bridge design life) equal to  $\beta = 2.60$  if no live load is considered. If one considers that a live load may occur within the  $\frac{1}{2}$  min when an earthquake is actively vibrating the bridge column, then the reliability index for the 76 MN-m column reduces to  $\beta = 2.59$ . The reduction is small. However, if one wishes to increase the reliability index from 2.59 back to the original 2.60, then the moment capacity of the column should be increased. By interpolation, the moment capacity that will produce a reliability index equal to  $\beta = 2.60$  when both earthquake loads and live loads are considered should be  $M_{cap} = 77$  MN-m (56,840 kip-ft) or an increase of 1207 kN-m (890 = 56,840 – 55,950 kip-ft).

The  $M_{design}$  value 76 MN-m (55,950 kip-ft) includes the effect of the resistance factor for bending,  $\phi = 0.90$ . The moment calculated from the applied earthquake force is equal to  $M_{EQ} = 68$  MN-m (50,355 kip-ft). Also, the applied live load from the HL-93 live loading will produce a moment in

the column equal to  $M_{LL} = 4,100$  kN-m (3,048 kip-ft). The live load factor that should be used for the combination of earthquakes and live load should be determined such that

$$\phi M_{req} = \gamma_{EQ} M_{EQ} + \gamma_{LL} M_{LL} \tag{3.32}$$

or

$$0.90 M_{req} = \gamma_{EQ} 68 \text{ MN-m} + \gamma_{LL} 4100 \text{ kN-m.}$$

The calibration of the load combination factor involves the determination of the values of  $\gamma_{EQ}$  and  $\gamma_{LL}$  needed to produce the required column moment capacity  $M_{req} = 77$  MN-m (56,840 kip-ft). If the value for  $\gamma_{EQ}$  is preset at 1.0, then  $\gamma_{LL}$  is calculated to be equal to 0.26. Many other options are available to reach the required 77 MN-m (56,840 kip-ft). However, in this example, it is assumed that the load factor for the moment obtained from the analysis of the earthquake effects is always equal to  $\gamma_{EQ} = 1.0$ . It is noted that in the examples solved in this section, the dynamic properties of the bridge system—particularly, the mass of the system—are not altered because of the presence of live load. The presence of live

TABLE 3.16 Summary of live load factors for combination of EQ plus LL.

Site	$M_{req}$ (kip-ft)	$M_{EQ}$	$M_{LL}$	$\gamma_{LL}$ for LL+EQ
San Francisco	56,840	50,351	3,048	0.26
Seattle	28,855	25,488	3,048	0.16
Memphis	21,597	18,945	3,048	0.17
New York	7,285	5,830	3,048	0.24
St. Paul	4,826	1,503	3,048	0.93
Average				0.21

loads on the bridge will increase the mass applied on the structure. However, since the vehicles may slide because of the effect of the earthquake, not all the mass will actually be active. Hence, the results shown in Table 3.16 assume that the mass of the system remains essentially constant despite the presence of the live load. A sensitivity analysis is performed further below to check the effect of this assumption on the final results.

Similar calculations are executed for all the five sites analyzed in this report—namely, San Francisco, Seattle, Memphis, New York, and St. Paul. The results from the five sites are summarized in Table 3.16. Notice that for all the sites considered except for St. Paul, the live load factor remains below 0.26 with an average value of 0.21. Based on the results shown in Table 3.16, it would seem appropriate to recommend that a live load factor of  $\gamma_{LL} = 0.25$  associated with an earthquake factor of  $\gamma_{EQ} = 1.00$  be used to account for the combination of live loads and earthquake loads for typical bridge bents supporting medium-span bridges. These proposed load factor values are on the lower side of the range of  $\gamma_L = 0.25$  to 0.50 proposed by Nowak (1999) for heavy traffic sites (annual daily truck traffic = 5,000 trucks per day or 1,000 heavy trucks per day). Nowak suggests that lower values should be used for sites with low traffic volume and longer span lengths. (It is noted that only a range of values and no specific values are provided in the preliminary work of Nowak [1999].) Longer spans will produce lower live load factors, because as the span length increases, the mass of the bridge becomes dominant compared with the applied live loads and the contributions of the live loads become less significant. Assuming that all other parameters remain constant, a higher mass will produce higher dynamic forces.

The results for the St. Paul site, which produces a load factor  $\gamma_{LL} = 0.93$ , are removed from consideration because for this site, the live load dominates the design. In fact, if the bridge is designed for live loads alone, the required moment capacity is 8 MN-m (5,927 kip-ft), which is higher than the moment capacity required to produce a reliability index of 2.88 for the combined effects of earthquakes and live loads.

The analysis performed above ignored the effect of the truck's mass on the dynamic response of the bridge system. This assumption is justified because the truck is not rigidly attached to the structure. However, the existence of friction between the truck tires and the bridge deck may require that at least a portion of a truck's mass would contribute to changing the dynamic properties of the system. Because, to the knowledge of the authors, no information is available in the literature about the mass contributions of trucks to the dynamic response of bridges, a value of 20% of the truck masses is included in order to study how the load factors might change. This 20% value has been selected based on a rule of thumb that some seismic engineers have used in the past. The reliability analysis and the load calibration process is then repeated following the same model described above to yield the results described in Table 3.17. The results shown in Table 3.17

**TABLE 3.17 Summary of live load factors considering contributions from truck masses to dynamic properties of system**

Site	$M_{req}$ (kip-ft)	$M_{EQ}$	$M_{LL}$	$\gamma_{LL}$ for LL+EQ
San Francisco	57,137	50,590	3,048	0.27
Seattle	29,274	25,616	3,048	0.24
Memphis	21,835	19,015	3,048	0.21
New York	7,347	5,856	3,048	0.25
St. Paul	4,826	1,529	3,048	0.92
<i>Average</i>				<i>0.24</i>

demonstrate that although the required load factor is slightly higher than that factor observed in Table 3.16, it remains close to the  $\gamma_{LL} = 0.25$  value recommended above.

The calibration executed above is for the foundation system that was designed using a response modification factor  $R_m = 1.5$ . To study the effects of the different response modification factors that may be used for different bridge components, the calibration process is repeated assuming that a response modification factor  $R_m = 6.0$  is used for the design of the bridge column. In this case, as explained in Appendix H, the reliability index,  $\beta$ , for the bridge subjected to earthquakes alone is lower than that obtained when  $R_m = 1.5$  by more than 1.0. Using the lower reliability index as the target that should be reached when combining earthquake and live load effects would yield the results shown in Table 3.18. The results reported in Table 3.18 clearly show that the live load factor that would be required to maintain the same reliability index as that obtained when  $R_m = 6$  is used with earthquakes alone remains essentially similar to that shown in Table 3.17. In Table 3.18, the results for the New York City site, however, must also be removed because when using  $R_m = 6$ , the required moment capacity for the bridge column will be dominated by the effects of the live load alone, as explained above for the St. Paul site.

Another sensitivity analysis is performed to study how the combination of load factors would change if the load factor for earthquakes is not preset at  $\gamma_{EQ} = 1.0$ . This is achieved by using an optimization algorithm with an objective function set to minimize the sum of the squared difference between

**TABLE 3.18 Summary of live load factors considering contributions from truck masses to dynamic properties of system for bridge columns designed using  $R_m = 6.0$**

Site	$M_{req}$ (kip-ft)	$M_{EQ}$	$M_{LL}$	$\gamma_{LL}$ for LL+EQ
San Francisco	12,189	10,275	3,048	0.23
Seattle	6,889	5,412	3,048	0.26
Memphis	5,296	4,085	3,048	0.22
New York	4,114	1,339	3,048	0.78
St. Paul	3,931	362	3,048	1.04
<i>Average</i>				<i>0.24</i>

the results of Equation 3.32 and those of  $M_{req}$  that are given in the first column of Table 3.16 when  $M_{EQ}$  and  $M_{LL}$  are plugged into Equation 3.32 with unknown values of  $\gamma_{EQ}$  and  $\gamma_{LL}$ . The results show that the square of the difference would be minimized when the combination  $\gamma_{EQ} = 1.00$  and  $\gamma_{LL} = 0.18$  is used. This is only slightly different than the results shown in Table 3.16. Hence, for the sake of conservatism, the combination  $\gamma_{EQ} = 1.00$  with  $\gamma_{LL} = 0.25$  is recommended for use when designing bridges that are susceptible to threats from the combined effects of earthquakes and live loads. Please note that these results are very conservative given the previous assumptions that the earthquake is assumed to last for 30 sec at its peak value and the live load model follows the conservative assumptions described by Nowak (1999).

### 3.3.2 Combination of Wind and Live Loads (WS + LL)

The single-column bent described in Figure 3.1 is analyzed to illustrate how the combined effects of wind and live loads will affect the bent's reliability. The wind data from three sites—St. Louis, Austin, and Sacramento—are selected as representative for low, medium, and high wind intensity sites. Table 2.7 of Chapter 2 provides the basic wind intensity data for the three sites. The live load data are obtained from the models developed by Nowak (1999) for NCHRP Project 12-33 as described in Section 2.4.1 of Chapter 2 (Table 2.3). The reliability calculations follow the Ferry-Borges model described in Section 2.5. The following assumptions are made:

- All winds last for 4 h, during which time the moment at the base of the column remains at its highest value. The intensity of the wind response is constant, as is shown in Figure 2.15 for the 4-h duration of the wind.
- The winds are independent from each other.
- Each site is on the average exposed to 200 winds in 1 year.
- The probability distribution of the maximum wind speed follows a Gumbel distribution, which may be used to find the probability distribution for a single event using Equation 2.14.
- The live load model assumes that for each one-lane loading event, the load effect is on the average 0.79 times the load effect obtained from the HL-93 loading configuration for one lane of traffic with a COV of 10%. For two lanes, the average load effect for one event is 1.58 times the effect of one lane of HL-93 with a COV of 7%.
- Each site is exposed to 1,000 single-lane heavy truck events and 67 two-lane truck events in 1 day based on the assumptions of Nowak (1999) and Moses (2001).
- Equation 2.11 is used to find the probability distribution of the live load for different return periods. In particular, the live load for a 4-h period is calculated for combination with the wind load effects when a windstorm is on.

- The effect of each wind is combined with the effect of the 4-h live load magnitude and is projected to provide the maximum expected combined load in the 75-year bridge design life period using the Ferry-Borges model described in Section 2.5. The calculations account for the cases in which the wind occurs with the 4-h live load and the cases in which the live load arrives when no wind is on.
- The reliability calculations are executed for a column bending failure and column overturning limit states.
- The reliability calculations account for the uncertainties associated with predicting the wind speed intensity, determining the bridge response given a wind load, the uncertainty in projecting the live load magnitude, and the uncertainty in estimating the column capacities and soil resistance properties.
- The failure equation for bending may be represented as follows:

$$Z = M_{col} + \frac{3\gamma DK_p f^3}{6} - M_{WS+LL,75} \quad (3.33)$$

where

- $M_{col}$  = the column's moment capacity;
- $\gamma$  = the specific weight of the soil;
- $D$  = the column diameter;
- $K_p$  = the Rankine coefficient,
- $f$  = the distance below the soil level at which the maximum bending moment occurs; and

$M_{WS+LL,75}$  = the applied moment caused by the combined effects of the live load,  $LL$ , and the wind load,  $WS$ , in a return period of  $T = 75$  years.

The maximum effect of the combined load can be represented as follows:

$$M_{WS+LL,75} = \max \left\{ \begin{array}{l} \max_{n_1} \left[ c_{WS} V^2 + \max_{n_2} [c_{LL} I_{LL}] \right] \\ \max_{n_3} [c_{LL} I_{LL}] \end{array} \right\} \quad (3.34)$$

where

- $n_1$  = the number of winds expected in a 75-year period ( $n_1 = 200 \times 75$ );
- $n_2$  = the number of live loads expected in a 4-h period when the wind is on ( $n_2 = 167$  for one-lane loading and  $n_2 = 11$  for two-lane loading);
- $n_3$  = the number of live load events expected in a period equal to 75 years minus the times when a windstorm is on (i.e.,  $n_3 =$  number of live load events in 75 years  $- n_1 \times 4$  h);

$V$  = the wind speed for one windstorm;  
 $I_{LL}$  = the intensity of the live load for one event; and  
 $c_{WS}$  and  $c_{LL}$  = the analysis coefficients that convert the wind speed and the live load intensity to moment effects (e.g., Equations 3.16 and 3.17 show how to convert the intensity of the live load into a moment effect, and Equations 3.18 through 3.20 show how to convert the wind speed into a moment effect).

The effect of wind load on moving trucks is taken into consideration during the simulation. However, following the suggestion of the AASHTO LRFD specifications, the effect of the wind loads on live loads, and the effects of live loads in combination with wind loads are considered only if the wind speed at 10 m (30.5 ft) is less than 90 km/h (56 mph). For the cases in which the wind speed exceeds 90 km/h (56 mph), only the wind load on the structure is considered. The justification is that there is no truck traffic under extreme windstorms.

The results of the reliability analysis are provided in Figure 3.28 for the bending limit state of the 7.6-m (25-ft) bridge bent. Figure 3.29 gives the results for overturning. The data are presented for the three representative wind sites for combination of wind loads and live loads and for wind loads alone. The effect of the soil in resisting bending and overturning are included in the reliability analysis. Similarly, the contributions of the permanent load in resisting overturning

are also included. The same calculations are performed for a 23-m (75-ft) high pier in order to study the influence of bridge height on the results. In this case, only the wind data from the St. Louis site are used.

The results of the calibration are summarized in Table 3.19. As an example, the calibration process follows this logic: if the 7.6-m (25-ft) bridge column is designed to satisfy the AASHTO LRFD specifications, then the required moment capacity for the column will be  $M_{cap} = M_{design} = 2.5$  MN-m (1,835 kip-ft). Choosing  $M_{design} = 2.5$  MN-m (1,835 kip-ft) for the Austin wind data will produce a reliability index (for a 75-year bridge design life) equal to  $\beta = 3.92$  if no live load is considered. When the bridge column is designed for live load, then the required moment capacity is  $M_{cap} = M_{design} = 8$  MN-m (5,917 kip-ft), producing a reliability index  $\beta = 3.71$ . If one considers that live loads may occur within the 4-h period when a windstorm is acting on the bridge column as well as when no wind is on, then the reliability index of the column is reduced as shown in Figure 3.28. To increase the reliability index back to the original  $\beta = 3.71$  obtained for gravity loads alone, the moment capacity of the column should be increased. By interpolation, the moment capacity that will produce a reliability index equal to  $\beta = 3.71$  when both wind loads and live loads are considered should be  $M_{required} = 8.2$  MN-m (6,038 kip-ft) or an increase of 200 kN-m (121 = 6,038 – 5,917 kip-ft).

For the case in which wind alone is applied, the design moment capacity ( $M_{design}$ ) value is 2.5 MN-m (1,835 kip-ft), which includes the effect of the resistance factor for bending of  $\phi = 0.90$  and a wind load factor of  $\gamma_{WS} = 1.4$  (see Equation

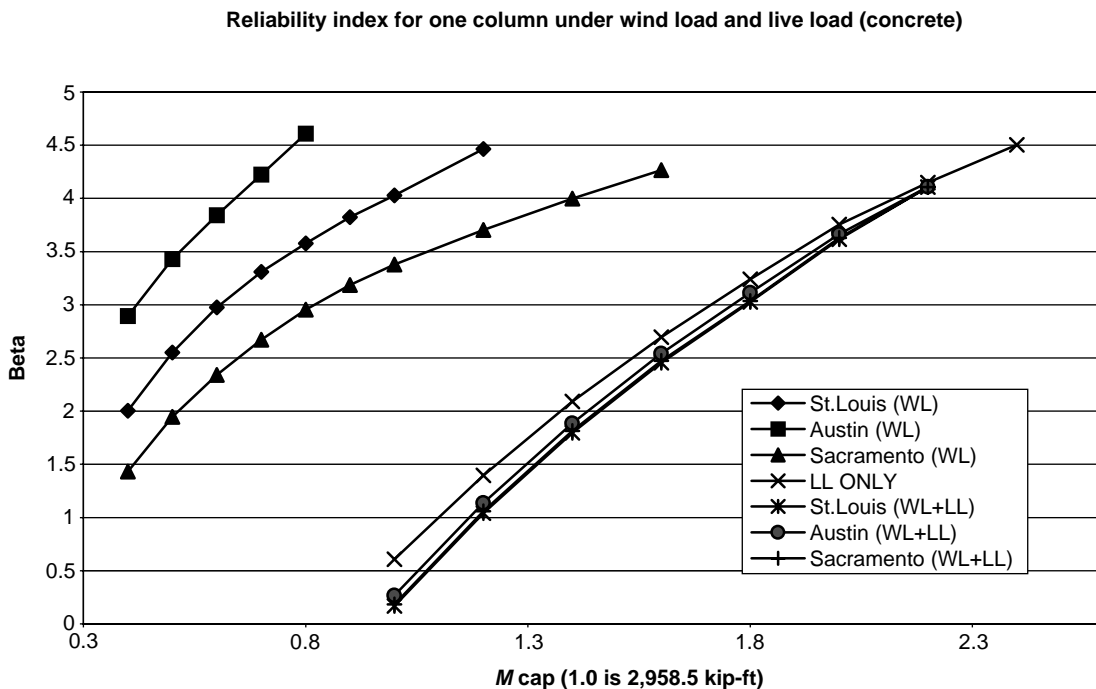


Figure 3.28. Reliability index for combination of wind loads and live load for moment capacity limit state.

Reliability index for overtopping of one column under wind load and live load

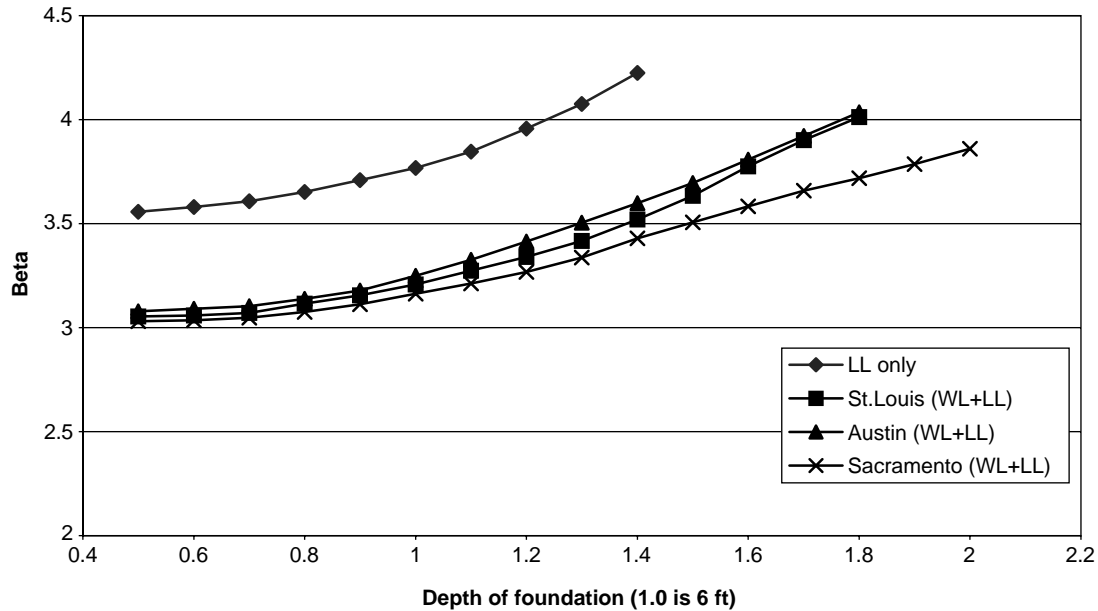


Figure 3.29. Reliability index for combination of wind loads and live load for overtopping.

3.4 and Table 3.2). The moment calculated from the wind load is equal to  $M_{WS} = 1.6 \text{ MN-m}$  (1,180 kip-ft) for a design wind speed of 145 km/h (90 mph). Also, when the live load is on the structure, the AASHTO LRFD requires the consideration of the wind load on live load. For a 90 km/h (56 mph)

wind speed, the AASHTO LRFD recommends applying a distributed force of 1.46 kN/m (0.1 kip/ft). This would result in a moment at the base of the column equal to  $M_{WL} = 513 \text{ kN-m}$  (378 kip-ft). Finally, the applied live load from the HL-93 live loading produces a moment in the column equal

TABLE 3.19 Summary of live load factors for combination of WS + LL for moment capacity

Site	$M_{req}$ (kip-ft)	$M_{WS}$	$M_{WL}$	$M_{LL}$	$\gamma_{LL}$	$\gamma_{WS} = \gamma_{WL}$
St. Louis (25-ft)	6,086	1,180	378	3,048	1.35	0.87
Austin (25-ft)	6,038	1,180	378	3,048	1.35	0.85
Sacramento (25-ft)	6,074	1,180	378	3,048	1.35	0.87
St. Louis (75-ft)	13,532	4,927	2,673	3,048	1.35	1.10
<b>Average</b>						<b>0.92</b>
St. Louis (25-ft)	6,086	1,180	378	3,048	1.50	0.58
Austin (25-ft)	6,038	1,180	378	3,048	1.50	0.55
Sacramento (25-ft)	6,074	1,180	378	3,048	1.50	0.57
St. Louis (75-ft)	13,532	4,927	2,673	3,048	1.50	1.00
<b>Average</b>						<b>0.68</b>
St. Louis (25-ft)	6,086	1,180	378	3,048	1.75	0.09
Austin (25-ft)	6,038	1,180	378	3,048	1.75	0.06
Sacramento (25-ft)	6,074	1,180	378	3,048	1.75	0.09
St. Louis (75-ft)	13,532	4,927	2,673	3,048	1.75	0.90
<b>Average</b>						<b>0.47</b>



$$\begin{aligned}
& 0.5 \frac{3 * 9.4 \text{ kN/m}^3 * 1.8 * 3.68 L_{\text{req}}^3}{3x2} + 0.9 * 6.5 * 10^3 \left( \frac{1.8}{2} \right) \\
& = \gamma_{\text{WS}} 141(8.8 + L_{\text{req}}) + \gamma_{\text{WS}} 26.7(3.6 + L_{\text{req}}) \\
& \quad + \gamma_{\text{WL}} 42.3(12.1 + L_{\text{req}}) + \gamma_{\text{LL}} 3.1 * 10^3
\end{aligned} \tag{3.36'}$$

given that  $L_{\text{req}} = 2.9$  m (9.57 ft) and solving for  $\gamma_{\text{WS}} = \gamma_{\text{WL}}$ , given a value of  $\gamma_{\text{WL}}$  will provide the appropriate load combination factors to be considered. These are provided in Table 3.20. Differences are observed between the results for overturning and bending moment failures and for different column heights in Tables 3.19 and 3.20. These differences are mainly due to the different influences of the statistical uncertainties associated with modeling the soil resistance and column bending capacity.

The results of Tables 3.19 and 3.20 show that the lower live load factors,  $\gamma_{\text{LL}}$ , would provide more uniform ranges of  $\gamma_{\text{WS}} = \gamma_{\text{WL}}$  values. In particular, if the current AASHTO recommended value of  $\gamma_{\text{LL}} = 1.35$  is used, then the corresponding average wind load factor set obtained from overturning and column bending is  $\gamma_{\text{WS}} = \gamma_{\text{WL}} = 0.80$ . This 0.80 value is higher than the current AASHTO LRFD set of  $\gamma_{\text{WS}} = \gamma_{\text{WL}} = 0.40$ , indicating that the current code produces relatively low safety levels. An optimization algorithm is also used to determine the load combination factors that would minimize the sum of the square of the differences between the required moment capacities and those that would be obtained from the right hand side of Equations 3.35 and 3.36. The optimization algorithm indicates that the differences are minimized when the combination of  $\gamma_{\text{WS}} = \gamma_{\text{WL}} = 1.17$  and  $\gamma_{\text{LL}} = 1.06$  is used. Based on these results, it is herein recommended that the combination  $\gamma_{\text{WS}} = \gamma_{\text{WL}} = 1.20$  and  $\gamma_{\text{LL}} = 1.00$  be used for bridges subjected to the combined threats of wind loads and live loads.

### 3.3.3 Combination of Scour and Live Loads (SC + LL)

In this section, the single-column bent described in Figure 3.1 is analyzed to illustrate how the combined effects of scour and live loads will affect the bent's reliability. Scour data from three river sites—the Schohaire, Sandusky, and Rocky—are selected as representative data. Table 2.8 of Chapter 2 provides the basic river discharge data for the selected sites. The live load data are obtained from the models developed by Nowak (1999) for NCHRP Project 12-33 as described in 2.4.1 (Table 2.3). The reliability calculations follow the Ferry-Borges model described in Section 2.5. During the calculations, the following assumptions are made:

- Scour depths last for 6 months, during which time the erosion of the soil around the column base remains at its highest value. The scour depth remains constant throughout the 6-month period.

- The scour depths are independent from year to year.
- Each site is on the average exposed to one major scour in 1 year.
- The probability distribution of the maximum yearly discharge rate follows a lognormal distribution. This maximum yearly discharge rate is assumed to control the scour depth for the year.
- The live load model assumes that for each one-lane loading event, the live load effect is on the average 0.79 times the effect of the HL-93 loading configuration with a COV of 10%. For two lanes, the average event produces an average load effect equal to 1.58 times the effect of one lane of HL-93 with a COV of 7%.
- Each site will be exposed to 1,000 single-lane heavy truck and 67 two-lane truck events in 1 day based on the assumptions of Nowak (1999) and Moses (2001).
- Equation 2.11 is used to find the probability distribution of the live load for different return periods. In particular, the live load for a 6-month period is calculated for studying the reliability caused by the application of live loads when scour is on.
- The effect of the scour depth in reducing the soil resistance around the column base is combined with the effects of the 6-month live load magnitude and projected to provide the maximum expected combined load in the 75-year bridge design life period using the Ferry-Borges model described in Section 2.5. The calculations account for the cases in which the live load occurs with the 6-month scour on and the cases in which the live load occurs with no scour on.
- The reliability calculations are executed for column overturning because the bending moment in deeply embedded columns is not affected by the presence of scour.
- The reliability calculations account for the uncertainties associated with predicting the discharge rate, estimating the scour depth given a discharge rate, projecting the live load magnitude, estimating the counter effect because of the dead loads, and estimating the soil resistance properties.
- Referring to Figure 3.4(a), the failure equation for overturning may be represented as follows:

$$Z = 0 - \max \left\{ \begin{array}{l} \max_{n_1} \left[ \frac{3\gamma DK_p (L - y_{\text{sc}})^3}{6} + F_{\text{DC}} \frac{D}{2} - F_{\text{LL}}^* \left( e_3 - \frac{D}{2} \right) \right] \\ \max_{n_2} \left[ \frac{3\gamma DK_p (L)^3}{6} + F_{\text{DC}} \frac{D}{2} - F_{\text{LL}}^{**} \left( e_3 - \frac{D}{2} \right) \right] \end{array} \right\} \tag{3.37}$$

where

- $F_{\text{DC}}$  = the dead weight applied on the column,
- $F_{\text{LL}}^*$  = the live load that occurs when scour is on,
- $F_{\text{LL}}^{**}$  = the live load when there is no scour,
- $\gamma$  = the specific weight of the soil,
- $D$  = the column diameter,

- $K_p$  = the Rankine coefficient,
- $L$  = the foundation depth,
- $e_3$  = the eccentricity of the live load relative to the center of the column, and
- $y_{sc}$  = the scour depth.

In this case,  $F_{LL}^*$  is the maximum live load effect that may occur within the 6-month period when scour occurs.  $n_1$  represents the number of scours expected in a 75-year period ( $n_1 = 75$ ).  $n_2$  is the number of live load events expected when there is no scour (e.g.,  $n_2 = 75 * 6 * 30 * 1,000$  for one-lane loading events).

The results of the reliability analysis are provided in Figure 3.30 for overtipping of the single-column bent. The data are presented for the three representative river sites for combination of scour and live loads and for live loads alone. The results are also summarized in Table 3.21. As an example, if the 7.6-m (25-ft) bridge column is designed to resist overtipping caused by the application of the HL-93 live load of the AASHTO LRFD specifications, then the column should be embedded a distance  $L = 1.8$  m (6 ft) into the soil. Choosing  $L = 1.8$  m (6 ft) with no scour would produce a reliability index of  $\beta = 3.68$ . If scour occurs because of a river having the discharge rate of the Rocky River, then the reliability index reduces to  $\beta = -2.0$  because of the possible combination of live load and scour in the 75-year bridge design life of a bridge column with a foundation depth  $L = 1.8$  m. However, if one wishes to increase the reliability index from  $-2.0$  back to the original 3.68, then the depth of the column should be increased. By interpolation, the required foundation depth that will produce a reliability index equal to  $\beta = 3.68$  when both scour and live loads are considered should be  $L_{req} = 7.4$  m (24.4 ft) or an increase by a factor of 4.1. Table 3.4 shows

that the expected scour depth from the Rocky River is 3.7 m (12.3 ft). Hence, to go from  $L = 1.8$  m to  $L = 7.4$  m (6 ft to 24.4 ft), one needs to include 1.50 times the design scour depth. Thus, the load factor for scour would be equal to  $\gamma_{sc} = 1.50$ . In other words, for determining the required design scour for the combination of scour plus live loads, one should use the scour HEC-18 equation (Equation 2.22) then multiply the value obtained by a load factor equal to 1.50.

Similar calculations are executed for all three scour site data selected in this section: the Schohaire, Sandusky, and Rocky Rivers. The results for all these cases are summarized in Table 3.21. The average scour factor for the three cases analyzed is  $\gamma_{sc} = 1.79$ , which indicates that a scour factor of  $\gamma_{sc} = 1.80$  associated with a live load factor of  $\gamma_{LL} = 1.75$  is reasonable when studying the combination of scour and live loads.

The recommended scour load factor  $\gamma_{sc} = 1.80$  reflects the fact that the current scour model provides a low reliability level compared with that for the live loads. As seen above, the scour alone model gives an average reliability index close to 1.0 as compared with  $\beta = 3.50$  to 3.70 for live loads. If the goal is to have bridges with foundations set in water channels satisfy the same safety requirements as bridges not subject to scour, then a live load factor  $\gamma_{LL} = 1.75$  should be used in combination with a scour factor  $\gamma_{sc} = 1.80$ . One should note that even for multicolumn bents, failure caused by scour will generally result in the collapse of the system as the bent system would provide little redundancy when one column loses its ability to carry load in a sudden (brittle) failure. Hence, using a system factor of 0.80 in addition to the member resistance factor would be appropriate during the design of column bents for combination of scour and other loads. The application of system factors during the design and safety

Reliability index for overtipping of one column under live load and scour

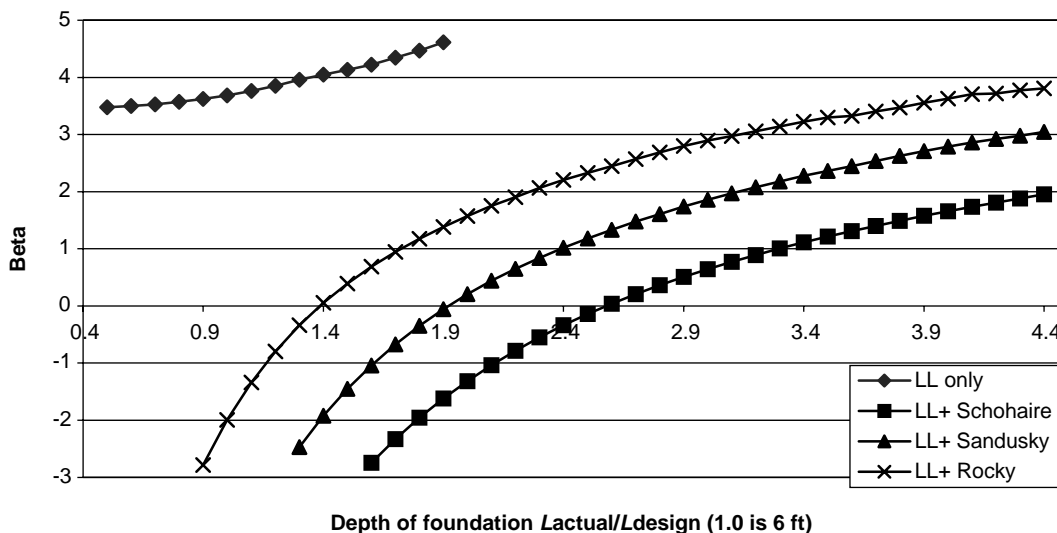


Figure 3.30. Reliability index for combination of scour and live load.

**TABLE 3.21 Summary of live load factors for combination of SC plus LL**

Site	$L_{req}$ (ft)	$L_{SC}$	$L_{LL}$	$\gamma_{SC}$ for LL + SC
Schohaire	41.0 ft	17.3 ft	6 ft	2.02
Sandusky	32.3 ft	14.3 ft	6 ft	1.84
Rocky	24.4 ft	12.3 ft	6 ft	1.50
<i>Average</i>				<b>1.79</b>

evaluation of bridge bents has been discussed elsewhere by Liu et al. (2001).

### 3.3.4 Combination of Scour and Wind Load (SC + WL)

The single-column bent described in Figure 3.1 is analyzed to illustrate how the combined effects of scour and wind loads will affect the bent's reliability. Scour data from three river sites—the Schohaire, Sandusky, and Rocky—are selected as representative sites. Table 2.8 of Chapter 2 provides the basic river discharge data for the selected sites. In addition, wind speed data from Austin, Sacramento, and St. Louis are selected as representatives of wind speed data. The reliability calculations follow the Ferry-Borges model described in Section 2.5. The following assumptions are made:

- Scour depths last for 6 months, during which time the erosion of the soil around the column base remains at its highest value. The scour depth remains constant throughout the 6-month period.
- Scour depths are independent from year to year.
- Each site is on the average exposed to one major scour in 1 year.
- The probability distribution of the maximum yearly discharge rate follows a lognormal distribution. This maximum yearly discharge rate is assumed to control the scour depth for the year.
- The wind speed data are assumed to follow a Gumbel distribution with mean and COV values as shown in Table 2.7.
- Each site will be exposed to 200 winds in a year.
- Equation 2.14 is used to find the probability distribution of the wind load for a 6-month period. This is used for studying the reliability caused by the application of wind loads when scour is on.
- The effect of the scour depth in increasing the moment arm of the wind load is combined with the effects of the 6-month wind load and projected to provide the maximum expected combined load in the 75-year bridge design life period using the Ferry-Borges model described in Section 2.5. The calculations account for the cases in which the wind load occurs with the 6-month scour on and the cases in which the wind occurs when no scour is on.

- The reliability calculations are executed for column bending because overturning is mostly balanced by the weight of the structure and is not significantly affected by the presence of scour.
- The reliability calculations account for the uncertainties associated with predicting the discharge rate, estimating the scour depth given a discharge rate, projecting the wind load magnitude, estimating the counter effect caused by the soil resistance, and estimating the moment capacity of the column.
- Referring to Figure 3.4, the failure equation for bending in the column may be represented as follows:

$$Z = M_{col} + \frac{3\gamma DK_p(f)^3}{6} \lambda_{cyc} - \max \left\{ \begin{array}{l} \max_{n_1} \left[ \left( \max_{n_2} F_{WS}^* \right) (e_1 + y_{sc} + f) \right] \\ \max_{n_3} [F_{WS}^{**} (e_1 + f)] \end{array} \right\} \quad (3.38)$$

where

$M_{col}$  = the bending moment capacity of the column;  
 $F_{WS}^*$  = the resultant wind load on the structure that occurs when scour is on (it accounts for wind on superstructure and wind on column);

$F_{WS}^{**}$  = the resultant wind load on the structure when there is no scour;

$\gamma$  = the specific weight of the soil;

$D$  = the column diameter;

$K_p$  = the Rankine coefficient;

$f$  = the distance below the soil level at which the maximum bending moment occurs;

$\lambda_{cyc}$  = the factor that accounts for the effect of cyclic loads on foundation strength;

$e_1$  = the eccentricity of the resultant wind load relative to the soil level (before scour);

$y_{sc}$  = the scour depth;

$n_1$  = the number of scours expected in a 75-year period ( $n_1 = 75$ );

$n_2$  = the number of wind loads expected when there is scour ( $n_2 = 100$ ); and

$n_3$  = the number of wind loads that occur during the design life of the bridge when there is no scour ( $n_3 = 75 * 100$ ).

The results of the reliability analysis are provided in Figure 3.31 for bending of the single-column bent. The data are presented for the three representative river sites for combination of scour and three different wind loads and for wind loads alone. The results are also summarized in Table 3.22. As an example, if the 8-m (25-ft) bridge column is designed to resist failure in bending caused by the application of the AASHTO design wind load, then the column should have a design moment capacity of  $M_{design} = 2.5 \text{ MN-m}$  (1,835 kip-ft). If the bridge is situated in a region in which the wind data are similar to that observed in Austin, then without the application of any live load the reliability index would be  $\beta = 3.92$ . If scour occurs because of a river having the discharge rate of the Schohaire, then the reliability index reduces to  $\beta = 3.63$  because of the possible combination of wind load and scour in the 75-year bridge design life when the column has a bending capacity of  $M_{cap} = M_{design} = 2.5 \text{ MN-m}$  (1,835 kip-ft). However, if one wishes to increase the reliability index from 3.63 back to the original 3.92, then the column capacity should be increased. By interpolation, the required moment capacity that will produce a reliability index equal to  $\beta = 3.92$  when both scour and wind loads are considered should be  $M_{cap} = 2.9 \text{ MN-m}$  (2,139 kip-ft) or an increase by a factor of 1.15. The scour depth that should be included to achieve this required  $M_{cap}$  is calculated from Equation 3.39:

$$\phi M_{req} = \gamma_{WS} M_{WS} \tag{3.39}$$

or

$$0.90 M_{req} = \gamma_{WS} F_{WS1} (8.8 \text{ m} + \gamma_{SC} y_{sc}) + \gamma_{WS} F_{WS2} (3.6 \text{ m} + \gamma_{SC} y_{sc})$$

where

$M_{WS}$  = the moment exerted on the column because of the applied design wind pressure when the moment arm of the force has been extended by the required factored scour depth;

$F_{WS1} = 140 \text{ kN}$  (31.6 kips), the wind design force on the superstructure located at a distance of 8.8 m (29 ft) above the original soil level;

$F_{WS2} = 27 \text{ kN}$  (6 kips), the wind design force on the column located at a distance of 3.6 m (11.8 ft) above the original soil level.

Given that the scour equation produces  $y_{sc} = 5.3 \text{ m}$  (17.3 ft) for the Schohaire River data and using a wind factor  $\gamma_{WS} = 1.40$  as stipulated by the AASHTO LRFD for wind on structures, the required scour factor is calculated to be  $\gamma_{SC} = 0.60$ .

Similar calculations are executed for all three wind site data (St. Louis, Austin, and Sacramento) and for the three scour site data selected in this section (the Schohaire, Sandusky, and Rocky Rivers). The results for all these cases are summarized in Table 3.22. It is noticed that the range of values for  $\gamma_{SC}$  is between a low of 0.53 and a high of 0.91. The reason for this spread in the results is due to the large range in the reliability index associated with the wind loads and the scour depths. This observation confirms the need to develop new wind maps that would better reflect the actual variations in the wind speeds at different sites in the United States as well as the development of new scour design equations that would reduce the observed differences for rivers with different discharge rates.

From the results shown in Table 3.22, it seems appropriate to conclude that a load factor on scour equal to  $\gamma_{SC} = 0.70$

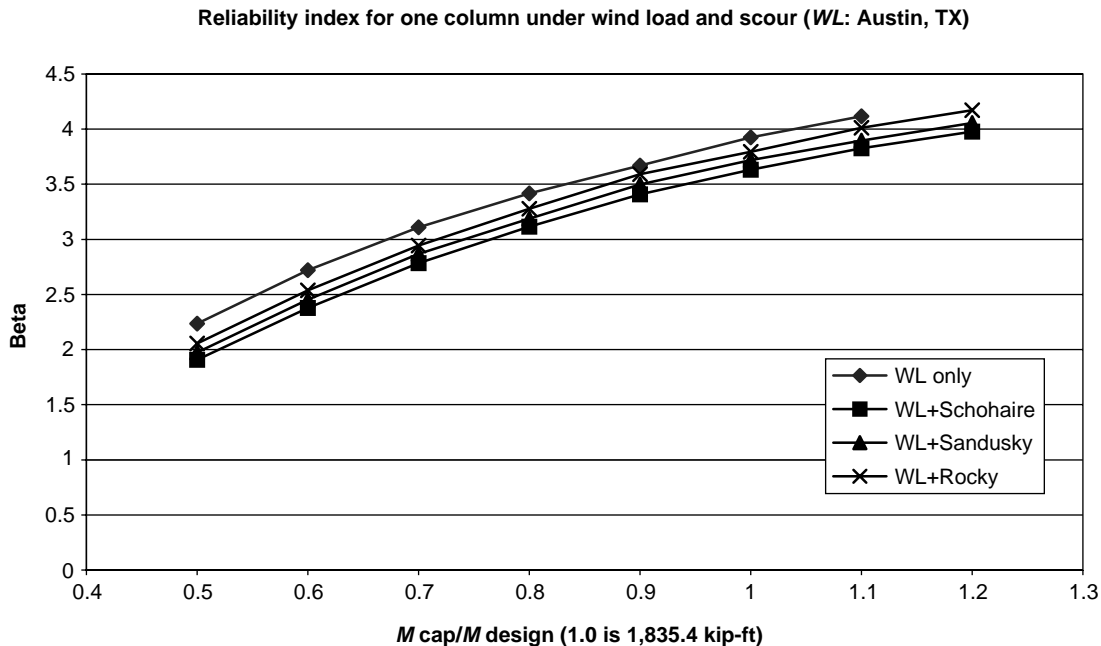


Figure 3.31. Reliability index for combination of wind loads plus scour.

**TABLE 3.22 Summary of live load factors for combination of SC plus WS**

Wind data	Scour data	$M_{req}$	$F_{WS1}$	$F_{WS2}$	$y_{sc}$ (ft)	$\gamma_{sc}$ for WS + SC
Austin	Schohaire	2,139 (kip-ft)	31.6 (kips)	6 (kips)	17.3	0.60
Austin	Sandusky	2,050	31.6	6	14.3	0.62
Austin	Rocky	1,945	31.6	6	12.3	0.57
Sacramento	Schohaire	2,314	31.6	6	17.3	0.77
Sacramento	Sandusky	2,260	31.6	6	14.3	0.87
Sacramento	Rocky	2,191	31.6	6	12.3	0.91
St. Louis	Schohaire	2,072	31.6	6	17.3	0.53
St. Louis	Sandusky	2,004	31.6	6	14.3	0.56
St. Louis	Rocky	1,959	31.6	6	12.3	0.59
<i>Average</i>						<b>0.67</b>

in combination with a wind load factor of  $\gamma_{ws} = 1.40$  is appropriate for use when studying the combination of scour and wind loads. This  $\gamma_{sc} = 0.70$  value is lower than that used for combining scour and live loads because there are fewer wind storms expected in the 75-year design life of a bridge structure as compared with the number of truck loading events. Fewer load occurrences imply a lower chance for combining high wind load intensity with high scour depth.

### 3.3.5 Combination of Scour and Vessel Collision (SC + CV)

The single-column bent described in Figure 3.1 is analyzed to illustrate how the combined effects of scour and vessel collision forces will affect the bent's reliability. Scour data from the Mississippi River at the location of the I-40 bridge are used in combination with the barge traffic at that location. Appendix C provides the basic river discharge data for the selected site. In addition, vessel collision forces as assembled in Figure 2.13 are used. The reliability calculations follow the Ferry-Borges model described in Section 2.5. The following assumptions are made:

- Scour depths last for 6 months, during which time the erosion of the soil around the column base remains at its highest value. The scour depth remains constant throughout the 6-month period.
- The scour depths are independent from year to year.
- The site is on the average exposed to one major scour in 1 year.
- The probability distribution of the maximum yearly discharge rate follows a lognormal distribution. This maximum yearly discharge rate is assumed to control the scour depth for the year. It is noted that because Equation 2.31 was developed based on data from small rivers, this model may not be valid for rivers with high discharge rates. For this reason, this analysis is based on the model developed in Appendix B based on the data provided by Johnson and Dock (1998) as expressed in

Equation 2.30 with a scour modeling variable,  $\lambda_{sc}$ , having a mean value equal to 0.55 and a COV of 52%.

- The collision force data are assumed to follow the probability distribution curve shown in Figure 2.13.
- Each site will be exposed to 0.83 barge flotilla collisions in 1 year.
- Equation 2.11 is used to find the probability distribution of the wind load for a 6-month period for studying the reliability caused by the application of wind loads when scour is on.
- The effect of the scour depth in increasing the moment arm of the collision force is combined with the effects of the 6-month collision force and projected to provide the maximum expected combined load in the 75-year bridge design life period using the Ferry-Borges model described in Section 2.5. The calculations account for the cases in which the collision occurs with the 6-month scour on and the cases in which the collision occurs when no scour is on.
- The reliability calculations are executed for column bending because overturning is mostly balanced by the weight of the structure and is not significantly affected by the presence of scour.
- The reliability calculations account for the uncertainties associated with predicting the discharge rate, estimating the scour depth given a discharge rate, projecting the collision force magnitude, estimating the counter effect caused by the soil resistance, and estimating the moment capacity of the column.
- Referring to Figure 3.4, the failure equation for bending in the column may be represented as follows:

$$Z = M_{col} + \frac{3\gamma DK_p(f)^3}{6} \lambda_{cyc} - \max \left\{ \max_{n_1} \left[ \left( \max_{n_2} F_{CV}^* \right) (e_1 + y_{sc} + f) \right] \right. \\ \left. \max_{n_3} [F_{CV}^{**} (e_1 + f)] \right\} \quad (3.40)$$

where

- $M_{col}$  = the bending moment capacity of the column,
- $F_{CV}^*$  = the collision force on the structure that occurs when scour is on,
- $F_{CV}^{**}$  = the collision force on the structure when there is no scour,
- $\gamma$  = the specific weight of the soil,
- $D$  = the column diameter,
- $K_p$  = the Rankine coefficient,
- $f$  = the distance below the soil level at which the maximum bending moment occurs,
- $\lambda_{cyc}$  = the factor that accounts for the effect of cyclic loads on foundation strength,
- $e_1$  = the eccentricity of the collision force relative to the soil level (before scour),
- $y_{sc}$  = the scour depth,
- $n_1$  = the number of scours expected in a 75-year period ( $n_1 = 75$ ),
- $n_2$  = the number of collisions expected within 1 year when there is scour ( $n_2 = 0.42$ ), and
- $n_3$  = the number of collisions that occur when there is no scour ( $n_3 = 0.42 * 75$ ).

The results of the reliability analysis are provided in Figure 3.32 for bending of the single-column bent. The results show that if the 150-ft bridge column is designed to resist failure in bending caused by the application of the collision forces determined using the AASHTO specifications and following the model of Whitney et al. (1996), the column should

have a design moment capacity  $M_{design} = 464 \text{ MN-m}$  (342,333 kip-ft). The corresponding reliability index—assuming that no scour is possible—would be  $\beta = 2.78$ . If the bridge is exposed to scour because of a river having the discharge rate of the Mississippi and the channel profile shown in Figure 3.6, then the reliability index reduces to  $\beta = 2.05$  because of the possible combination of collision forces and scour in the 75-year bridge design life when the column capacity of  $M_{cap} = M_{design} = 464 \text{ MN-m}$  (342,333 kip-ft). However, if we wish to increase the reliability index from 2.05 back to the original 2.78, then the column capacity should be increased. By interpolation, the required moment capacity that will produce a reliability index equal to  $\beta = 2.78$  when both scour and vessel collisions are considered should be  $M_{cap} = 715 \text{ MN-m}$  (527,200 kip-ft) or an increase by a factor of 1.54. To achieve this  $M_{cap}$ , the following design equation should be satisfied:

$$\phi M_{req} = \gamma_{CV} M_{CV} \tag{3.41}$$

or

$$0.90 M_{req} = \gamma_{CV} F_{CV} (4.9m + \gamma_{SC} y_{SC} + f) - \frac{3\gamma D K_p f^3}{6}$$

where

$M_{CV}$  = the moment exerted on the column caused by the applied design wind pressure when the moment arm

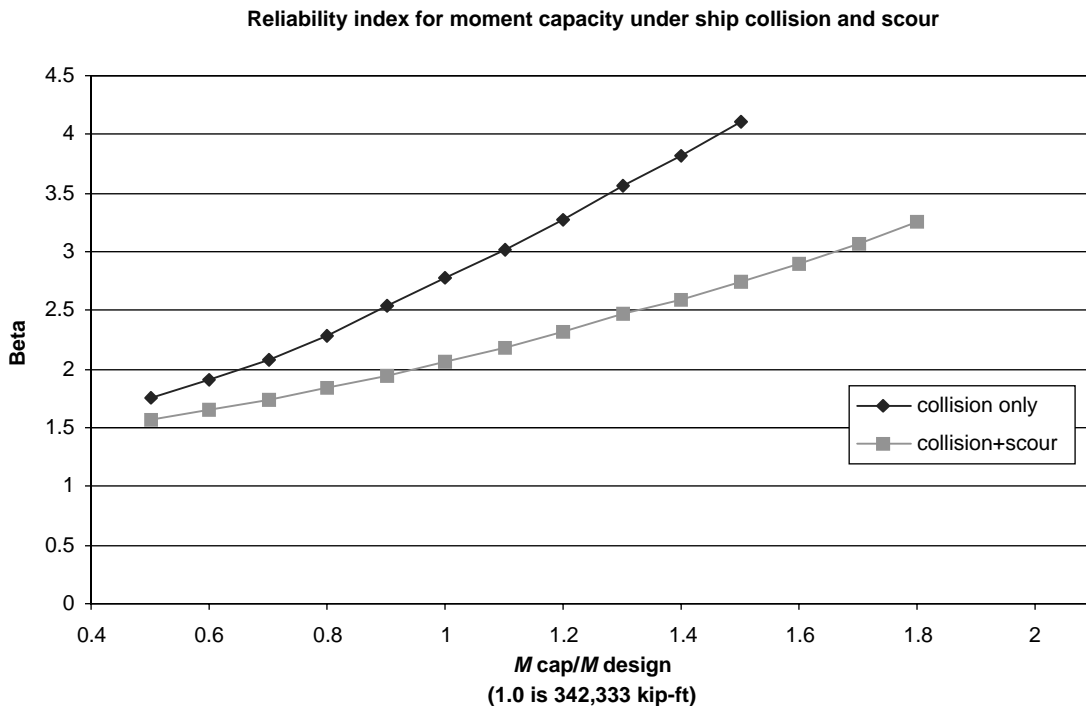


Figure 3.32. Reliability index for combination of collision and scour.

of the force has been extended by the required factored scour depth;

$\gamma$  = the specific weight of the soil;

$D$  = the column diameter;

$K_p$  = the Rankine coefficient;

$F_{CV} = 35 \text{ MN (7,900 kips)}$ , the vessel collision design force on the column applied at a distance of 16 ft above the original soil level; and

$f = 10.5 \text{ m (34.5 ft)}$  = the depth to the point of maximum moment.

Note that in this equation the effect of the soil resistance is included because  $f$  is reasonably deep. For the cases analyzed above (e.g., wind loads),  $f$  is relatively small and the contributions of the soil resistance does not significantly affect the design capacity of the column. Given that the scour equation produces  $y_{sc} = 10.4 \text{ m (34.2 ft)}$  for the Mississippi River data and using a vessel collision factor  $\gamma_{CV} = 1.0$  as stipulated by the AASHTO LRFD for collision forces, the required scour factor is calculated to be  $\gamma_{SC} = 0.62$ .

From the calculations shown above, it seems appropriate to conclude that a load factor on scour equal to  $\gamma_{SC} = 0.60$  associated with  $\gamma_{CV} = 1.0$  is reasonable for use when studying the combination of scour and ship collision forces. This value is lower than that used for combining scour and live loads and for combining wind and scour because there are fewer collisions expected in the 75-year design life of a bridge structure as compared with the number of truck loading events or windstorms. Fewer load occurrences imply a lower chance for combining high vessel collision forces with high scour depths. Also, the target reliability index selected for the calibration is lower than that used for live loads and is lower than that obtained from the average of different wind data. The lower target reliability index is selected to match the reliability index observed for the cases in which vessel collisions occur without risk of scour.

### 3.3.6 Combination of Vessel Collision and Wind Loads (CV + WS)

In this section, the single-column bent described in Figure 3.1 is analyzed to illustrate how the combined effects of vessel collision forces and wind loads will affect its reliability. It is herein assumed that wind load data collected in Knoxville, Tennessee, are applicable for this bridge site. This Knoxville wind data are used in combination with the barge traffic at the location of the I-40 bridge in Memphis. In addition, vessel collision forces as assembled in Figure 2.13 are used. The reliability calculations follow the Ferry-Borges model described in Section 2.5. The following assumptions are made:

- The wind speed data are assumed to follow a Gumbel distribution, with a yearly mean value equal to 77.8 km/h (48.6 mph) and COV of 14%.
- The site is exposed to 200 winds in 1 year.

- Equation 2.14 is used to find the probability distribution of the wind load for a 6-month period for studying the reliability caused by the application of wind loads when scour is on.
- The collision force data are assumed to follow the probability distribution curve shown in Figure 2.13.
- Each site will be exposed to an average of 0.83 barge flotilla collisions in 1 year.
- Equation 2.14 is used to find the probability distribution of the wind load for a 6-month period for studying the reliability caused by the application of a collision force when the wind is on.
- A correlation between the wind speed and the number of collisions is assumed based on the data provided by Larsen (1993). According to this model, the rate of collisions increases by a factor of 3 (from 0.83 to 2.50 collisions/year) when the wind speed increases from 6 m/sec (13 mph) to 14 m/sec (31 mph). Below 6 m/sec (13 mph), the number of collisions remains at 0.83 collisions/year; beyond 14 m/sec (31 mph), the number of collision remains at a rate of 2.50/year. Although barges and flotilla may not travel when the wind speeds exceed the 14 m/sec (31 mph) limit, it is herein assumed that vessels and barges may break from their moorings when there is a large windstorm such that collisions are still possible.
- The effect of the moment from wind forces is combined with the effects of the collision force and projected to provide the maximum expected combined load in the 75-year bridge design life period using the Ferry-Borges model described in Section 2.5. The calculations account for the cases in which the collision occurs during a windstorm and the cases in which the collision occurs when no wind is on.
- The reliability calculations are executed for column bending because overturning is mostly balanced by the weight of the structure.
- The reliability calculations account for the uncertainties associated with predicting the wind speed, estimating the wind forces, projecting the collision force magnitude, estimating the counter effect caused by the soil resistance, and estimating the moment capacity of the column.
- Referring to Figure 3.4, the failure equation for bending in the column may be represented as follows:

$$Z = M_{col} + \frac{3\gamma DK_p (f)^3}{6} \lambda_{cyc} - \max \left\{ \begin{array}{l} \max_{n_1} \left[ F_{ws} (e_2 + f) + \left( \max_{n_2} F_{cv}^* \right) (e_2 + f) \right] \\ \max_{n_3} \left[ F_{cv}^{**} (e_2 + f) \right] \end{array} \right\} \quad (3.42)$$

where

$M_{col}$  = the bending moment capacity of the column,

- $F_{CV}^*$  = the collision force on the structure that occurs when a wind is on,
- $F_{CV}^{**}$  = the collision force on the structure when there is no wind,
- $\gamma$  = the specific weight of the soil,
- $D$  = the column diameter,
- $K_p$  = the Rankine coefficient,
- $f$  = the distance below the soil level at which the maximum bending moment occurs,
- $\lambda_{cyc}$  = the factor that accounts for the effect of cyclic loads on foundation strength,
- $e_2$  = the eccentricity of the collision force relative to the soil level,
- $e_1$  = the moment arm of the resultant wind force,
- $n_1$  = the number of winds expected in a 75-year period ( $n_1 = 200 \times 75$ ),
- $n_2$  = the number of collisions expected when there is a wind, and
- $n_3$  = the number of collisions that occur when there is no wind.

In order to study the effects of the winds on the structure and calculate the wind force,  $F_{WS}$ , the results provided in Appendix F are used. The results essentially show that at a wind of 70 mph the wind force is equal to 18.6 MN (4,180 kips) and that the resultant force will be applied at an eccentricity  $e_1 = 68$  m (223 ft) from the soil's surface. Interpolation as a func-

tion of  $V^2$  (where  $V =$  wind velocity) is used to find the wind forces for different wind speeds. Notice that the force eccentricity is larger than the column height because of the effect of the superstructure.

The results of the reliability analysis are provided in Figure 3.33 for bending of the single-column bent. For example, if the 46-m (150-ft) bridge column is designed to resist failure in bending caused by the application of the collision forces determined using the AASHTO specifications and following the model of Whitney et al. (1996), then the column should have a design moment capacity of  $M_{design} = 464$  MN-m (342,333 kip-ft). If the bridge was originally designed without taking into consideration the possibility of windstorms, the reliability index would be  $\beta = 2.78$ . If the bridge is exposed to winds in addition to collision forces, then the reliability index reduces to  $\beta = 0.82$  in the 75-year bridge design life when the column has a capacity  $M_{cap} = M_{design} = 464$  MN-m (342,333 kip-ft). However, if one wishes to increase the reliability index from 0.82 back to the original 2.78, then the column capacity should be increased. By interpolation, the required moment capacity that will produce a reliability index equal to  $\beta = 2.78$  when both vessel collision forces and wind loads are considered should be  $M_{cap} = 896$  MN-m (660,700 kip-ft) or an increase by a factor of 1.93. To achieve this  $M_{cap}$ , load combination factors should be used in the design equations. The determination of the appropriate load factors is executed using the following equation:

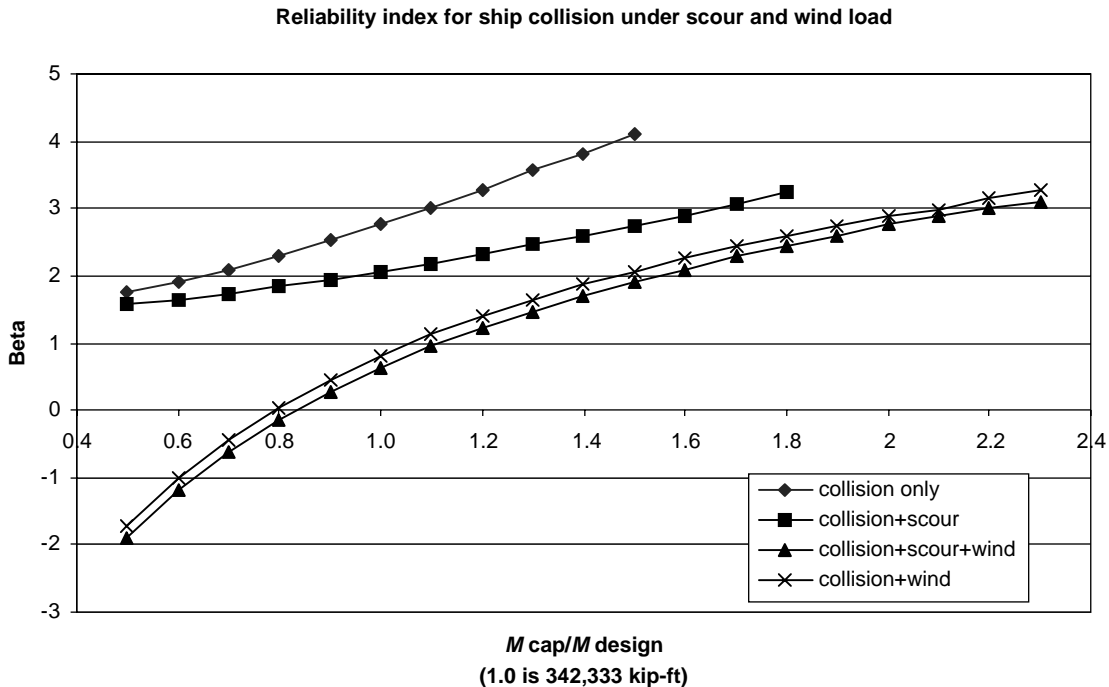


Figure 3.33. Reliability index for combination of vessel collision plus wind loads and scour.

$$\phi M_{\text{req}} = \gamma_{\text{WS}} M_{\text{WS}} + \gamma_{\text{CV}} M_{\text{CV}} \quad (3.43)$$

or

$$0.90 M_{\text{req}} = \gamma_{\text{WS}} 18.6 \text{ MN} * (68 \text{ m} + 2f/3) \\ + \gamma_{\text{CV}} 35 \text{ MN} * (4.9 \text{ m} + 2f/3).$$

By trial and error, it has been determined that a  $\gamma_{\text{WS}} = 0.27$  associated with  $\gamma_{\text{CV}} = 1.0$  would lead to a point of maximum moment located at a distance of  $f = 11.3 \text{ m}$  (37 ft) below the soil level. These factors will produce a required moment capacity  $M_{\text{req}} = 896 \text{ MN}\cdot\text{m}$  (660,700 kip-ft), which will lead to a reliability index of  $\beta = 2.78$  for the combination of wind loads and vessel collisions. The  $\beta = 2.78$  is the same reliability index obtained from vessel collision forces alone.

In addition to showing how the reliability index varies for the cases in which vessel collision forces are applied alone on the bridge, Figure 3.33 shows how the combination of wind forces, collision forces, and scour affect the reliability index. It is noted that the probability of having all three extreme events simultaneously is very small. Hence, the drop in the reliability index from the case in which wind and vessel collision forces are combined to the case in which wind, scour, and vessel collision are combined is less than 0.1. Therefore, it is not necessary to check this possible combination. Based on the calculations performed in this section it is recommended to use a wind load factor of  $\gamma_{\text{WS}} = 0.30$  in combination with  $\gamma_{\text{CV}} = 1.0$  when checking the safety of bridges under the combined effects of winds and vessel collisions. The 0.30 wind factor proposed is lower than the 0.80 factor used for combinations involving live loads. This is justified based on the lower number of vessel collisions expected when compared with the number of live load events, meaning there is a lower chance of combination even though a correlation between the rate of collisions is made with the intensity of the wind while a negative correlation is made with the number of live load events with wind speeds. In addition, the target reliability index selected for wind plus vessel collision is lower than that used for live loads with winds.

### 3.3.7 Combination of Earthquakes and Scour (EQ + SC)

In this section, the single-column bent described in Figure 3.1 is analyzed to illustrate how the combined effects of earthquakes and scour will affect its reliability. The data from the five earthquake sites with probability distribution curves described in Figure 2.4 are used. The scour data are obtained from the USGS website for the Schohaire, Sandusky, and Rocky Rivers, as described in Section 2.4.4 (Table 2.8). The reliability calculations follow the Ferry-Borges model described in Section 2.5. The following assumptions are made:

- Scour depths last for 6 months, during which time the erosion of the soil around the column base remains at its highest value. The scour depth remains constant throughout the 6-month period.
- Scour depths are independent from year to year.
- Each site is on the average exposed to one major scour in 1 year.
- The probability distribution of the maximum yearly discharge rate follows a lognormal distribution. This maximum yearly discharge rate is assumed to control the scour depth for the year.
- The intensity of the earthquake response is as shown in Figure 2.15.
- The number of earthquakes expected in 1 year is 8 for the San Francisco site data, 2 for Seattle, 0.50 for Memphis, 0.40 for New York, and 0.01 for St. Paul. This means that there will be 600 earthquakes in a 75-year return period for San Francisco, 150 earthquakes for Seattle, 38 in Memphis, 30 in New York, and 1 in St. Paul.
- The probability distribution of the maximum yearly earthquake may be used to find the probability distribution for a single event using Equation 2.14.
- Equation 2.14 is used to find the probability distribution of the earthquake intensities for different return periods. In particular, the earthquake intensity for  $t = 1/2$ -year period is calculated for combination with the earthquake load effects when the foundation is scoured.
- The effects of each scour are combined with the effects of the  $1/2$ -year earthquake intensity and projected to provide the maximum expected combined load in the 75-year bridge design life period using the Ferry-Borges model described in Section 2.5. The calculations account for the cases in which the earthquake occurs with the  $1/2$ -year scour period and the cases in which an earthquake occurs when there is no scour.
- The reliability calculations are executed for the column overturning limit state. The column bending limit state was not considered because the results of Figure 3.18 show that the foundation depth does not significantly affect the reliability index for column bending. Thus, when a large length of the column is exposed because of scour, the reduced column stiffness that ensues will result in lower bending moment on the column base, and the reliability index remains practically unchanged. On the other hand, for column overturning, the remaining soil depth may sometimes not be sufficient to resist overturning even though the forces are reduced.
- The reliability calculations account for the uncertainties associated with predicting the *EQ* intensity, estimating the bridge response given an *EQ* intensity, projecting the scour depth, and estimating the soil capacity to resist overturning.
- The failure equation for bending of the column under the combined effect may be represented as follows:

$$Z = \max \left\{ \begin{array}{l} \max_{n_1} \left\{ \frac{3\gamma DK_p (L - y_{scour})^3}{6} - \max_{n_2} [F_{EQ}^*(e + L)] \right\} \\ \max_{n_3} \left\{ \frac{3\gamma DK_p (L)^3}{6} - F_{EQ}^{**}(e + L) \right\} \end{array} \right\} \quad (3.44)$$

where

- $\gamma$  = the specific weight of the soil;
- $D$  = the column diameter;
- $K_p$  = the Rankine coefficient;
- $L$  = the foundation depth before scour;
- $e$  = the distance from the original soil level to the point of application of the inertial force;
- $F_{EQ}^*$  = the inertial force when the scour is on;
- $F_{EQ}^{**}$  = the inertial force when no scour is on;
- $n_1$  = the number of scours expected in a 75-year period (75 scours);
- $n_2$  = the number of earthquakes expected in a 1/2-year period when scour is on; and
- $n_3$  = the number of earthquake events expected in a period equal to 75 years minus the times when a scour is on (i.e.,  $n_3$  is the number of earthquakes in a period equal to 37.5 years [75/2]).

The results of the reliability analysis are provided in Figure 3.34 for the San Francisco earthquake data for different values of foundation depth. The results that were obtained by considering the reliability of the bridge structure when only earthquakes are considered (i.e., by totally ignoring the effects

of scour) are also illustrated in Figure 3.34. The results for the San Francisco site are summarized as shown in Table 3.23. For example, if the bridge column is designed to satisfy the proposed revised AASHTO LRFD specifications (the seismic provisions) developed under NCHRP Project 12-49 (ATC and MCEER, 2002), then the required foundation depth for the column using a 2,500-year earthquake return period is  $L = L_{design} = 26.06$  m (85.5 ft). This would produce a reliability index for overtipping (for a 75-year bridge design life) equal to  $\beta = 2.26$  for sites having earthquake intensities similar to those observed in San Francisco but that are not subject to scour. If one considers that the foundation may be weakened by the presence of scour that would occur because of the river having the discharge rate of the Schohaire, then the reliability index for the column with a foundation depth of  $L = 26.06$  m (85.5 ft) reduces to  $\beta = 2.24$ . If one wishes to increase the reliability index from 2.24 back to the original 2.26, then the depth of the foundation should be increased. By interpolation, the required foundation depth that will produce a reliability index equal to  $\beta = 2.26$ , when both earthquake loads and scour are considered, should be  $L = 26.33$  m (86.4 ft) or an increase of 0.27 m (0.9 ft).

The  $L_{design}$  value 26.06 m (85.5 ft) includes the effect of the resistance factor for a lateral soil capacity of  $\phi = 0.50$ . The scour factor that should be used for the combination of earthquakes and scour should be determined such that

$$0.50 \frac{3\gamma DK_p L^3}{6} = \gamma_{EQ} F_{EQ}(e + \gamma_{SC} y_{SC} + L') \quad (3.45)$$

Reliability index for overtipping of one column under EQ and scour (San Francisco)

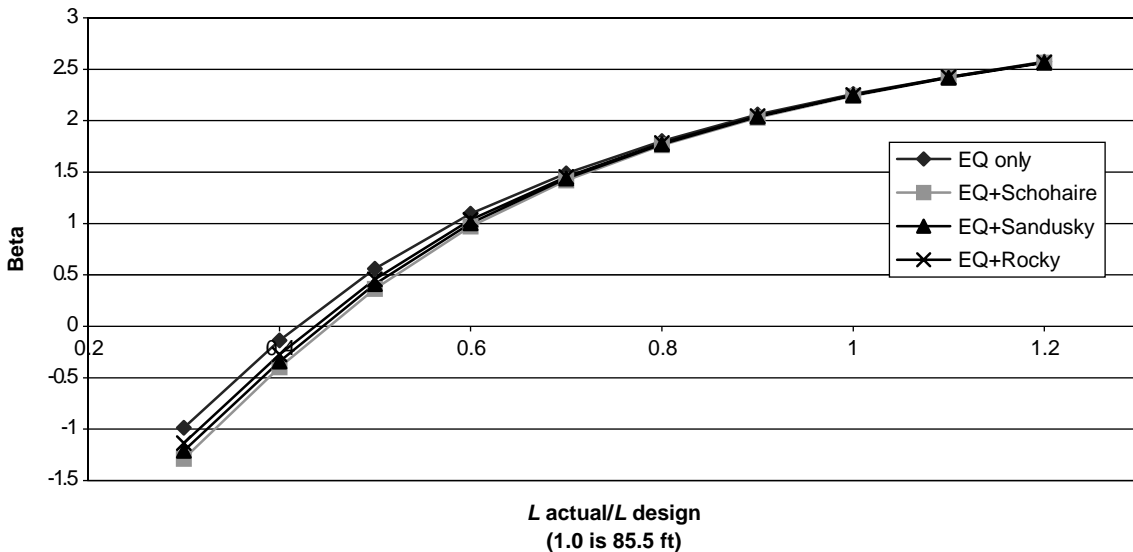


Figure 3.34. Reliability index for earthquakes and scour for overtipping (San Francisco).

**TABLE 3.23 Summary of live load factors for combination of EQ plus SC**

Earthquake site	Scour data	$\beta$ target	Original foundation depth (ft)	Required foundation depth (ft)	Scour depth (ft)	$\gamma_{sc}$
San Francisco	Schohaire	2.259	85.5	86.42	17.34	0.36
	Sandusky			86.19	14.33	0.36
	Rocky			85.99	12.32	0.34
Seattle	Schohaire	2.635	66	67.04	17.34	0.18
	Sandusky			66.80	14.33	0.17
	Rocky			66.46	12.32	0.12
St. Paul	Schohaire	2.368	20	28.64	17.34	0.55
	Sandusky			23.97	14.33	0.32
	Rocky			22.08	12.32	0.20
New York	Schohaire	2.491	37	41.06	17.34	0.32
	Sandusky			39.39	14.33	0.23
	Rocky			38.55	12.32	0.18
Memphis	Schohaire	2.488	58.6	60.00	17.34	0.18
	Sandusky			59.59	14.33	0.16
	Rocky			59.20	12.32	0.12
<b>Average</b>						<b>0.25</b>

where

- 0.50 = the soil resistance factor;
- $\gamma$  = the specific weight of the soil;
- $D$  = the column diameter;
- $K_p$  = the Rankine coefficient;
- $L'$  = the foundation depth after scour ( $L' = L_{\text{required}} - \gamma_{sc}\gamma_{sc}$ );
- $e$  = the distance from the original soil level to the point of application of the inertial force;
- $\gamma_{EQ}$  = the load factor for earthquake forces;
- $F_{EQ}$  = the inertial force;
- $\gamma_{sc}$  = the design scour depth as shown in Table 3.4, which for the Schohaire River is 5.3 m (17.3 ft); and
- $\gamma_{SC}$  = the scour factor that should be used when considering the combination of earthquakes and scour.

It is noted that the inertial force,  $F_{EQ}$ , is a function of  $L'$  and the product  $\gamma_{sc}\gamma_{sc}$ . Hence the scour factor can only be found from Equation 3.45 by trial and error.

The calibration of the load combination factor involves the determination of the values of  $\gamma_{sc}$  needed to produce the required foundation depth  $L_{\text{req}} = 26.3$  m (86.4 ft). If the value for  $\gamma_{EQ}$  is preset at 1.0, then  $\gamma_{sc}$  is calculated to be equal to 0.36. This would lead to a foundation  $L'$  after scour erosion equal to 24.2 m (79.3 ft). Notice that the  $L' = 24.2$  m (79.3 ft) is lower than the original  $L = 26.1$  m (85.5 ft). This reduction in the required effective foundation depth is due to the additional flexibility of the column caused by the presence of scour. In fact, when scour occurs, the clear height of the column increases and the remaining foundation depth decreases; as long as the foundation is not totally washed out, this phenomenon would reduce the stiffness of the system and would lead to a higher natural period. When the natural period increases, the inertial forces decrease. Although the moment

arm of the force increases, the required foundation depth after scour would be lower than originally required if no scour were considered. It is noted however that adding 24.2 m (79.3 ft) plus 0.36 times the design scour depth (5.3 m = 17.3 ft) would still lead to a total foundation depth = 26.3 m (86.4 ft), which is higher than the original no scour depth  $L = 26.1$  m (85.5 ft). It is also noted that in the examples solved in this section, the mass of the system is not altered because of the presence of scour or changes in foundation depth.

Similar calculations are executed for five earthquake sites and three discharge data. Namely, the earthquake data used correspond to those data from San Francisco, Seattle, Memphis, New York, and St. Paul. The scour data used correspond to those data from the Schohaire, Sandusky, and Rocky Rivers. The results from all 15 cases considered are summarized in Table 3.23. Notice that for all the cases considered, the scour factor remains below 0.55, with an average value of 0.25. Based on the results shown in Table 3.23, it would seem appropriate to recommend that a scour factor of  $\gamma_{sc} = 0.25$  associated with an earthquake factor of  $\gamma_{EQ} = 1.00$  be used to account for the combination of scour and earthquakes. The 0.25 scour factor is lower than that observed for the combination of scour and vessel collisions because the target reliability level used for the combination of scour and earthquakes is lower than that used for collisions and scour (e.g., for San Francisco,  $\beta_{\text{target}} = 2.26$  versus  $\beta_{\text{target}} = 2.78$  for vessel collisions). Another reason is because the earthquake analysis model accounts for the additional flexibility of the system when scour occurs and for the reduction in inertial force that this causes. The flexibility of the column is not directly considered when analyzing the effect of vessel collision forces.

All the analyses for combinations involving scour assume that scour lasts for a period of 6 months, during which time the scour remains at its highest value. Because no models are

currently available to study the duration of live bed scours at bridge piers and how long it would take for the foundation of drilled shafts to regain their original strengths, a sensitivity analysis is performed to study the effect of scour duration on the results of the reliability analysis and the proposed load factor if the duration of scour is changed from 6 months to either 4 or 8 months. The results are provided in Table 3.24, which shows a change in the load factor on the order of 0.05 for each 2-month change in the scour duration. It is noted that in all cases considered, the scour is assumed to be at its highest value, which does provide a conservative envelope to the scour combination cases.

### 3.4 SUMMARY AND RECOMMENDATIONS

In this chapter, a reliability analysis of bridge bents is performed when the bridges are subjected to effects of live loads, wind loads, scour, earthquakes, vessel collisions, and combinations of these extreme events. Load combination factors are proposed such that bridges subjected to a combination of these events would provide reliability levels similar to those of bridges with the same configurations but situated in sites in which one threat is dominant. Thus, the proposed load factors are based on previous experiences with “safe bridge structures” and provide balanced levels of safety for each load combination. The results of this study found that different threats produced different reliability levels. Therefore, the target reliability indexes for the combination of events are selected in most cases to provide the same reliability level associated with the occurrence of the individual threat with the highest reliability index. Thus, when dealing with the combination of live load plus wind load or live load plus scour,

the reliability index associated with live loads is used as target. When studying the reliability of bridges subjected to the combination of wind loads and scour, the reliability index associated with wind loads alone is chosen for target. Similarly, when studying the reliability of bridges subjected to vessel collisions with scour or vessel collision with wind load, the reliability index associated with vessel collisions is used for target. For combinations involving earthquake loads, it is the reliability index associated with earthquakes alone that is used for target. Combinations involving earthquakes are treated differently than are other combinations because of the large additional capacity that would be required to increase the reliability levels of bridges subjected to earthquake risks. This approach is consistent with current earthquake engineering practice, which has determined that current earthquake design methods provide sufficient levels of safety given the costs that would be involved if higher safety levels were to be specified.

Results of the reliability analyses indicate that there are large discrepancies among the reliability levels implied in current design practices for the different extreme events under consideration. For example, the AASHTO LRFD was calibrated to satisfy a target member reliability index equal to 3.5 for gravity loads. The calculations performed in this study confirm that bridge column bents provide reliability index values close to the target 3.5 for the different limit states considered. These limit states include column bending, axial failure, bearing failure of the soil for one-column and multicolumn bents, and overturning of one-column bents. The reliability index values calculated for each of these limit states show that  $\beta$  ranges from about 2.50 to 3.70. The lowest value is for foundation failures in bearing capacity. This is due to the large level of uncertainty associated with determining the strengths of foundation systems. The highest value is for bending

**TABLE 3.24 Sensitivity of results to scour duration period**

Earthquake site	Scour data	Required foundation depth (ft) (4 months)	Required foundation depth (ft) (6 months)	Required foundation depth (ft) (8 months)	$\gamma_{sc}$ (4 months)	$\gamma_{sc}$ (6 months)	$\gamma_{sc}$ (8 months)
San Francisco	Schohaire	86.15	86.42	86.43	0.29	0.36	0.36
	Sandusky	86.01	86.19	86.38	0.30	0.36	0.42
	Rocky	85.87	85.99	86.07	0.29	0.34	0.38
Seattle	Schohaire	66.84	67.04	67.56	0.15	0.18	0.25
	Sandusky	66.68	66.80	67.24	0.15	0.17	0.25
	Rocky	66.16	66.46	66.75	0.04	0.12	0.19
St. Paul	Schohaire	28.58	28.64	28.68	0.55	0.55	0.56
	Sandusky	23.76	23.97	24.28	0.30	0.32	0.34
	Rocky	21.52	22.08	22.40	0.15	0.20	0.23
New York	Schohaire	40.15	41.06	41.52	0.25	0.32	0.35
	Sandusky	38.67	39.39	39.81	0.17	0.23	0.27
	Rocky	38.11	38.55	38.98	0.13	0.18	0.23
Memphis	Schohaire	59.85	60.00	60.57	0.16	0.18	0.25
	Sandusky	59.49	59.59	60.12	0.15	0.16	0.24
	Rocky	59.12	59.20	59.58	0.11	0.12	0.19
<b>Average</b>				<b>0.21</b>	<b>0.25</b>	<b>0.30</b>	

moment capacity. These reliability indexes are for member failures. If there is sufficient redundancy, the system reliability is higher as explained by Ghosn and Moses (1998) and Liu et al. (2001).

The system reliability index for bridge bents subjected to earthquakes is found to be on the order of 2.80 to 3.00 for the moment capacity of drilled shafts supporting single- and multicolumn bents or 2.20 to 2.60 for overtopping of single-column bents. These values are for bridges designed following the proposed specifications developed under NCHRP Project 12-49 (ATC and MCEER, 2002). These reliability levels decrease to as low as 1.75 when studying the safety of bridge columns under earthquakes. The large difference is due to the differences in the response modification factors recommended for use during the design process. In fact, *NCHRP Report 472* recommends the use of different response modification factors for bridge subsystems depending on the consequences of failure (ATC and MCEER, 2002). Unlike the analysis for other hazards, the earthquake analysis procedure accounts for system capacity rather than for member capacity because failure is defined by accounting for plastic redistribution of loads and the ductility capacity of the columns. Although relatively low compared with the member reliability index for gravity loads, the engineering community is generally satisfied with the current safety levels associated with current earthquake design procedures. For this reason, the target reliability index for load combination cases involving earthquakes is chosen to be the same reliability index calculated for the case in which earthquakes alone are applied. In fact, the results of this study indicate that very little improvement in the earthquake reliability index can be achieved even if large increases in the load factor are implemented. This is because much of the uncertainties in assessing the earthquake risk for bridge systems are due to the difficulty in predicting the earthquake intensities over the design life of the bridge. Improvement in the overall earthquake design process can only be achieved after major improvements in the seismologists' ability to predict future earthquakes.

The reliability index for designing bridge piers for scour for small-size rivers is on the order of 0.45 to 1.7, which is much lower than the 3.5 target for gravity loads and even lower than the range observed for earthquakes. In addition, failures caused by scour generally result in total collapse as compared with failures of members under gravity loads. This observation is consistent with the observation made by Shirole and Holt (1991) that, by far, most U.S. bridge collapses are due to scour. Because of the high risks of major collapses caused by scour, it is recommended to increase the reliability index for scour by applying a scour safety factor equal to 2.00. The application of the recommended 2.00 safety factor means that if current HEC-18 scour design procedures are followed, the final depth of the foundation should be 2.00 times the value calculated using the HEC-18 approach. Such a safety factor would increase the reliability index for scour from an average of about 1.00 to slightly more than 3.0, which

will make the scour design methods produce average safety levels for small rivers more compatible with the methods for other threats. However, the wide range in safety levels will require a review of current scour evaluation procedures.

Current AASHTO LRFD bridge design methods for wind loads provide average member reliability index values close to 3.00. However, there are large differences between the reliability indexes obtained for different U.S. sites. In fact, for the sites analyzed in this report, the reliability index ( $\beta$ ) ranges between 2.40 and 4.00. The wind design approach is based on member safety. If sufficient levels of redundancy exist, the system reliability would be higher. The system reliability could increase by 0.25 to 0.50 over member reliability, depending on the number of columns in the bridge bent and the level of confinement of the columns. However, the large variations observed in the reliability index indicate that there should be major research effort placed on improving the current wind design procedures. This effort should be directed toward better understanding the behavior of bridges subjected to wind loads and toward developing new wind design maps that would provide more uniform safety levels for different regions of the United States.

The AASHTO vessel collision model produces a reliability index of about 3.15 for shearing failures and about 2.80 for bending failures. The higher reliability index for shear is due to the implicit biases and conservatism associated with the AASHTO LRFD shear design procedures as reported by Nowak (1999). The presence of system redundancy caused by the additional bending moment resistance by the bents, abutments, or both that are not impacted would increase the reliability index for bending failures to more than 3.00, making the safety levels more in line with those for shearing failures and those of bridge members subjected to the other threats considered.

The results of the reliability index calculations for individual threats are used to calibrate load combination factors applicable for the design of short- to medium-span bridges. The recommended load combination factors are summarized in Appendix A in a format that is implementable in the AASHTO LRFD specifications.

The load combination factors proposed in this study illustrate that the current load factors for the combination of wind plus gravity loads lead to lower reliability indexes than do those of either load taken separately. Hence, this study has recommended increasing the load factors for wind on structures and wind on live loads from the current 0.40 to 1.20 in combination with a live load factor of 1.00, which replaces the live load factor of 1.35. If the 1.35 live load factor is maintained, then the wind factor should be set equal to 0.80.

The commonly used live load factor equal to 0.50 in combination with earthquake effects leads to conservative results. This report has shown that a load factor of 0.25 on live load effects when they are combined with earthquake effects would still provide adequate safety levels for typical bridge configurations subjected to earthquake intensities similar to

those observed on the West or the East Coast. These calculations are based on conservative assumptions on the recurrence of live loads when earthquakes are actively vibrating the bridge system.

For the combination of vessel collision forces and wind loads, a wind load factor equal to 0.30 is recommended in combination with a vessel collision factor of 1.0. The low wind load factor associated with vessel collisions compared with that recommended for the combination of wind loads plus live loads partially reflects the lower rate of collisions in the 75-year design life of bridges as compared with the number of live load events.

A scour factor equal to 1.80 is recommended for use in combination with a live load factor equal to 1.75. The lower scour load factor for combination of scour and live loads as compared with the load factor proposed for scour alone reflects the lower probability of having the maximum possible 75-year live load occur when the scour erosion is also at its maximum 75-year depth.

A scour factor equal to 0.70 is recommended in combination with a wind load factor equal to 1.40. The lower scour factor observed in combination involving wind loads as compared with those involving live loads reflect the lower number of wind storms expected in the 75-year design life of the structure.

A scour factor equal to 0.60 is recommended in combination with vessel collision forces. The lower scour factor observed in combinations that involve collisions reflects the lower number of collisions expected in the 75-year bridge design life.

A scour factor equal to 0.25 is recommended in combination with earthquakes. The lower scour factor with earthquakes reflects the fact that as long as a total wash out of the foundation does not occur, bridge columns subjected to scour exhibit lower flexibilities that will help reduce the inertial forces caused by earthquakes. This reduction in inertial forces partially offsets the scour-induced reduction in soil depth and the resulting soil resisting capacity.

With regard to the extreme loads of interest to this study, the recommended revisions to the AASHTO LRFD specifications (1998) would address the extreme loads by ensuring that the factored member resistances are greater than the maximum load effects obtained from the following combinations:

- Strength I Limit State:  $1.25 DC + 1.75 LL$
- Strength III Limit State:  $1.25 DC + 1.40 WS$
- Strength V Limit State:  $1.25 DC + 1.00 LL$   
 $+ 1.20 WS + 1.20 WL$
- Extreme Event I:  $1.25 DC + 0.25 LL$   
 $+ 1.00 EQ$
- Extreme Event II:  $1.25 DC + 0.25 LL$   
 $+ 1.00 CV$ , or  
 $1.25 DC + 0.30 WS$   
 $+ 1.00 CV$  (3.46)

- Extreme Event III:  $1.25 DC$ ;  $2.00 SC$ ,  
or  
 $1.25 DC + 1.75 LL$ ;  
 $1.80 SC$
- Extreme Event IV:  $1.25 DC + 1.40 WS$ ;  
 $0.70 SC$
- Extreme Event V:  $1.25 DC + 1.00 CV$ ;  
 $0.60 SC$
- Extreme Event VI:  $1.25 DC + 1.00 EQ$ ;  
 $0.25 SC$

In the above equations,  $DC$  represents the dead load effect,  $LL$  is the live load effect,  $WS$  is the wind load effect on the structure,  $WL$  is the wind load acting on the live load,  $EQ$  is the earthquake forces,  $CV$  is the vessel collision load, and  $SC$  represents the design scour depth. The dead load factor of 1.25 would be changed to 0.9 if the dead load counteracts the effects of the other loads.

Notice that no calculations for the combination of vessel collisions and live loads are performed in this study because no live load models are currently available to cover the long-span bridges most susceptible to this combination. The  $\gamma_{LL} = 0.25$  factor proposed under Extreme Event II is projected from the calibration for the combination of earthquakes and live loads under Extreme Event I.

Unlike the other extreme events, scour does not produce a load effect. Scour changes the geometry of the system and reduces the load-carrying capacity of the foundation in such a way as to increase the risks from other failures. The presence of scour is represented in the above set of Equations 3.46 through the variable  $SC$ . The semicolon indicates that the analysis for load effects should assume that a maximum scour depth equal to  $\gamma_{SC} SC$  exists when the load effects of the other extreme events are applied where  $g_{SC}$  is the scour factor by which scour depths calculated from the current HEC-18 method should be multiplied. When scour is possible, the bridge foundation should always be checked to ensure that the foundation depth exceeds  $2.00 SC$ . For the cases involving a dynamic analysis, such as the analysis for earthquakes, it is very critical that the case of zero scour depth be checked because in many cases, the presence of scour may reduce the applied inertial forces. The resistance factors depend on the limit states being considered. When a linear elastic analysis of single and multicolumn bents is used, the system factors developed under NCHRP Project 12-47 should also be applied (Liu et al., 2001).

Equation 3.46 does not include any combinations of three different threats. This is because several analyses executed as part of this study have shown that the reductions of the reliability indexes for the combination of three different extreme events are small. This is due to the low probability of a simultaneous occurrence of three extreme events with high enough intensities to affect the overall risk. This is illustrated in Figure 3.33 for the combination of ship collisions with scour and winds loads and in Figure 3.35 for the combination of live load, wind, and scour.

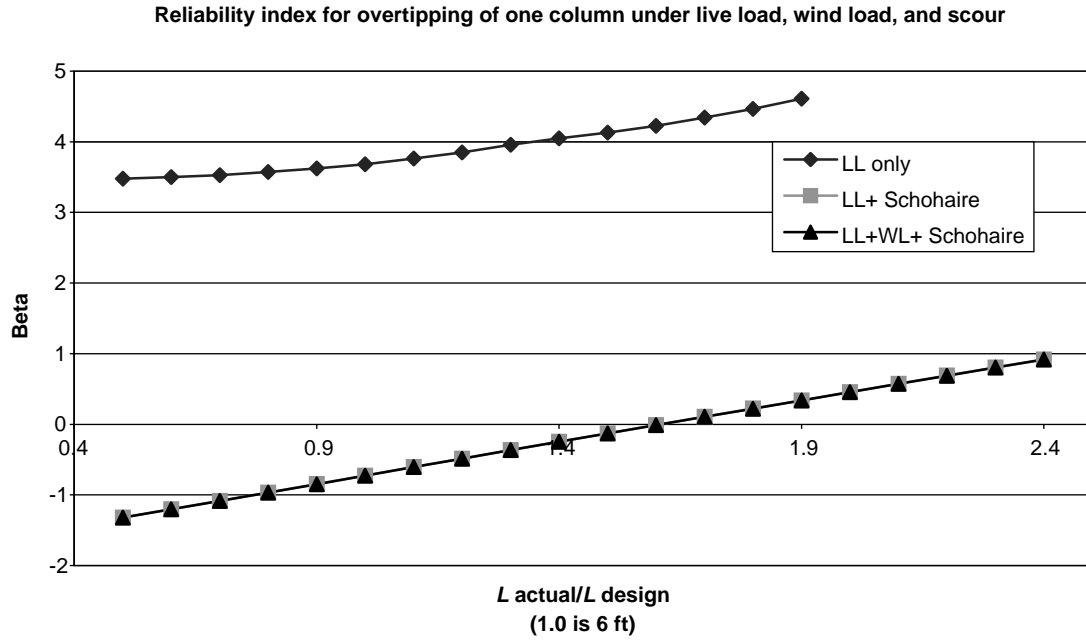


Figure 3.35. Reliability index for combination of live load, wind, and scour.

